ESCOLA DE MEDICINA
PROGRAMA DE PÓS-GRADUAÇÃO EM PEDIATRIA E SAÚDE DA CRIANÇA
MESTRADO EM PEDIATRIA E SAÚDE DA CRIANÇA

JOSIANE SILVA SILVEIRA

PARTICIPAÇÃO DO VÍRUS SINCICIAL RESPIRATÓRIO, DAS ESPÉCIES REATIVAS DE OXIGÊNIO E DA AUTOFAGIA NA FORMAÇÃO DE REDES EXTRACELULARES DE EOSINÓFILOS NA ASMA

Porto Alegre
2018

JOSIANE SILVA SILVEIRA

PARTICIPAÇÃO DO VÍRUS SINCICIAL RESPIRATÓRIO, DAS ESPÉCIES REATIVAS DE OXIGÊNIO E DA AUTOFAGIA NA FORMAÇÃO DE REDES EXTRACELULARES DE EOSINÓFILOS NA ASMA

Dissertação de Mestrado apresentada como requisito para a obtenção do grau de Mestre em Saúde da Criança pelo Programa de Pós-graduação em Pediatria e Saúde da Criança da Pontifícia Universidade Católica do Rio Grande do Sul.

Orientadora: Profª. Dra. Aline Andrea da Cunha

Porto Alegre

2018

Ficha Catalográfica

S587p Silveira, Josiane Silva

Participação do vírus sincicial respiratório, das espécies reativas de oxigênio e da autofagia na formação de redes extracelulares de eosinófilos na asma / Josiane Silva Silveira . – 2018.

151 f.

Dissertação (Mestrado) – Programa de Pós-Graduação em Medicina/Pediatria e Saúde da Criança, PUCRS.

Orientadora: Profa. Dra. Aline Andrea Cunha.

1. asma. 2. autofagia. 3. espécies reativas de oxigênio. 4. redes extracelulares de eosinófilos. 5. vírus sincicial respiratório. I. Cunha, Aline Andrea. II. Título.

Elaborada pelo Sistema de Geração Automática de Ficha Catalográfica da PUCRS
com os dados fornecidos pelo(a) autor(a).
Bibliotecária responsável: Salete Maria Sartori CRB-10/1363

JOSIANE SILVA SILVEIRA

PARTICIPAÇÃO DO VÍRUS SINCICIAL RESPIRATÓRIO, DAS ESPÉCIES REATIVAS DE OXIGÊNIO E DA AUTOFAGIA FORMAÇÃO DE REDES EXTRACELULARES DE EOSINÓFILOS NA ASMA

Dissertação de Mestrado apresentada como requisito para a obtenção do grau de Mestre em Saúde da Criança pelo Programa de Pós-graduação em Pediatria e Saúde da Criança da Pontifícia Universidade Católica do Rio Grande do Sul.

Aprovado em _____ de _____ de _____.

BANCA EXAMINADORA

_____

Prof. Dr. Fernando Spiller (UFSC)

_____

Prof. Dr. Jarbas Rodrigues de Oliveira (PUCRS)

_____

Prof. Dr. Márcio Vinícius Fagundes Donadio (PUCRS)

_____

Profª. Drª. Aline Andrea da Cunha (Orientadora)

Porto Alegre

2018

‘‘Conheça todas as teorias, domine todas as técnicas, mas ao tocar uma alma humana, seja apenas outra alma humana’’.
(Carl Jung)

AGRADECIMENTOS

Primeiramente agradeço a Deus pela vida, por trilhar meu caminho sempre da melhor maneira e por me permitir finalizar mais esta etapa da minha vida.

Agradeço à minha família por todo o amor e por sempre estarem ao meu lado me apoiando, compreendendo e incentivando meus estudos. Amo muito vocês.

À minha orientadora e amiga Aline Andrea da Cunha por ter despertado em mim o amor pela pesquisa. Agradeço a todos os ensinamentos, paciência, confiança e incentivo. Você é muito especial e um grande exemplo para mim. Muito obrigada por tudo!

Ao professor Paulo Pitrez pela oportunidade de trabalhar em seu laboratório no início da minha graduação e a todos os ensinamentos transmitidos.

A todos os colegas e amigos do Laboratório de Respirologia Pediátrica Géssica Luana Antunes, Carolina Luft, Rodrigo Godinho de Souza, Mariana Severo, Daniela Kaiber, Keila Abreu e Taila Piva. Muito obrigada pela amizade, paciência, companheirismo e ajuda em tudo que precisei durante todos esses anos.

À professora Angela Wyse e aos alunos Eduardo Marques e Fernanda Ferreira do Laboratório de Neuroproteção e Doenças Metabólicas pela realização das técnicas de extresse oxidativo e metabolismo energético mitocondrial.

Aos colegas do Laboratório de Imunologia Celular e Molecular principalmente ao Rodrigo Gassen pelo auxílio na técnica de citometria de fluxo e Rodrigo Dorneles pelo ajuda com os equipamentos de Western Blot.

Ao Ricardo Breda pela realização das imagens de imunofluorescência confocal.

À Betânia Souza pelo auxílio na revelação do Western Blot.

Aos técnicos do Laboratório Central de Microscopia e Microanálise (LaBCEMM) pela ajuda na realização da microscopia eletrônica de varredura.

Aos colegas do Laboratório de Imunologia Clínica e experimental principalmente à Krist Helen Antunes pelo auxílio na realização do Western Blot.

Aos colegas e amigos do Laboratório de Biofísica Celular e Inflamação pelos momentos de descontração e trocas de conhecimento, especialmente à Gabriela Viegas Haute.

À equipe do Centro de Modelos Biológicos Experimentais (CeMBE) pelo fornecimento dos animais utilizados no estudo.

À secretária da pós-graduação Carla Rothmann pela paciência e ajuda sempre que precisei.

Ao Conselho Nacional de Desenvolvimento Científico e Tecnológico (CNPq) pela bolsa de mestrado concedida.

RESUMO

INTRODUÇÃO: a asma é uma doença inflamatória crônica caracterizada pela secreção de elevados níveis de citocinas do perfil *T helper 2* (Th2) como interleucina (IL)-4, IL-5 e IL-13, espécies reativas de oxigênio (EROs), aumento da autofagia e formação redes extracelulares de eosinófilos (EETs). A infecção pelo vírus sincicial respiratório (VSR) pode facilitar o desenvolvimento da sensibilização alérgica bem como exacerbar os sintomas da doença. Recentemente, estudos têm demonstrado o aumento da autofagia em eosinófilos das vias de pacientes asmáticos, contribuindo para o aumento da resposta inflamatória nas vias aéreas. Na asma, a produção excessiva de EETs pode causar dano tecidual e aumento da viscosidade do muco, podendo contribuir para o aumento da obstrução da via aérea e redução da função pulmonar. Entretanto, os mecanismos de formação das EETs e seu papel fisiopatológico na asma são pouco compreendidos.

OBJETIVO: esta dissertação teve como objetivo elucidar alguns mecanismos envolvidos na liberação de EETs na asma. Avaliamos a participação do VSR *in vitro,* das EROs e da autofagia nos mecanismos envolvidos na liberação das EETs em eosinófilos do lavado broncoalveolar (LBA) em um modelo experimental de asma.

METODOLOGIA: para o desenvolvimento do modelo experimental de asma, camundongos BALB/cJ foram sensibilizados com duas injeções subcutâneas de ovalbumina (OVA) nos dias 0 e 7 seguidos por três desafios intranasais com OVA nos dias 14, 15 e 16 do protocolo. No artigo científico 1, eosinófilos do LBA de animais do grupo OVA e do grupo controle foram estimulados com VSR (10^3 PFU/mL) *in vitro* por 3 horas. Após este período, o sobrenadante da cultura foi coletado para a realização das técnicas avaliadas conforme os objetivos específicos deste artigo científico. No artigo cientifico 2, durante o protocolo experimental de asma, os animais foram tratados via intranasal com um inibidor da nicotinamida adenina dinucleotídeo fosfato oxidase (NADPH oxidase), difenileno-iodônio (DPI), ou com um precursor da glutationa, N-acetilcisteína (NAC), 45 minutos antes dos três desafios intranasais com OVA. Já no artigo cientifico 3, os animais foram tratados via intranasal com um inibidor de autofagia, 3-metiladenina (3-MA), 45 minutos antes dos três desafios intranasais com OVA. Ao final do protocolo o LBA e o tecido pulmonar foram coletados para a realização das técnicas avaliadas em cada um dos artigos científicos, conforme seus objetivos específicos.

RESULTADOS: no artigo cientifico 1, observamos um aumento na liberação de EETs em eosinófilos do LBA de animais submetidos ao modelo experimental de asma e estimulados com VSR *in vitro*. Por outro lado, o VSR *in vitro* foi capaz de diminuir os níveis de IFN-γ no sobrenadante da cultura de eosinófilos do LBA. Em relação aos resultados do artigo científico 2, verificamos que no grupo OVA tratado com NAC ocorreu uma diminuição no número de células inflamatórias no LBA bem como uma redução no infiltrado inflamatório pulmonar. Além disso, os animais do grupo OVAM tratados com DPI ou NAC apresentaram uma redução da enzima EPO, hiperplasia de células caliciformes, citocinas inflamatórias e da proteína fator nuclear kappa B (NFκB p65). Os tratamentos com DPI ou NAC foram capazes de reduzir a formação de EROs, aumentar a atividade da enzima catalase antixidante (CAT). Por outro lado, parâmetros do metabolismo energético mitocondrial aumentaram somente com o tratamento com NAC. Por fim, demonstramos que os tratamentos com DPI ou NAC foram capazes de reduzir a formação de EETs do LBA. No artigo científico 3, observamos que no grupo OVA tratado com o inibidor de autofagia, 3-MA, ocorreu uma diminuição no número de células inflamatórias no LBA bem como uma redução do infiltrado inflamatório pulmonar. Além disso, os animais tratados com 3-MA apresentaram uma redução nos níveis da enzima EPO, hiperplasia de células caliciformes, citocinas inflamatórias e da proteína NFκB p65. O tratamento com 3-MA foi capaz de reduzir a formação de EROs bem como aumentar os níveis da enzima antioxidante CAT. O tratamento com 3-MA também melhorou parâmetros do metabolismo energético mitocondrial e a atividade da enzima Na^+,K^+ATPase. Demonstramos também que o tratamento com 3-MA diminuiu o imunoconteúdo da proteína *light chain 3B* (LC3B) em eosinófilos do LBA e no tecido pulmonar e reduziu a formação de EETs no LBA.

CONCLUSÃO: Nossos resultados demonstram um importante papel do VSR na indução da liberação de EETs. Além disso, verificamos que os tratamentos com DPI, NAC e 3-MA foram capazes de reduzir a inflamação das vias aéreas, o estresse oxidativo e a liberação de EETs no LBA. Demonstramos que o VSR, as EROs e a autofagia participam dos mecanismos que regulam o processo de liberação das EETs na asma. Assim, a identificação de alguns desses mecanismos envolvidos na liberação de EETs na asma pode contribuir para uma melhor compreensão da patogênese desta doença inflamatória crônica que prejudica a qualidade de vida dos

pacientes e é responsável por um alto custo econômico para o Sistema Único de Saúde (SUS).

PALAVRAS-CHAVE: asma, autofagia, espécies reativas de oxigênio, redes extracelulares de eosinófilos, vírus sincicial respiratório.

ABSTRACT

INTRODUCTION: asthma is a chronic inflammatory disease characterized by secretion of elevated levels of cytokines (interleukin (IL)-4, IL-5 and IL-13), reactive oxygen species (ROS), autophagy and eosinophil extracellular traps (EETs) release in airway. Moreover, respiratory syncytial virus (RSV) infection may facilitate allergic sensitization development as well as exacerbate asthma symptoms. Recently, studies have demonstrated an increase of autophagy in eosinophils of asthmatic patients, contributing to an increase in inflammatory response. In asthma, an increase in EETs release may cause tissue damage and an increase in mucus viscosity, which contribute to airway obstruction and reduction of lung function. However, the mechanism of EETs formation and its pathophysiologic role in asthma are poorly understood.

OBJECTIVE: the aim of this dissertation was to elucidate some mechanisms involved in EETs release in asthma. We investigated whether the respiratory syncytial virus (RSV) could induce EETs *in vitro* in bronchoalveolar lavage fluid (BALF) eosinophils of an experimental asthma model. Moreover, we evaluated ROS and autophagy participation in mechanisms involved in EETs formation.

METHODS: in order to perform the experimental model of asthma, BALB/cJ mice were sensitized with two subcutaneous injections of ovalbumin (OVA) on days 0 and 7, followed by three intranasal challenges with OVA on days 14, 15 and 16 of the protocol. In paper 1, BALF eosinophils of OVA group and control group were stimulated with RSV (10^3 PFU/mL) *in vitro* for 3 hours. After that, culture supernatant was collected in order to perform the analyses proposed in this study which were evaluated according to the specific objectives of this paper. In paper 2, during the experimental asthma protocol, mice were treated intranasally with a nicotinamide adenine dinucleotide phosphate oxidase (NDPH oxidase) inhibitor, diphenyleneiodonium (DPI), or a glutathione precursor, N-acetylcysteine (NAC). In paper 3, mice were treated intranasally with an autophagy inhibitor, 3-Methyladenine (3-MA). Treatments were performed 45 minutes before of the three intranasal administrations with OVA. At the end of the protocol, BALF and lung tissue were collected to perform the techniques discribed in each of the papers, according to their specific objectives.

RESULTS: in paper 1, we verified an increase in EETs release in BALF eosinophils from OVA group stimulated with RSV *in vitro*. RSV *in vitro* decreased IFN-γ in BALF cells when compared to the OVA group. In paper 2, we showed that in NAC-treated OVA group there was a decrease in the inflammatory cells in BALF and lung tissue. DPI or NAC treatments reduced EPO activity, goblet cells hyperplasia, inflammatory cytokines and NFκB p65 immunocontent in lung, and they helped in decreasing ROS production in lung. Furthermore, NAC increased catalase (CAT) activity in lur However, only NAC treatment improved mitochondrial energy metabolism in lung. We showed that DPI or NAC reduced EETs formation in BALF from the OVA group. In paper 3, we showed that in 3-MA-treated OVA group there was a decrease in the inflammatory cells, EPO activity, goblet cells hyperplasia, inflammatory cytokines, NFκB p65 immunocontent, and oxidative stress in airway. Moreover, 3-MA was able to improve mitochondrial energy metabolism and increase Na^+,K^+-ATPase activity. We also demonstrated that 3-MA decreased light chain 3B (LC3B) in BALF cells and lung tissue as well as reduced EETs formation in BALF.

CONCLUSION: our results verified an important role for RSV in the induction of EETs release. Moreover, DPI, NAC and 3-MA treatments decreased airway inflammation, oxidative stress and EETs release in asthma. Our data suggested that RSV, ROS and autophagy participate in the mechanisms for EETs release in asthma. Thus, identification of mechanisms that regulate EETs formation in asthma may contribute to a better understanding of the pathogenesis of this chronic inflammatory disease which damages patients' quality of life and is responsible for a high economic cost for the Brazilian Single Health System (SUS).

KEYWORDS: asthma, autophagy, eosinophil extracellular traps, reactive oxygen species, respiratory syncytial virus.

LISTA DE FIGURAS

LISTA DE ABREVIATURAS

Atg – Proteína relacionada à autofagia

ATG5 – Gene 5 relacionado à autofagia

ATP – Adenosina trifosfato

ANOVA – Análise da variância

AKT – Proteína quinase B

AO – Laranja de acridina

AVOs – Organelas vesiculares ácidas

BETs – Redes extracelulares de basófilos

BSA – Albumina sérica bovina

CAT – Catalase

CD4 – Cluster de diferenciação 4

CeMBE – Centro de modelos biológicos experimentais

CEUA – Comissão de ética no uso de animais

CTE – Cadeia transportadora de elétrons

CO_2 – Ácido carbônico

DCF – Diclorofluoresceína

DCIP – 2,6-dicloroindofenol

DMEM – *Dulbecco's Modified Eagle's medium*

DNA – Ácido Desoxirribonucleico

DGC – Doença granulomatosa crônica

DPBS – *Dulbecco phosphate-buffered saline*

DPI – Difenileno-iodônio

ECP – Proteína catiônica eosinofílica

EDN – Neurotoxina derivada do eosinófilo

EDTA – Ácido etilenodiamino tetra-acético

EPO – Peroxidase eosinofílica

EROs – Espécies reativas de oxigênio

EETs – Redes extracelulares de eosinófilos

FOT – Técnica de oscilação forçada

G – *Tissue damping* (amortecimento do tecido)

GATA3 – Proteína de ligação Gata 3

GINA – Iniciativa global contra a asma

GPx – Glutationa peroxidase

H – *Tissue elastance* (elastância do tecido)

HCl – Ácido clorídrico

H2DCF-DA – 2’7’ diclorofluoresceína

H&E – Hematoxilina e eosina

H_2O – Água

H_2O_2 – Peróxido de hidrogênio

HOCL – Ácido hipocloroso

H_2SO_4 – Ácido sulfúrico

IFN-α – Interferon α

IFN-β – Interferon β

IFN-γ – Interferon γ

IgE – Imunoglobulina E

IL – Interleucina

iNOS – Óxido nítrico sintase induzível

KCl – Cloreto de sódio

KH_2PO_4 – Fosfato de potássio

LBA – Lavado broncoalveolar

LC3 – *Light chain 3*

3-MA – 3-metiladenina

MAPK – Proteínas quinases ativadas por mitógenos

MBP – Proteína básica principal

MCETs – Redes extracelulares de mastócitos

METs – Redes extracelulares de macrófagos

$MgCl_2$ – Cloreto de magnésio

NAC – N-acetilcisteína

NADPH – Nicotinamida adenina dinucleotídeo fosfato

NADPH oxidase – Nicotinamida adenina dinucleotídeo fosfato oxidase

NaCl – Cloreto de magnésio

Na_3PO_4 – Fosfato de sódio

NETs – Redes extracelulares de neutrófilos

NFκB – Fator nuclear kappa B

NK – Células natural killer

O_2 – Oxigênio

$O_2^{\bullet-}$ – Ânion superóxido

OH^- – Radical hidroxil

OMS – Organização mundial da saúde

OPD – O-fenilenodiamina

OVA – Ovalbumina

PBS – Tampão fosfato salino

PCR - Reação em cadeia da polimerase

P_i – Fosfato inorgânico

PFA – Paraformaldeído

PFU – Unidades Formadoras de Placa

pH – Potencial de hidrogênio

PI – Iodeto de propídio

PMA – Forbol-12-miristato-13-acetato

PMSF – Fluoreto de fenilmetilsulfonil

PI3K de classe III – Fosfatidilinositol 3-quinase de classe III

rhDNase – Desoxirribonuclease recombinante humana

Rn – Resistência newtoniana (resistência das vias aéreas)

RNA – Ácido ribonucleico

rpm – Rotações por minuto

SOD – Superóxido dismutase

SDH – Succinato desidrogenase

SFB – Soro fetal bovino

SPF – Livres de patógenos específicos

STAT6 - Ativador da transcrição 6

RPMI – Roswell Park Memorial Institute

Th2 – *T helper 2*

TGF-β – Fator de transformação do crescimento β

TLR4 – Receptor do tipo Toll 4

TNF-α – Fator de necrose tumoral α

VSR – Vírus sincicial respiratório

SUMÁRIO

1. INTRODUÇÃO

A asma é uma doença inflamatória crônica altamente prevalente com alta morbidade e mortalidade no mundo. A Organização Mundial da Saúde (OMS) estima que a asma acometa aproximadamente 300 milhões de pessoas no mundo com um índice de mortalidade mundial de 250.000 pessoas ao ano.[1] A asma é uma doença complexa caracterizada por secreção nas vias aéreas de elevados níveis de imunoglobulina E (IgE), citocinas pró-inflamatórias como interleucina (IL)-4, IL-5 e IL-13 e aumento dos níveis de espécies reativas de oxigênio (EROs) e redução de defesas antioxidantes causando hiper-responsividade das vias aéreas, hipersecreção de muco, remodelamento e estreitamento das vias aéreas.[2-4] Eosinófilos são granulócitos envolvidos ativamente na resposta imune da asma e possuem atividades citotóxicas através da liberação de suas proteínas granulares contribuindo para o dano tecidual, diminuição da função pulmonar e aumento do processo inflamatório nas vias aéreas.[5] Além disso, recentes estudos têm demonstrado o aumento da autofagia em eosinófilos das vias de pacientes asmáticos, podendo contribuir para o aumento da resposta inflamatória da doença.[6-8]

Há evidências de que os vírus respiratórios são responsáveis por mais de 80% dos casos de exacerbação da asma em crianças.[9] Além disso, há vários estudos que sugerem que infecções graves pelo vírus sincicial respiratório (VSR) no início da vida podem contribuir para o risco de asma na infância.[10] O VSR atinge aproximadamente 100% das crianças até dois anos.[11] E apesar de ser altamente infeccioso, o VSR não induz uma memória imunológica eficaz em resposta à infecção, com isso, infecções repetidas são muito frequentes.[12,13] Além de contribuir para a doença no lactente, o VSR pode facilitar o desenvolvimento da sensibilização alérgica, mas os mecanismos imunológicos envolvidos na exacerbação da asma pelo VSR são pouco compreendidos.[14]

As redes extracelulares de ácido desoxirribonucleico (DNA) têm sido descritas como um mecanismo de resposta imune inata eficiente do hospedeiro.[15-17] Os eosinófilos quando estimulados liberam rapidamente seu DNA para o meio extracelular, juntamente com as suas proteínas granulares, formando as extracelulares de eosinófilos (EETs) capazes de aprisionar patógenos extracelularmente.[15] Apesar das propriedades vantajosas das EETs, sua produção excessiva já foi demonstrada em várias condições inflamatórias, desencadeando a

exacerbação da inflamação e provocando dano tecidual.[18,19] Neste contexto, estudos demonstram que o VSR é capaz de induzir a formação de redes extracelulares de neutrófilos (NETs), entretanto, não há na literatura nenhum estudo avaliando a capacidade deste vírus induzir a formação de EETs.[20,21] Em 2011, Dworski e colaboradores demonstraram a presença de EETs nas vias aéreas de pacientes asmáticos.[22] Cunha e colaboradores observaram um aumento na formação de EETs no lavado broncoalveolar (LBA) em um modelo murino de asma.[23] Além disso, recentes estudos demonstram que as EROs e a autofagia desempenham um papel crucial na formação de redes extracelulares de DNA, entretanto pouco se sabe sobre o envolvimento desses mecanismos na liberação de EETs na asma.[24]

Durante minha iniciação científica no Laboratório de Respirologia Pediátrica, demonstramos pela primeira vez a formação de EETs nas vias aéreas de camundongos submetidos a um modelo experimental de asma.[23] Este trabalho foi publicado na revista *Allergy* em 2014. Em um estudo posterior, demostramos que o tratamento com desoxirribonuclease recombinante humana (rhDNase) (fármaco que promove a degradação do DNA) reduz a formação de EETs e melhora parâmetros da mecânica ventilatória pulmonar.[25] Assim, a proposta deste projeto de mestrado foi avaliar quais os mecanismos e estímulos induzem a liberação de EETs em um modelo experimental de asma. Visando contemplar este objetivo geral, realizamos três artigos científicos. No artigo científico 1 em formato de *short communication*, mostramos a capacidade do VSR *in vitro* de induzir a formação de EETs em eosinófilos do LBA. Já no artigo científico 2, avaliamos a participação das EROs na formação de EETs. A fim de avaliar este mecanismo, tratamos os animais com um inibidor da nicotinamida adenina dinucleotídeo fosfato oxidase (NADPH oxidase), difenileno-iodônio (DPI), ou com um precursor da glutationa, N-acetilcisteína (NAC). Finalmente no artigo científico 3, avaliamos o papel da autofagia na liberação das EETs. Para avaliarmos este mecanismo, tratamos os animais com um inibidor de autofagia, o 3-metiladenina (3-MA). Assim, nesta dissertação avaliamos a participação do VSR *in vitro*, das EROs e da autofagia nos mecanismos envolvidos na liberação de EETs em eosinófilos do LBA em um modelo experimental de asma com ovalbumina (OVA). Desta forma essa dissertação visa contribuir para uma melhor compreensão dos mecanismos necessários para liberação das EETs bem como avaliar sua participação na resposta imune da asma.

2. REVISÃO DE LITERATURA

2.1 ASMA

2.1.1 Definição e epidemiologia da asma

A asma é uma doença altamente prevalente com elevada morbidade e mortalidade.[1,26] Segundo a Organização Mundial da Saúde (OMS), estima-se que a asma acomete aproximadamente 300 milhões de pessoas no mundo e possui um índice de mortalidade mundial de 250.000 pessoas ao ano.[1] Estima-se que no Brasil existem 20 milhões de asmáticos, considerando a prevalência global de 10%, ocupando a oitava posição mundial na prevalência desta doença.[27,28] A asma atinge todas as idades e entre 10 a 15% dos pacientes estão na faixa etária pediátrica, provocando ansiedade e um grande impacto na qualidade de vida do paciente e de seus familiares.[29] Em um estudo prévio do nosso grupo, demostramos que a prevalência da asma em crianças no sul do Brasil é de 28,6% e 42,7% das crianças estão com a asma mal controlada, apresentando uma taxa de hospitalização de 7,6%.[30] Esta doença causa elevada morbidade e custos para os sistemas de saúde, resultando em perdas escolares, faltas no trabalho, limitações aos exercícios, risco de hospitalizações, aumento de visitas em consultas médicas e salas de emergência e é associada com transtornos emocionais.[31]

A asma é uma doença complexa causada tanto por fatores genéticos quanto ambientais, e recentemente, tem sido reconhecida como uma síndrome, devido a sua complexidade, por apresentar diferentes graus severidade, fenótipos, morbidades e resposta a tratamentos variáveis.[32] Além disso, a asma apresenta como principais sintomas sibilos, dispneia, tosse e opressão torácica, piorando à noite ou no início da manhã, sendo que esses sintomas são desencadeados frequentemente por exposição à alérgenos ou a substâncias irritantes, exercício, mudanças no clima ou principalmente por infecções respiratórias virais.[1]

O tratamento medicamentoso da asma baseia-se em duas linhas principais de abordagem: medicação de controle (glicocorticoide inalatório e broncodilatadores de longa duração) e de resgate (broncodilatadores de curta duração). Entretanto, os tratamentos disponíveis para asma persistente moderada e grave, principalmente o uso de glicocorticoide inalatório, nem sempre é capaz de controlar os sintomas da

doença ou o remodelamento das vias aéreas, complicação patológica presente em alguns pacientes.[33]

2.1.2 Resposta imune da asma

A asma é uma doença caracterizada por uma inflamação crônica das vias aéreas inferiores associada a uma hiper-responsividade brônquica, broncocostrição e limitação variável do fluxo aéreo.[1] Além disso, é uma doença heterogenia apresentando diferentes fenótipos resultantes da interação entre diversas células inflamatórias, citocinas e mediadores inflamatórios.[29] A inflamação é o aspecto central do desenvolvimento da asma. Ao entrar em contato com alérgenos específicos diversas células são ativadas e citocinas e mediadores inflamatórios são secretados. A participação de células inflamatórias, IgE específica para alérgenos e linfócitos T *helper* 2 (Th2) exercem um papel fundamental na fisiopatologia da doença, ocorrendo também a participação de diversas citocinas (IL-4, IL-5 e IL-13), EROs, leucotrienos e histamina.[31] Nas vias aéreas dos pacientes asmáticos ocorre um aumento da infiltração de células inflamatórias como neutrófilos, macrófagos, mastócitos e eosinófilos.[34] A principal célula que participa da resposta imune da asma são os eosinófilos. Estas células são leucócitos derivadas da medula óssea e são associados com doenças alérgicas ou helmínticas.[35] Os eosinófilos secretam enzimas citotóxicas presentes em seus grânulos como proteína básica principal (MBP), peroxidase eosinofílica (EPO), proteína catiônica eosinofílica (ECP) e neurotoxina derivada do eosinófilo (EDN) que estão envolvidas nas alterações fisiopatológicas da asma.[36] Além disso, há um aumento do remodelamento das vias aéreas em pacientes asmáticos ocorrendo à deposição de colágeno, espessamento da musculatura lisa e aumento da angiogênese, contribuindo para a redução da função pulmonar.[37]

A resposta imune da asma se inicia quando as células apresentadoras de antígeno das vias aéreas reconhecem, processam e apresentam o antígeno aos linfócitos T naive e estes se diferenciam ao fenótipo Th2.[38,39] Os linfócitos Th2 são importantes para a defesa do organismo contra infecções helmínticas, mas também são característicos de doenças alérgicas, como a atopia e a asma.[40] Estas células secretam citocinas específicas como IL-5 que promove a diferenciação e a migração

de eosinófilos, IL-4 que estimula a secreção de IgE alérgeno-específico pelos linfócitos B que é responsável pela sensibilização dos mastócitos, IL-13 induz a hiperplasia de células caliciformes e IL-9 que promove a migração e a diferenciação dos mastócitos.[41,42]

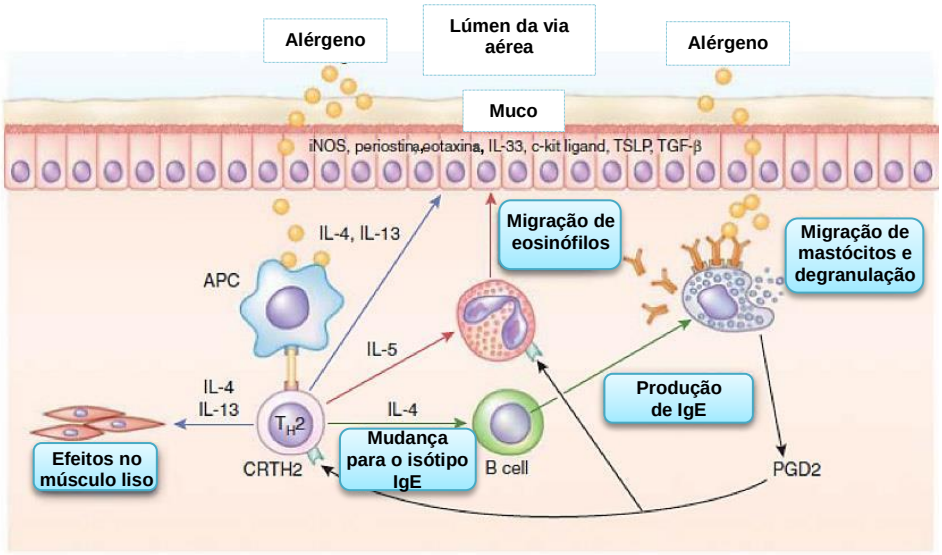

Figura 1: Resposta imune da asma. APC: célula apresentadora de antígeno; CRTH2: molécula homóloga ao receptor quimioatraente expresso em *T helper 2*; IL: interleucina; iNOS: óxido nítrico sintase induzível; IgE: imunoglobulina E; TGF-β: fator de transformação do crescimento β; Th2: *T helper 2*; TSLP: proteína estromal tímica (Adaptado de Wenzel).[43]

2.1.3 A infecção pelo VSR e a resposta imune na asma

Os sintomas da asma podem ser desencadeados por diversos fatores, porém, infecções virais possuem um papel central na exacerbação desta doença. Há evidências de que os vírus respiratórios são responsáveis por mais de 80% dos casos de exacerbação da asma em crianças.[9] Além disso, há vários estudos que sugerem que infecções graves pelo VSR no início da vida podem contribuir para o risco de asma na infância por alterar o sistema imunológico e interferir no desenvolvimento pulmonar.[10] Em torno de 31% dos lactentes que apresentam pelo menos um episódio de bronquiolite, desenvolvem asma em idade escolar.[44]

Globalmente, o VSR causa por ano, cerca de 33,8 milhões novos casos de infecções do trato respiratório inferior em crianças menores de cinco anos.[45] Além disso, estima-se que o VSR atinja cerca de 100% das crianças até dois anos de

idade.[11] Apesar de ser altamente infeccioso, VSR não induz uma memória imunológica eficaz em resposta à infecção, com isso, infecções repetidas são muito frequentes.[12,13] O VSR é um vírus envelopado, com ácido ribonucleico (RNA) de fita simples, pertencente à ordem *Mononegavirales* e a família *Pneumoviridae.*[46] O VSR possui duas proteínas de superfície principais, a proteína G que promove a adesão e a proteína F que promove a fusão entre o vírus e a superfície da célula alvo.[47] Possui também proteínas não estruturais, como a NS1 e NS2 que constituem o componente viral chave envolvido no ciclo infeccioso e na evasão da resposta imune do hospedeiro ao VSR.[46]

As células epiteliais das vias respiratórias constituem o alvo inicial para a infecção do VSR, bem como o primeiro local para a ativação da resposta imune inata. Quando ocorre o contato do VSR com as células epiteliais respiratórias, a proteína F presente no envelope viral é reconhecido pelo receptor do tipo Toll 4 (TLR4) da superfície celular, promovendo a ativação do fator nuclear kappa B (NFκB) e a secreção das citocinas IL-8, IL-10 e IL-6.[48] Assim, durante as primeiras horas da infecção pelo VSR, uma expressão aumentada de genes relacionados com respostas inflamatórias, processamento de antígenos e quimioatração são observados no epitélio pulmonar.[49] Estes processos promovem a produção de quimiocinas e o recrutamento de eosinófilos, neutrófilos, monócitos, células *natural killer* (NK) e células T cluster de diferenciação 4 $(CD4)^+$ para as vias aéreas.[50] Diferente da maioria dos vírus, a infecção pelo VSR promove uma resposta enfraquecida ao interferon tipo I (IFN tipo I) nos tecidos infectados, bloqueando a sinalização de IFN-α e IFN-β. Este mecanismo utilizado pelo VSR provavelmente permite o sucesso viral e a sua replicação dentro de tecidos infectados.[51] Durante a infecção pelo VSR as células T $CD4^+$ frequentemente diferenciam-se em linfócitos Th2, fenótipo que não é adequado para remoção viral, e produzem ou promovem a secreção das citocinas IL-4, IL-5 e IL-13.[52,53] A alteração causada pelo VSR na polarização dos linfócitos T $CD4^+$ em direção a um fenótipo Th2, caracterizado por ser um fenótipo alérgico, pode propiciar a sensibilização a aeroalérgenos e favorecer o desenvolvimento da asma.[54,55] Assim, a infecção pelo VSR altera a reatividade das vias aéreas ainda imaturas e em desenvolvimento do lactente, podendo causar lesões, redução da função pulmonar e alterações imunomoduladoras.[11,56]

2.1.4 Envolvimento das EROs, do metabolismo energético mitocondrial e da enzima Na^+,K^+ATPase na asma

As EROs produzidas pelo organismo são resultantes do metabolismo celular normal e são essenciais para muitas funções biológicas.[57] Porém em altas concentrações, as EROs, produzem modificações adversas nos componentes das células, como nos lipídios, proteínas e DNA.[58] As principais EROs são o ânion superóxido ($O_2^{\bullet-}$), peróxido de hidrogênio (H_2O_2) e o radical hidroxila (OH^-). O organismo possui mecanismos antioxidantes que neutralizam as ações deletérias das EROs. Entre as defesas antioxidantes podemos destacar a superóxido dismutase (SOD), catalase (CAT) e glutationa peroxidase (GPx), que são defesas enzimáticas e, como defesas não enzimáticas as vitaminas A, C, E, glutationa reduzida, polifenóis, entre outros. A enzima SOD é responsável por catalisar a dismutação de $O2^{\bullet-}$ em H_2O_2 e oxigênio (O_2).[59] H_2O_2 resultante dessa reação é reduzido pelas enzimas CAT e GPx.[59] Além disso, a N-acetilcisteína (NAC) é um clássico tiol antioxidante que é utilizado como alternativa terapêutica. NAC atua como um "*scavanger"* de EROs por possuir cisteína em sua composição a qual é precursora da glutationa.[60] Em situações onde há um desequilíbrio entre a produção de EROs e das defesas antioxidantes ocorre o estresse oxidativo e é associado a diversas patologias.[59]

Estudos demonstram que pacientes asmáticos apresentam um aumento na produção de EROs, promovendo uma diminuição na capacidade antioxidante do trato respiratório.[61,62] Além disso, a produção excessiva de EROs causa danos aos pulmões, aumentando a inflamação e a hiper-reatividade das vias aéreas, exacerbando o quadro fisiopatológico da doença.[63] As células inflamatórias presentes na resposta imune da asma, como os eosinófilos, neutrófilos e macrófagos, e as células que compõe as vias aéreas como o epitélio e a musculatura lisa, são capazes de produzir EROs.[64] Macrófagos, neutrófilos e eosinófilos contêm uma enzima chamada nicotinamida adenina dinucleotídeo fosfato oxidase (NADPH oxidase) associada à membrana, que produz $O_2^{\bullet-}$ e outras EROs, responsáveis por atividades bactericida, tumoricida e pró-inflamatória.[65] Esse sistema enzimático é responsável pela geração de $O_2^{\bullet-}$ que forma um sistema de transporte de elétrons transmembrana que resulta na oxidação de NADPH na superfície celular e na geração de $O_2^{\bullet-}$ na superfície externa da membrana, que

pode sofrer a ação da enzima antioxidante SOD e formar H_2O_2. Uma vez formado, o potencial oxidante do H_2O_2 pode ser amplificado pela ação de peroxidases derivadas de eosinófilos e neutrófilos, a EPO e a mieloperoxidase (MPO), respectivamente, formando ácido hipocloroso (HOCL).[61] Neste contexto substâncias são utilizadas visando a inibição da NADPH oxidase, um exemplo é o difenileno-iodônio (DPI) que é considerado um potente inibidor da NADPH oxidase. O DPI retira um elétron da oxidase, levando à formação de um aduto com o FAD e inibindo deste modo, a formação de $O_2^{\bullet-}$.[66]

Outro importante local de formação de EROs nas células é na cadeia transportadora de elétrons (CTE) na membrana mitocondrial. A CTE é composta por quatro complexos proteicos (I, II, III, IV), que interagem através da ubiquinona e da proteína citocromo c visando à produção de adenosina trifosfato (ATP) no complexo V ou ATP sintase.[67] O alto fluxo de elétrons na CTE predispõe a formação de EROs. Assim, cerca de 5% do O_2 utilizado na CTE é incompletamente reduzido a água (H_2O) e é convertido em EROs. Neste contexto, a exposição de células a EROs pode causar dano mitocondrial e inativar a CTE e consequentemente diminuir a produção de ATP.[68,69] Além disso, estudos mostraram uma associação entre disfunção mitocondrial e doenças inflamatórias pulmonares.[70,71] Mabalirajan e colaboradores demonstraram que em um modelo experimental de asma há uma redução da atividade do complexo I e IV mitocondrial e uma diminuição dos níveis de ATP no pulmão.[72] Assim, o estresse oxidativo que ocorre na asma causa uma importante disfunção mitocondrial que pode contribuir para o aumento da inflamação e do remodelamento nas vias aéreas.[72]

A atividade da enzima Na^+,K^+-ATPase controla o gradiente iônico celular e sua atividade é suscetível a um aumento na formação de EROs e à depleção de ATP.[73] As consequências da redução na atividade da Na^+,K^+-ATPase incluem alteração do potencial elétrica da membrana, ativação de leucócitos, regulação negativa de respostas a β-agonistas em receptores β-adrenérgicos e broncocostrição.[74-76]. Estudos demonstram que a diminuição da atividade desta enzima em células do sangue periférico de pacientes asmáticos.[74] Além disso, a inibição da Na^+,K^+-ATPase com oubaína, causa constrição do músculo liso *in vitro* e aumento da hiper-responsividade brônquica em modelo animal.[75] Assim, o aumento na formação de EROs diminui a atividade da CTE e, consequentemente, pode

reduzir a produção de ATP, contribuindo para a redução da atividade da Na^+, K^+-ATPase, pois a taxa de consumo de ATP desta enzima é muito alta.[68]

2.1.5 Autofagia e asma

A autofagia é um processo fisiológico fundamental para a sobrevivência celular durante a restrição de nutrientes, diferenciação e controle normal do crescimento celular e promove a remoção de proteínas danificadas e organelas senescentes ou danificadas.[76] É definida como o processo de sequestrar proteínas citoplasmáticas ou até mesmo organelas inteiras para o lisossomo.[77] A autofagia se inicia com o envolvimento de porções citoplasmáticas e organelas da célula por uma membrana dupla, denominada autofagossoma ou vacúolo autofágico. Por fim, o autofagossoma funde-se com um lisossomo para formar o autolisossoma ou o vacúolo autofágico degradativo. Dentro do autolisossoma, o conteúdo é degradado por hidrolases lisossômicas.[78]

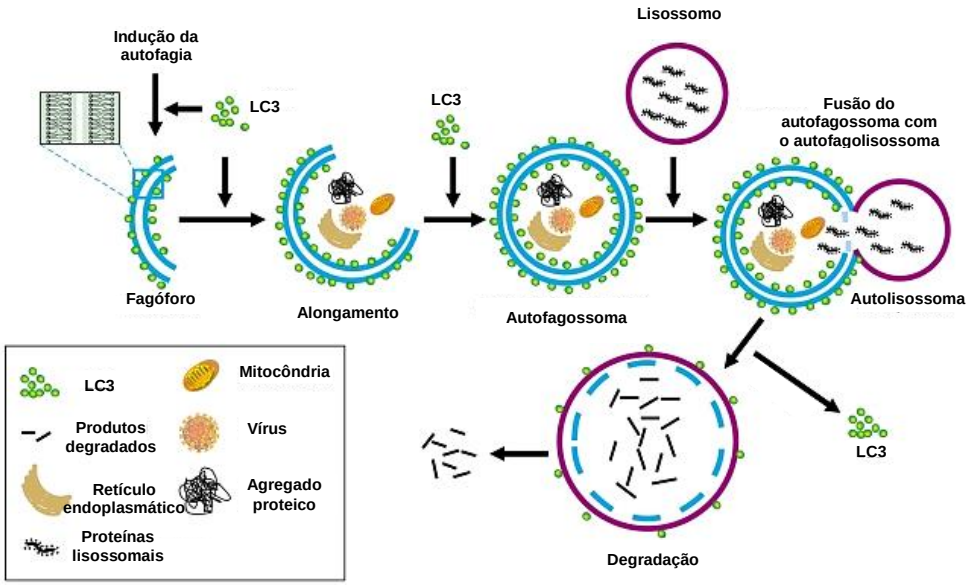

Figura 2: Autofagia. LC3: *light chain* 3 (Adaptado de Jing e colaboradores).[79]

A autofagia desempenha um papel crucial no desenvolvimento da resposta imune inata e adaptativa, regulando a proliferação, ativação e função de várias células imunes.[80,81] Vários processos imunológicos são altamente dependentes da autofagia, incluindo reconhecimento e destruição de patógenos, apresentação de

antígenos e regulação inflamatória.[82,83] Porém poucos são os estudos que descrevem o mecanismo pelo qual a autofagia participa na patogênese de doenças inflamatórias. Os fatores que desencadeiam a autofagia no pulmão incluem hipóxia, exposição ao fumo, condições pró-inflamatórias e estresse oxidativo, porém poucos estudos foram realizados no pulmão e o significado funcional da autofagia em doenças pulmonares permanece um enigma.[84] As EROs vem sendo relatadas como indutores de autofagia, sendo que as mitôcondrias representam a principal fonte de EROs necessária para a realização da autofagia.[85,86] O aumento da geração de EROs promove a ativação da fosfatidilinositol 3-quinase de classe III (PI3K de classe III), uma proteína crucial para o início da autofagia.[86]

Recentes estudos demonstram que a autofagia desempenha um importante papel na resposta imune da asma.[8,87] Ban e colaboradores observaram que os granulócitos do escarro e neutrófilos e eosinófilos do sangue periférico de pacientes com asma severa apresentam níveis mais elevados da proteína *light chain 3 II* (LC3-II), proteína presente ma membrana do autofagossomo, quando comparados com pacientes com asma não severa e controles saudáveis.[87] Além disso, estudos demontran que variantes do gene 5 relacionado à autofagia (ATG5) estão associadas à promoção do remodelamento das vias aéreas e redução da função pulmonar em crianças com asma.[6] A autofagia também é descrita por ter a capacidade de atrasar a apoptose de fibroblastos, aumentando a produção do fator de transformação do crescimento beta (TGF-β), promovendo um aumento na síntese de colágeno e o remodelamento nas vias aéreas.[6] A autofagia também é essencial para a secreção de muco nas vias aéreas, sendo este processo dependente de IL-13.[7] Em um modelo experimental de asma em camundongos realizado com OVA, observou-se um aumento da proteína LC3II nas células do LBA avaliado por imunofluorescência e Western Blot, quando comparado ao grupo controle. Já o tratamento com um inibidor de autofagia, foi capaz de diminuir a hiper-responsividade das vias aéreas, o infiltrado inflamatório e as células caliciformes.[8]

2.2 FORMAÇÃO DE REDES EXTRACELULARES DE DNA

2.2.1 Redes extracelulares de DNA

As redes extracelulares de DNA são descritas como um mecanismo de eficiente de defesa do hospedeiro e apresentam um importante papel na resposta imune inata. As redes extracelulares de DNA foram descritas inicialmente em neutrófilos[88] como uma nova forma de morte celular, distinta da apoptose e da necrose e foram chamadas posteriormente de NETose.[89] Entretanto, estudos posteriores demonstraram que os neutrófilos permanecem viáveis após a liberação das redes extracelulares de neutrófilos (NETs), além de permanecerem com sua capacidade fogocítica.[90,91] As NETs são compostas principalmente de DNA, histonas e por proteínas presentes em seus grânulos, como a enzima mieloperoxidase (MPO). A presença de DNA é um componente estrutural e importante na formação das NETs, uma vez que, estudos já demonstraram que o tratameto prévio com DNase promove a desintegração das redes extracelulares formadas.[89]

A formação das NETs desempenham um importante papel no combate à infecções, servindo como uma “armadilha” para bactérias e outros patógenos.[92] Apesar das propriedades vantajosas, a produção excessiva das NETs pode levar a uma exacerbação da inflamação e sua formação já foi demonstrada em várias doenças inflamatórias.[93,94] Nas doenças respiratórias, as NETs já foram identificadas na fibrose cística, lesão pulmonar aguda (LPA), infecções bacterianas, fúngicas, virais e na asma.[22,95-99] Na fibrose cística, o acúmulo de NETs pode promover dano ao tecido pulmonar e exacerbação da doença pelo espessamento da camada de muco.[95] Em um recente estudo realizado com neutrófilos de sangue periférico de doadores saudáveis, a proteína F do VSR foi capaz de induzir a formação de NETs.[20] Além disso, um aumento de NETs no escarro de pacientes asmáticos foi correlacionado com uma fenótipo mais severo da doença.[100]

As redes extracelulares de DNA têm sido recentemente documentadas por não serem exclusivamente liberadas pelos neutrófilos, podendo ser produzidas também por macrófagos (METs)[101], mastócitos (MCETs)[102], basófilos (BETs)[103] e eosinófilos (EETs) [15].

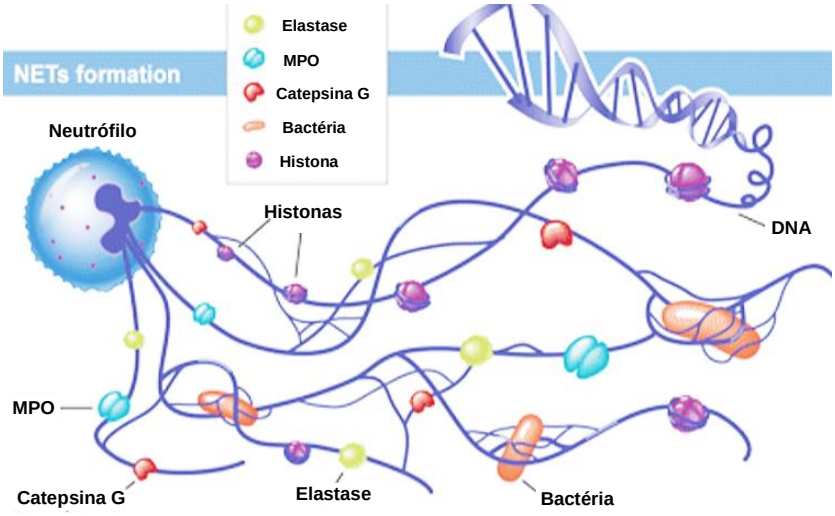

Figura 3: Redes extracelulares de neutrófilos (NETs). MPO: mieloperoxidase (Adaptado de Miyata e colaboradores).[104]

2.2.2 EETs e asma

Os eosinófilos quando estimulados, perdem forma bilobular do seu núcleo, seguido da desintegração do envelope nuclear e derramamento da cromatina nuclear para o citoplasma. Então, a membrana plasmática dos eosinófilos se rompe, permitindo a expulsão das redes de DNA e liberação dos grânulos dos eosinófilos intactos, formando as EETs.[105] Estudos posteriores demonstraram que o DNA liberado pelas EETs também pode ser de origem mitocondrial.[16,22,] Neste contexto, eosinófilos sensibilizados com IL-5 ou IFN-γ e estimulados com lipopolissacarídeo (LPS), eotaxinas ou proteína do complemento (C5a), liberam seu DNA mitocondrial e proteínas granulares para o meio extracelular, formando redes bactericidas no espaço extracelular.[15] Dados da literatura sugerem que a atividade fagocítica dos eosinófilos é em grande parte limitada quando comparada com outras células fagocíticas, sugerindo que sua atividade bactericida possa ocorrer extracelularmente, provavelmente através da liberação de EETs.[106]

Em 2004, Brinkmann e colaboradores demonstraram que a formação de NETs é um processo que envolve morte celular.[89] Estudos subsequentes verificaram que pós a liberação das EETs, os eosinófilos permanecem viáveis e não apresentam evidências de morte celular.[15,16,23] Cunha e colaboradores observaram que a liberação de EETs nas vias aéreas de um modelo de asma não foi devida a

apoptose ou necrose.[23] No entanto, Ueki e colaboradores demonstraram que a liberação das EETs em secreções de pacientes com rinossinusite ou otite eosinofílica foi resultado de morte celular.[107] Além disso, em EETs não está completamente esclarecido se o seu DNA está associado à liberação de DNA nuclear ou mitocondrial. Yousefi e colaboradores utilizando a técnica de reação em cadeia da polimerase (PCR) demonstraram que as EETs continham sequências de DNA mitocondrial.[15] Já Muniz e colaboradores verificaram que as EETs foram co-localizadas com histona H3 citrulinada, o que sugere que os EETs formadas contêm DNA de origem de nuclear.[17]

Os eosinófilos são encontrados nas vias aéreas de indivíduos asmáticos, sendo a célula predominante na inflamação inicial e tardia da asma.[108] Em 2011, Dworski e colaboradores demonstraram pela primeira presença de EETs co-localizadas com MBP nas vias aéreas de pacientes asmáticos através de biópsias brônquicas analisadas por imunofluorescência.[22] No entanto, embora esta seja uma descoberta importante, foi realizada por meio de uma técnica muito invasiva. Em um estudo realizado pelo nosso grupo, demonstramos um aumento nos níveis de DNA extracelular no escarro induzido de crianças asmáticas que possuíam diferentes padrões de células inflamatórias (dados submetidos à publicação). Além disso, nosso grupo publicou o primeiro estudo demonstrando a presença de EETs co-localizadas com EPO em eosinófilos do LBA e do tecido pulmonar de animais submetidos a um modelo experimental de asma com OVA.[23] Posteriormente, demonstramos que o tratamento com rhDNase (fármaco promove a degradação do DNA) via intranasal promoveu uma redução significativa na formação de EETs no LBA e no tecido pulmonar, além de verificarmos que o tratamento também promoveu uma melhora na mecânica respiratória pulmonar, além de diminuir a hiperplasia das células caliciformes.[25] A produção excessiva de EETs na asma pode causar dano tecidual e espessamento do muco das vias aéreas, contribuindo para as alterações patológicas da doença.

2.2.3 Participação das EROs e da autofagia na formação de redes extracelulares de DNA

Há diversos estudos que demonstram que as EROs desempenham um papel crucial na formação de redes extracelulares de DNA.[89,109] Esta observação foi feita primeiramente devido aos pacientes com doença granulomatosa crônica (DGC) apresentarem uma capacidade reduzida em formar NETs.[110] Os pacientes com DGC possuem uma deficiência na expressão da enzima NADPH oxidase a qual é responsável pela geração de $O^{2\bullet-}$. Da mesma forma, os eosinófilos de indivíduos com DGC, também não são capazes de liberar EETs após a estimulação com IL-5 ou com IFN-γ e LPS.[15] A inibição da produção de NADPH oxidase com DPI, antes da estimulação com linfopoetina estromal tímica (TSLP) (citocina que promove a diferenciação de linfócitos ao fenótipo Th2), bloqueou completamente a liberação de EETs em eosinófilos purificados do sangue periférico de doadores saudáveis, atópicos ou portadores de síndromes hipereosinofílicas.[16] Além disso, Choi e colaboradores demonstraram recentemente, que eosinófilos do sangue periférico de pacientes com asma eosinofílica severa tratados com o antioxidante NAC e posteriormente estimulados com IL-5 e LPS apresentaram uma redução na liberação de EETs.[111] No entanto, não está claro como as EROs participam da formação das redes extracelulares de DNA. Ueki e colaboradores demonstraram que a liberação das EETs é um mecanismo dependente de NADPH oxidase, esta enzima ativa a via citolítica, iniciando a dissolução da cromatina nuclear, formando as redes extracelulares de DNA.[18] As EROs podem contribuir também inativando as caspases, inibindo com isso a apoptose e favorecendo a autofagia, em um processo que leva a dissolução das membranas celulares contribuindo para liberação das redes extracelulares de DNA.[24]

A autofagia foi descrita recentemente por participar de um importante mecanismo da resposta imune inata, a formação de redes extracelulares de DNA.[24] A participação da autofagia no mecanismo de liberação das NETs, já foi descrita na estimulação *in vitro* com *Candida albicans,* induzida por plaquetas, na gota, no câncer de pâncreas e na asma.[112-116]. Remijsen e colaboradores demonstraram que a formação de NETs induzida pelo clássico indutor da liberação de redes extracelulares de DNA, o forbol-12-miristato-13-acetato (PMA), requer tanto a participação da autofagia como a produção de $O_2^{\bullet-}$. [24] Além disso, os neutrófilos do

sangue periférico de pacientes com asma severa apresentam um aumento no imunoconteúdo da proteína LC3II, proteína presente no autofagossoma, e este parâmetro, apresentou correlação positiva com o aumento da formação de NETs.[116]

Assim, nosso estudo busca investigar alguns mecanismos que podem estar relacionados com a liberação das EETs na asma. Já está estabelecido na literatura que ocorre a liberação de EETs na asma, mas quais mecanismos estão diretamente relacionados com sua formação ainda foram pouco estudados. Esta dissertação propõe a investigação do possível envolvimento do VSR, das EROs e da autofagia nos mecanismos de liberação das EETs na asma.

3. JUSTIFICATIVA

A asma é uma doença inflamatória crônica de elevada prevalência na infância, causando alta morbidade e mortalidade. Está doença é causa de altos custos para os sistemas de saúde, além de resultar em perdas escolares, faltas ao trabalho, limitações ao exercício, risco de hospitalizações, aumento de visitas em consultas médicas e salas de emergência.[31] As infecções virais têm sido crescentemente reconhecidas como a maior causa da exacerbação da asma[14], o que sugere que o VSR possa desempenhar um papel importante em amplificar a resposta inflamatória na asma.

O papel desempenhado por diferentes mecanismos inflamatórios na asma, tais como a liberação de redes extracelulares de DNA, formação de EROs e a autofagia constituem um assunto de grande interesse pela comunidade científica, por participarem dos mecanismos de defesa do hospedeiro contra agentes infecciosos e, ao mesmo tempo, causam dano tecidual através do recrutamento e/ou ativação de células inflamatórias. A formação das EETs constitui um importante mecanismo da resposta imune inata contra as infecções, sendo as EROs o principal estímulo para sua formação.[92] Além disso, a autofagia vem sendo descrita como essencial na liberação das redes extracelulares de DNA em doenças inflamatórias.[116] As EETs são produzidas como ferramentas eficientes contra agentes infecciosos, mas, por outro lado, sua produção excessiva pode contribuir para os danos característicos presentes nas vias aéreas de pacientes asmáticos. Entretanto, os mecanismos envolvidos na liberação de EETs e seu papel fisiopatológico na asma ainda são pouco compreendidos. Desta forma esta dissertação pretende contribuir esclarecendo alguns dos mecanismos imunológicos envolvidos na estimulação da liberação das EETs tais como o efeito do VSR, das EROs e da autofagia.

4. OBJETIVOS

O objetivo dessa dissertação é elucidar alguns dos mecanismos envolvidos na liberação das EETs na asma. O objetivo geral bem como os objetivos específicos estão subdivididos em artigos 1, 2 e 3 e serão apresentados na forma de artigos científicos como seguem.

4.1 Artigo Científico 1

4.1.1 Objetivo Geral

Investigar a capacidade do VSR em induzir a formação de EETs *in vitro* em eosinófilos do LBA de um modelo experimental de asma.

4.1.2 Objetivos Específicos

- Quantificar os níveis de DNA extracelular no sobrenadante da cultura de eosinófilos do LBA estimuladas com VSR *in vitro*;
- Verificar a liberação de EETs por imunofluorescência e sua co-localização com a EPO e histona H2B em eosinófilos do LBA estimulados com VSR *in vitro*;
- Determinar a morte em células do LBA estimuladas *in vitro* com VSR por citometria de fluxo através do kit de Anexina V e Iodeto de propídio (PI);
- Mensurar os níveis das citocinas IL-4 e IFN-γ no sobrenadante da cultura de eosinófilos do LBA estimuladas com VSR *in vitro*;
- Analisar a atividade da enzima EPO no sobrenadante da cultura de eosinófilos do LBA estimuladas com VSR *in vitro*.

4.2 Artigo Científico 2

4.2.1 Objetivo Geral

Avaliar o envolvimento das EROs no mecanismo de formação das EETs em um modelo experimental de asma.

4.2.2 Objetivos Específicos

Avaliar em um modelo experimental de asma o tratamento com um inibidor da NADPH oxidase, DPI, ou com um precursor da glutationa, NAC, sobre:

- A contagem total e diferencial de células, bem como a atividade da enzima EPO no LBA;
- As alterações histopatológicas no tecido pulmonar através da utilização da coloração hematoxilina e eosina (H&E) para avaliar o infiltrado inflamatório bem como a produção de muco e hiperplasia de células caliciformes através da coloração de alcian blue;
- Parâmetros de mecânica ventilatória pulmonar (resistência newtoniana (Rn), *tissue damping* (G) e *tissue elastance* (H));
- Os níveis das citocinas IL-5, IL-13, IFN-γ, IL1-β, fator de necrose tumoral (TNF)-α e IL-10 bem como a proteína NFκB p65 no tecido pulmonar;
- Os níveis de EROs pela técnica da diclorofluoresceína (DCF) e a atividade das enzimas antioxidantes SOD, CAT e GPx no tecido pulmonar;
- O metabolismo energético mitocondrial (complexo II, succinato desidrogenase (SDH) e complexo IV) e a atividade da enzima NA^+,K^+ATPase no tecido pulmonar;
- Os níveis de DNA extracelular no sobrenadante do LBA, formação de EETs por imunofluorescência e por microscopia eletrônica de varredura bem como a morte dos eosinófilos do LBA por citometria de fluxo através do kit de Anexina V e PI.

4.3 Artigo Científico 3

4.3.1 Objetivo Geral

Avaliar a participação da autofagia nos mecanismos de liberação das EETs em um modelo experimental de asma.

4.3.2 Objetivos Específicos

Avaliar em um modelo experimental de asma e em animais tratados com o inibidor da autofagia 3-MA:

- A contagem total e diferencial de células, bem como a atividade da enzima EPO no LBA;
- O infiltrado inflamatório através de morfometria pulmonar utilizando a coloração H&E bem como produção de muco e hiperplasia de células caliciformes com a coloração de alcian blue;
- Parâmetros de mecânica ventilatória pulmonar (Rn, G e H);
- Mensurar os níveis das citocinas IL-5, IL-13, IFN-γ, IL1-β, TNF-α e IL-10, bem como a proteína NFκB p65 no tecido pulmonar;
- Os níveis de EROs pela técnica do DCF, bem como a atividade das enzimas antioxidantes SOD, CAT e GPx no tecido pulmonar;
- O metabolismo energético mitocondrial (complexo II, SDH e complexo IV) e a atividade da enzima NA^{+},K^{+}ATPase no tecido pulmonar;
- Os níveis de DNA extracelular no sobrenadante do LBA, a formação de EETs por imunofluorescência bem como a morte de eosinófilos do LBA por citometria de fluxo através do kit de Anexina V e PI;
- A presença de organelas vesiculares ácidas (AVOs) nos eosinófilos do LBA através do corante laranja de acridina (AO) por imunoflorescência e por citometria de fluxo;
- A proteína light chain 3 B (LC3B) por imunoflorescência no tecido pulmonar e em eosinófilos do LBA;
- O imunoconteúdo por Western Blot de LC3B e da proteína quinase B (AKT) no tecido pulmonar.

5. MATERIAL E MÉTODOS

5.1.1 Animais

Os experimentos foram realizados com camundongos BALB/cJ fêmeas com idades entre 6 e 8 semanas, livres de patógenos específicos (SPF) e com peso aproximado de 20 g, provenientes do Centro de Modelos Biológicos experimentais (CeMBE). Os animais foram mantidos em ambiente com temperatura controlada (24 ± 2°C), alojados em gaiolas de acrílico com maravalha esterilizada e em um ciclo 12/12 horas de claro/escuro. Os animais tiveram acesso livre à ração padrão para roedores e água. Este projeto foi aprovado pela Comissão de ética no uso de animais (CEUA) sob o número 7910.

5.1.2 Protocolo de indução do modelo experimental de asma

Os camundongos foram sensibilizados com duas injeções via subcutânea de 20 µg de OVA (Grade V, Sigma, Missouri, EUA), diluída em 200 µL de *Dulbecco phosphate-buffered saline* (DPBS, Gibco, Massachusetts, EUA) nos dias 0 e 7 do protocolo. Em seguida, foram realizados três desafios intranasais com 100 µg de OVA, diluídas em 50 µL de DPBS, nos dias 14, 15 e 16 do protocolo.[25] Antes da realização dos desafios intranasais os animais foram previamente anestesiados em câmara anestésica com isoflurano por via inalatória para facilitar a aspiração pulmonar da OVA. O grupo controle negativo recebeu somente DPBS durante a sensibilização e o desafio.

5.1.3 Desenho experimental do protocolo de asma

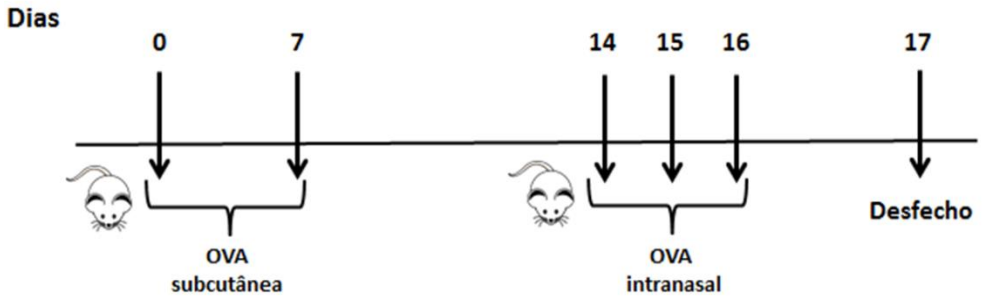

Figura 4: Desenho experimental do protocolo de asma com ovalbumina (OVA).

5.2 METODOLOGIA REFERENTE AO ARTIGO CIENTÍFICO 1

5.2.1 Cultivo celular e produção do VSR

Para a realização dos experimentos *in vitro,* utilizamos a cepa A2 do VSR, doada pelo Dr. Fernando Polack (Fundación Infant, Argentina). As células VERO (células renais de macaco verde africano) foram utilizadas para propagar o vírus. Monocamadas de células VERO foram cultivadas em meio *Dulbecco's Modified Eagle's medium* (DMEM) com 10% de soro fetal bovino (SFB), até 60% de confluência. Após o cultivo celular, as células foram inoculadas com 5 x 10^5 Unidades Formadoras de Placa (PFU)/mL de VSR e incubadas por 2 horas a 37°C em 5% de CO_2. Após a incubação, o meio foi removido e adicionado o meio Opti-MEM. Aproximadamente 3 a 4 dias após a infecção as células foram recolhidas para a extração do vírus. As células foram congeladas a -80°C *overnight*, para lise e posteriormente descongeladas e sonicadas por 60 segundos. Após este período, as células foram centrifugadas a 2500 rotações por minuto (rpm), por 10 minutos, a 4°C para a remoção dos debris celulares e o vírus presente no precipitado foi titulado. A titulação viral foi realizada através da detecção de PFU identificadas pela marcação com anticorpo anti-RSV (Millipore, MA, USA) em placa de lise com carboximetilcelulose. Após a realização da titulação as alíquotas de vírus foram armazenadas a -80ºC até sua utilização.[20]

5.2.2 Coleta do LBA

A coleta do LBA foi realizada no 17º dia do protocolo. Primeiramente, os animais foram anestesiados (0,4 mg/g de cetamina e 0,2 mg/g de xilazina). Em seguida a traqueia foi canulada com uma agulha de 20 gauges e foi instilado 1 mL de tampão fosfato salino (PBS) 2% de SFB. O LBA foi centrifugado e o sobrenadante foi descartado. O precipitado celular foi ressuspendido em 350 μL de PBS 2% de SFB para a realização da contagem total e diferencial de células no LBA. A contagem total de células e a morte celular foram determinadas pelo teste de exclusão por azul de tripan e foi realizado na câmara de Neubauer (BOECO, Hamburg, Germany). As lâminas para a contagem diferencial de células foram

realizadas em citocentrífuga (Eppendof, Wesseling, Germany) e coradas com H&E (Newprov, Paraná, Brasil). A contagem total e diferencial de células foi realizada apenas para o controle de qualidade da indução do modelo experimental de asma. Após a coleta do LBA, os animais foram eutanasiados através de exanguinação por punção cardíaca.

5.2.3 Estimulação de eosinófilos do LBA com VSR

Células do LBA (2 x 10^5/mL) de animais do grupo OVA e controle foram plaqueadas e estimuladas com VSR (10^3 PFU/mL) ou incubadas somente com meio *Roswell Park Memorial Institute* (RPMI) durante 3 horas a 37ºC com 5% de CO_2. Esta concentração viral foi utilizada porque concentrações mais altas (10^4 - 10^6 PFU/mL) foram citotóxicas para os eosinófilos. Em seguida as amostras foram centrifugadas e o sobrenadante da cultura foi coletado para a realização da quantificação do DNA extracelular, atividade da enzima EPO e determinação dos níveis de citocinas (IL-4 e IFN-γ). O pellet foi ressuspendido em tampão de citometria para a análise da morte celular por citometria de fluxo através do Kit Anexina V e PI.

5.2.4 Quantificação das redes extracelulares de DNA no sobrenadante da cultura de eosinófilos do LBA

A quantificação do DNA extracelular foi realizada no sobrenadante da cultura de eosinófilos do LBA estimuladas ou não com VSR (10^3 PFU/mL). Para a quantificação do DNA extracelular, inicialmente precipitamos o DNA contido no sobrenadante da cultura, adicionando 300 µL do sobrenadante da cultura em 750 µL de álcool etílico absoluto e 105 µL de acetato de sódio 3 M pH=5,2 e incubamos a amostra por 24 horas a -20ºC. Após esse período, a amostra foi centrifugada por 10 minutos a 13000 rpm. O sobrenadante foi descartado e adicionamos 100 µL de álcool etílico 70%. Em seguida, a amostra foi novamente centrifugada na velocidade citada anteriormente e após o descarte do álcool etílico 70% adicionamos 20 µL de água destilada livre de nucleasse. A quantificação do DNA foi realizada utilizando o Kit Quant-iT dsDNA HS (Invitrogen, Carlsbad, EUA) e mensuradas no fluorímetro

Quibit 2.0 (Invitrogen, Carlsbad, EUA), de acordo com as recomendações do fabricante.

5.2.5 Visualização das EETs por imunofluorescência em eosinófilos do LBA

Para a visualização da formação das EETs por microscopia de imunofluorescência confocal, as células do LBA (2 x 10^5/mL) foram plaqueadas em lâminas de 8 poços para cultura de células e estimuladas com PMA (50 nM) durante 1 hora. Após este período, as células foram estimuladas ou não com VSR 10^3 PFU/mL por 2 horas a 37°C e após fixadas com paraformaldeído (PFA) 4%. Em seguida as células foram marcadas com os anticorpos primários anti-EPO (1:250, Santa Cruz Biotechnology, EUA) e anti-histona H2B (1:250; Santa Cruz Biotechnology, EUA) durante 40 minutos. As células foram incubadas por 40 minutos com os anticorpos secundários FITC *anti-goat* (1:100; Santa Cruz Biotechnology, EUA) e alexa fluor 633 *anti-goat* (1:100, Invitrogen, EUA) e coradas com Hoechst 33342 (1:2000; Invitrogen, Carlsbad, EUA) durante 4 minutos. As Imagens foram obtidas em um microscópio de imunofluorescência confocal Leica TCS-SP8 (Leica Microsystem, Wetzlar, Germany).

5.2.6 Determinação da morte celular em eosinófilos do LBA

Os eosinófilos do LBA incubados com VSR foram analisados em relação à presença de morte celular através do Kit Anexina-V e PI seguindo as instruções do fabricante (BD Pharmingen). As células foram incubadas com Anexina V e PI por 15 minutos em temperatura ambiente e analisadas por citometria de fluxo (FACS Canto II, BD Bioscience). Os dados foram analisados utilizando o software FlowJo versão X.0.7 (TreeStar, Óregon, EUA).

5.2.7 Níveis de citocinas no sobrenadante da cultura de eosinófilos do LBA

Os níveis de IL-4 e IFN-γ foram avaliados pela técnica multiplex utilizando *beads* magnéticas (MAGPIX® TECHNOLOGY, MILLIPLEX® MAP, EUA) utilizando o

Kit ProcartaPlex Multiplex immunoassay (Thermo-Life Technology, Massachusetts, USA), de acordo com as instruções do fabricante e as análises foram realizadas no software xPONENT® solutions (Luminex Corporation).

5.2.8 Atividade da enzima EPO no sobrenadante da cultura de eosinófilos do LBA

A atividade da EPO foi realizada no sobrenadante da cultura de eosinófilos incubados ou não com VSR e foi determinada através de ensaio colorimétrico.[117] A atividade da enzima EPO foi mensurada através oxidação da O-fenilenodiamina (OPD) na presença de H_2O_2 Para a realização do protocolo 50 µL do sobrenadante da cultura foi transferido para uma placa de 96 poços, em seguida foi adicionado em cada amostra 50 µL do reagente de trabalho (OPD 0,1 mM, tris 0,05 M pH=8,0, triton X-100 e 1 mM de H_2O_2). A placa foi incubada protegida da luz por 1 hora. Após esse período a reação foi interrompida com de 50 µL de ácido sulfúrico (H_2SO_4) 1M. A absorbância foi medida com comprimento de onda de 492 nm em espectrofotômetro.

5.2.9 Análise estatística

Os dados foram analisados utilizando o software GraphPad Prism 5 (GraphPad Software, California, USA). A normalidade dos dados foi testada através do teste de *Shapiro-Wilk*. Os dados estão apresentados como média e desvio padrão da média e os resultados foram analisados através da análise da variância (ANOVA) de uma via seguido do pós-teste de *Tukey*, $p \leq 0,05$ foi considerado como estatisticamente significativo.

5.3 METODOLOGIA REFERENTE AOS ARTIGOS CIENTÍFICOS 2 E 3

Os modelos experimentais apresentados nesta dissertação na forma de artigos científicos 1, 2 e 3 apresentam modelos experimentais semelhantes entre si (conforme descrito acima), mudando apenas os tratamentos utilizados.

5.3.1 Tratamentos com DPI, NAC ou 3-MA

Em nosso estudo para investigarmos os mecanismos de liberação das EETs utilizamos três diferentes tratamentos durante o protocolo experimental de asma. No artigo científico 2, para a avaliação da participação das EROs na liberação das EETs os animais foram tratados com DPI (inibidor da NADPH oxidase) (Sigma, Missouri, EUA) na dose de 1 mg/Kg ou NAC (precursor da glutationa) (União Química, São Paulo, Brazil) na dose de 15 mg/100 g de peso.

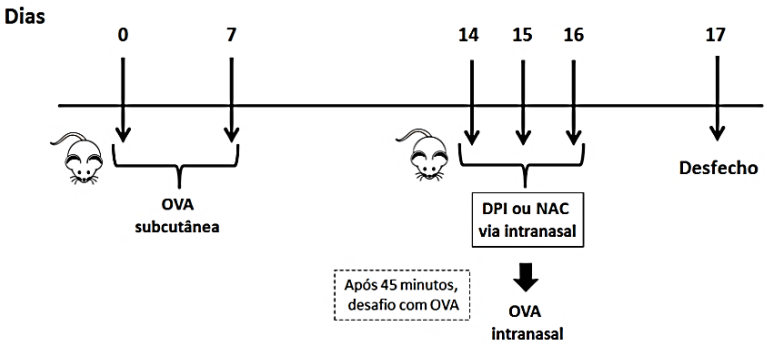

Figura 5: Desenho experimental do protocolo de asma com ovalbumina (OVA) e tratamentos com difenileno-iodônio (DPI) ou N-acetilcisteína (NAC).

Já para investigar a participação da autofagia na liberação das EETs utilizamos o 3-MA (inibidor da proteína PI3K de classe III que é uma proteína crucial para o início da autofagia) (Sigma, Missouri, EUA) na dose de 15 mg/Kg. Os tratamentos foram realizados 45 minutos antes dos desafios intranasais com OVA nos dias 14, 15 e 16.

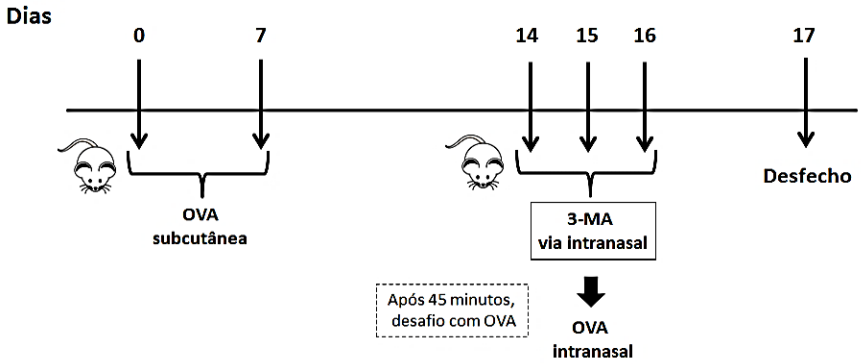

Figura 6: Desenho experimental do protocolo de asma com ovalbumina (OVA) e tratamento com 3-metiladenina (3-MA).

Antes da administração dos tratamentos via intranasal, os animais foram previamente anestesiados em câmara anestésica com isoflurano por via inalatória para facilitar a aspiração pulmonar dos tratamentos.

5.3.2 Avaliação da mecânica ventilatória pulmonar

No 17º dia do protocolo os animais foram anestesiados com cetamina (0,4 mg/g) e xilazina (0,2 mg/g). A avaliação da mecânica ventilatória foi realizada após canulação da traqueia através de uma traqueostomia. O animal foi conectado a um ventilador (flexiVent, SCIREQ, Montreal, Canadá), e mantido por 5 minutos antes do início do teste com uma frequência respiratório de 150 movimentos por minuto, após a administração de pancurônio intraperitoneal (1mg/Kg). Foram realizadas seis medidas de técnica de oscilação forçada (FOT), durante pausa do respirador (3 segundos). Durante as pausas da ventilação, um sinal oscilatório de 9 frequências (4-38 Hz) foi gerado por um alto-falante e passou através da cânula traqueal do animal. Um modelo de quatro parâmetros com a impedância do tecido de fase constante foi ajustada aos dados de Zrs para obter medidas de Rn, que equivale à resistência das vias aéreas no camundongo devido à complacência da parede torácica, G que representa a resistência das pequenas vias aéreas onde o movimento do ar ocorre principalmente por difusão e H que representa a elastância tecidual. Os dados foram analisados em software específico (flexiWare, SCIREQ, Montreal, Canadá), onde resistência das vias aéreas e propriedades elásticas (viscosidade e elasticidade) do pulmão foram mensuradas através da impedância pulmonar.[118,119] Após a realização das medidas de mecânica ventilatória, os animais foram eutanasiados através de exsanguinação por punção cardíaca.

5.3.3 Contagem total e diferencial de células do LBA

O LBA foi coletado no 17º dia do protocolo. Os animais foram anestesiados (0,4 mg/g de cetamina e 0,2 mg/g de xilazina), a traqueia foi canulada com uma agulha de 20 gauges e foi instilado 1 mL de PBS 2% de SFB para coletar o LBA. O LBA foi centrifugado e o sobrenadante foi utilizado para a quantificação do DNA

extracelular e mensuração da atividade da enzima EPO. O precipitado celular foi ressuspendido em 350 μL de PBS 2% de SFB para a realização da contagem total e diferencial de células no LBA. A contagem total de células e a morte celular foram determinadas pelo teste de exclusão por azul de tripan e realizadas na câmara de Neubauer (BOECO, Hamburg, Germany). Para a contagem diferencial de células as lâminas foram realizadas através de cytospin em citocentrífuga (Eppendof, Wesseling, Germany) e coradas com H&E (Newprov, Paraná, Brasil). Em seguida quatrocentas células foram contadas em microscópio óptico (Olympus, Tóquio, Japão). Após a coleta do LBA, os animais foram eutanasiados através de exanguinação por punção cardíaca.

5.3.4 Análise da atividade da enzima EPO no LBA

A atividade da enzima EPO foi mensurada através do teste colorimétrico baseado na oxidação da OPD (Sigma, Missouri, EUA) na presença de H_2O_2.[117] Está técnica está descrita detalhadamente no item 5.2.8 na metodologia do artigo científico 1.

5.3.5 Análise histopatológica do tecido pulmonar

Após a coleta do LBA, os pulmões dos animais foram perfundidos em uma coluna de gravidade com formalina tamponada 10% a uma pressão de 20 cmH_2O. Em seguida o pulmão esquerdo dos animais foi removido e fixado em formalina tamponada 10% por 24 horas. O tecido pulmonar passou por um gradiente de álcool e em seguida em xilol e finalmente foi recoberto com parafina. O tecido foi emblocado em parafina e foram realizados cortes histológicos de 5 micrômetros (µm). Para avaliar o infiltrado inflamatório as lâminas foram coradas com H&E. Para a realização da análise morfométrica pulmonar inicialmente as lâminas foram fotografadas em um aumento de 400x. Para a avaliação da extensão do infiltrado inflamatório peribrônquico e perivascular em µm, foram realizadas 10 medidas iniciando do final do epitélio do brônquio ou do vaso até o final do infiltrado inflamatório, utilizando o software Olympus CellSens Standart (Olympus, Tóquio,

Japão). No mínimo cinco brônquios foram avaliados para obter a média de cada animal. Para a avaliação da hiperplasia das células caliciformes e produção de muco, as lâminas foram coradas com alcian blue. As análises histológicas foram realizadas em microscópio óptico (Olympus, Tóquio, Japão).

5.3.6 Níveis de citocinas no tecido pulmonar

O tecido pulmonar foi homogeneizado em PBS 1x e em seguida foi centrifugado a 8000 rpm por 5 minutos e o sobrenadante foi coletado. Os níveis de IL-5, IL-13, IFN-γ, IL1-β, TNF-α e IL-10 foram mensurados no sobrenadante do tecido pulmonar por análise multiplex utilizando *beads* magnéticas com o Kit Milliplex MAP mouse (MILLIPLEX®, Millipore, Germany) e ProcartaPlex Multiplex immunoassay (Thermo-Life Technology, Massachusetts, USA) de acordo com as instruções do fabricante. As análises foram realizadas no equipamento Magpix® (Millipore, Germany). Os resultados foram analisados utilizando o software xPONENT® solutions (Luminex Corporation).

5.3.7 Preparo do tecido pulmonar para a realização das técnicas de estresse oxidativo, metabolismo energético mitocondrial e NA^+,K^+-ATPase

Para avaliar parâmetros de estresse oxidativo, os pulmões foram homogeneizados (1:10, peso (p)/volume (v)) em tampão de fosfato de sódio (Na_3PO_4) 20 mM contendo 140 mM de cloreto de sódio (KCl) com pH =7,4. Para as análises do metabolismo energético mitocondrial (complexo II, SDH e complexo IV), os pulmões foram congelados e descongelados três vezes para romper as membranas mitocondriais. Após este processo, os pulmões foram homogeneizados (1:20, p/v) em tampão SETH (sacarose 250 mM, ácido etilenodiamino tetra-acético (EDTA) 2 mM, base Trizma 10 mM e 50 UI/mL de heparina), pH=7,4. Para a análise da atividade de NA^+,K^+-ATPase, os pulmões foram homogeneizados (1:10, p/v) em solução de sacarose a 0,32 mM contendo HEPES 5,0 mM e EDTA 1,0 mM, pH=7,5. Os pulmões foram homogeneizados com os tampões específicos, centrifugados a

8000 rpm durante 10 minutos a 4°C e os sobrenadantes foram recolhidos e utilizados para as análises.

5.3.8 Produção de EROs no pulmão

A produção de EROs foi determinada através da técnica descrita por Lebel e colaboradores.[120] Primeiramente, o sobrenadante do tecido pulmonar foi incubado em meio contendo 100 µM de 2'7' diclorofluoresceína (H2DCF-DA) a 37ºC em placa preta durante 30 minutos. Ao final da reação é formado um composto fluorescente, diclorofluoresceína (DCF), que foi medido em espectrofotômetro em 488 nm de excitação e 525 nm de emissão. Os resultados foram expressos por DCF nmol/mg de proteína.

5.3.9 Atividade da enzima antioxidante GPx no pulmão

A Atividade da enzima GPx foi determinada de acordo com Wendel, utilizando tert-butil-hidroperóxido como substrato.[121] Foi adicionado ao sobrenadante do tecido pulmonar 2 mM de glutationa, 0,15 U/mL de glutationa redutase, 0,4 mM de azida, 0,5 mM de tert-butil-hidroperóxido e 0,1 mM de NADPH. Em seguida, o decaimento da NADPH foi monitorado a 340 nm em espectrofotômetro e foi lida por 4 minutos em intervalos de 30 segundos. 1 unidade de GPx é definida como 1 µMol de NADPH consumida por minuto. A atividade da GPx foi representada em unidades GPx/mg de proteína.

5.3.10 Atividade da enzima antioxidante SOD no pulmão

A atividade da SOD foi determinada de acordo com Marklund.[122] Esse método é baseado na capacidade de auto-oxidação do pirogalol, um processo altamente dependente de $O_2^{\bullet -}$, que é substrato para a SOD. Foram adicionados 0,8 mM de pirogalol ao sobrenadante do tecido pulmonar. A inibição da auto-oxidação desse composto ocorre na presença da SOD, cuja atividade pode ser indiretamente medida

em espectrofotômetro a 412 nm. A amostra foi lida durante 3 minutos a cada 30 segundos. Uma curva de calibração foi realizada com SOD purificada como padrão, para calcular a atividade da SOD presente nas amostras. A atividade da SOD foi representada em unidades de SOD/mg de proteína.

5.3.11 Atividade da enzima antioxidante CAT no pulmão

A atividade da CAT foi baseada na medida da diminuição do consumo de H_2O_2 em 240 nm, em uma reação contendo H_2O_2 20 mM com 0,1 de Triton X-100 e fosfato de potássio (KH_2PO_4) 10 mM com pH=7,0. Uma unidade de CAT é definida em 1 μM de H_2O_2 consumido por minuto. A atividade da CAT foi representada em unidades de CAT/mg de proteína.[123]

5.3.12 Atividade do complexo II, da SDH e do complexo IV no pulmão

A atividade do complexo II e SDH nos pulmões foram determinadas de acordo com Fisher e colaboradores.[124] Ao sobrenadante do tecido pulmonar foi adicionado um tampão contendo KH_2PO_4 40 mM pH=7,4, succinato de sódio 16 mM e 2,6-dicloroindofenol (DCIP) 8 mM e foi incubado a 30°C por 20 minutos. Depois disso, adicionamos 4 mM de azida de sódio, 7 mM rotenona e 40 mM de DCIP. A atividade enzimática do complexo II foi mensurada após a diminuição da absorbância pela a redução do DCIP a 600 nm. A reação foi monitorada por 5 minutos, foram realizadas leituras a cada 1 minuto e o resultado foi expresso em nmol/minuto/mg de proteína. A atividade enzimática do SDH foi mensurada após a diminuição da absorbância pela redução do DCIP a 600 nm na presença de metasulfato de fenazina. A reação foi iniciada com a adição de 1 mM de metasulfato de fenazina e foi monitorizada por 5 minutos realizando leituras a cada 1 minuto e os resultados foram expressos em nmol/minuto/mg de proteína. A atividade do complexo IV foi determinada de acordo com Rustin e colaboradores.[125] Ao sobrenadante foi adicionado o tampão de reação contendo KH_2PO_4 10 mM pH=7,0 e 0,6 mM n-dodecil-β-D-maltosídeo. A reação foi iniciada pela adição de 7 μg de citocromo c reduzido sendo a reação monitorada durante 10 minutos em 550 nm a 25ºC. A atividade enzimática foi mensurada

através da diminuição da absorbância pela oxidação do citocromo c reduzido. Os resultados foram expressos em nmol/min/mg de proteína.

5.3.13 Atividade da enzima NA^+,K^+-ATPase no pulmão

A Atividade da enzima NA^+, K^+-ATPase no pulmão foi determinada de acordo com Wyse e colaboradores.[126] O sobrenadante do tecido pulmonar foi incubado com cloreto de magnésio ($MgCl_2$) 5 mM, NaCl 80 mM, KCl 20 mM e Tris-HCl 40 mM em pH=7,4. Após a placa contendo as amostras foi aquecida por 10 minutos a 37ºC. A reação foi iniciada pela adição de ATP a uma concentração final de 3 mM e foi incubada por 20 minutos. Os controles foram realizados sob as mesmas condições com adição de ouabaína 1 mM. A atividade da enzima Na^+,K^+-ATPase foi calculada pela diferença entre os dois ensaios. O fosfato inorgânico (P_i) liberado foi medido pelo método de Chan e colaboradores.[127] A atividade específica foi expressa como nmol P_i liberada por minuto/mg de proteína.

5.3.14 Quantificação do DNA extracelular no sobrenadante do LBA

Para a quantificação do DNA extracelular, inicialmente precipitamos o DNA contido no sobrenadante do LBA. A precipitação do DNA foi realizada conforme descrita no item 5.2.4 do artigo científico 1. A quantificação de DNA da amostra foi analisada utilizando o kit Quant-iT dsDNA HS (Invitrogen, Carlsbad, EUA) e as leituras foram realizadas no fluorímetro Quibit 2.0 (Invitrogen, Carlsbad, USA) de acordo com as recomendações do fabricante.

5.3.15 Visualização da formação de EETs nos eosinófilos do LBA

Para a visualização da formação das EETs, eosinófilos obtidos do LBA (2 x 10^5/mL) foram plaqueadas em lâminas de 8 poços para cultura de células e incubadas a 37°C com 5% de CO_2 por 1 hora. Após este período as células foram fixadas com PFA 4 % por 45 minutos e incubadas com os anticorpos primários anti-

EPO e anti-histona H2B (1:250, Santa Cruz Biotecnology, Dallas, EUA) por 45 minutos. Posteriormente foram incubadas por 30 minutos com os anticorpos secundários FITC *anti-goat* (1:100, Santa Cruz Biotecnology, Dallas, EUA) e Alexa flúor 633 *anti-goat* (1: 100 em PBS, (Invitrogen, Carlsbad, EUA). Em seguida as células foram incubadas com o corante de DNA Hoechst 33342 (1:2000; Invitrogen, Carlsbad, EUA) por 4 minutos. As imagens foram realizadas em microscópio de fluorescência confocal (Zeiss LSM5, Oberkohen, Germany).

5.3.16 Avaliação da formação das EETs em eosinófilos do LBA por microscopia eletrônica de varredura

Os eosinófilos do LBA (2 x 10^5/mL) foram plaqueadas em placas de cultura de 6 poços com lamínulas pré-tratadas com poli-L-lisina (0.005%, Sigma, Missouri, USA). Em seguida, as células foram incubadas por 1 hora a 37°C e com 5% CO_2. O meio de cultura foi removido e as células foram fixadas com glutaraldeído 2,5%. As amostras foram lavadas três vezes com PBS 1x e pós-fixadas com uma solução de tetróxido de ósmio 2% por 45 minutos. As amostras foram novamente lavadas em PBS 1x, seguido de desidratação em gradiente de acetona 30%, 50%, 70%, 2x 95% e 2x 100% por 10 minutos em cada concentração. O ponto crítico foi realizado com CO_2, seguido da montagem metálica com fita de carbono. As amostras foram metalizadas com ouro e as imagens foram realizadas no microscópio eletrônico Inspecionar F50 (FEI, Oregon, EUA).

5.3.17 Análise da morte celular em eosinófilos do LBA

As células foram avaliadas quanto a presença de apoptose por Anexina V e necrose por PI (BD Pharmingen) e analisadas por citometria de fluxo (FACSCanto II), de acordo com as instruções do fabricante. Esta metodologia está descrita detalhadamente no item 5.2.6 da metodologia do artigo científico 1.

5.3.18 Detecção e quantificação de AVOs nos eosinófilos do LBA

A autofagia induz o sequestro citoplasmático de proteínas do componente lítico e é caracterizada pela formação de AVOs (Anderson et al, 1984).[128] Para a detecção dos compartimentos ácidos da célula, utilizamos o corante AO que emite fluorescência vermelha em vesículas ácidas e fluorescência verde no citoplasma e no núcleo. Para a visualização da formação de AVOs, eosinófilos do LBA (2 x 10^5/mL) foram plaqueados em lâminas para cultura de células e incubados a 37°C com 5% de CO_2 por 1 hora. Posteriormente, as células foram incubadas com o corante AO (Sigma, Missouri, USA) na concentração final de 1 µg/mL por 15 minutos em temperatura ambiente. Em seguida, as células foram fixadas com PFA 4% e visualizadas em microscópio confocal de fluorescência (Zeiss LSM5, Oberkohen, Germany). Para quantificar a formação de AVOs as células do LBA foram incubadas com AO na concentração final de 1µg/mL e foram analisadas por citometria de fluxo (FACS Canto II, BD Bioscience). Os dados foram analisados utilizando o software FlowJo versão X.0.7 (TreeStar, Óregon, EUA).

5.3.19 Análise da proteína LC3B nos eosinófilos do LBA

Eosinófilos do LBA (2 x 10^5/mL) foram plaqueados em lâminas de oito poços para cultura de células e incubadas a 37°C com 5% de CO_2 por 1 hora. Após este período as células foram fixadas com PFA 4% por 15 minutos e permeabilizadas com Triton X-100 0,1% em PBS por 15 minutos. Em seguida as células foram incubadas com o anticorpo primário anti-LC3B (0,5 µg/mL, Invitrogen, Carlsbad, EUA) por 1 hora, e posteriormente, foram incubadas por 40 minutos com o anticorpo secundário FITC *anti-rabbit* (1:100, Thermo-Life Tecnology, Waltham, EUA). As células foram incubadas com Hoechst 33342 (1:2000; Invitrogen, Carlsbad, EUA) por 4 minutos e visualizadas em microscópio confocal de fluorescência (Zeiss LSM5, Oberkohen, Germany).

5.3.20 Análise das proteínas NFκB p65 e LC3B no tecido pulmonar por imunofluorescência

O processamento histológico do tecido pulmonar foi realizado como descrito no item 5.3.5. Em seguida, foi realizada a recuperação antigênica nos cortes histológicos de pulmão com citrato de sódio 10 mM, pH=9,0 durante 10 minutos e após as peroxidases endógenas foram bloqueadas com H_2O_2 0,3% em metanol por 20 minutos. Os cortes foram bloqueados com albumina sérica bovina (BSA) 10% em PBS durante 30 minutos. Posteriormente, os cortes foram incubados durante 40 minutos com os anticorpos primários anti-NFκB p65 (1: 500 em PBS, Thermo-Life Tecnology, Massachusetts, EUA) ou anti-LC3B (0,5 µg/mL, Invitrogen, Carlsbad, EUA). Em seguida, foram incubados com anticorpo secundário FITC *anti-rabbit* (1:250, Thermo-Life Tecnology, Massachusetts, EUA) por 30 minutos. E finalmente, os cortes foram incubados com o corante de DNA Hoechst 33342 (1: 2000; Invitrogen, Carlsbad, EUA) por 4 minutos. As imagens foram realizadas em microscópio de fluorescência confocal (Zeiss LSM5, Oberkohen, Germany).

5.3.21 Análise de AKT total e LC3B por Western Blot no tecido pulmonar

O tecido pulmonar foi lisado em tampão de lise CHAPS (Tris-HCl 10 mM, pH 7,5, $MgCl_2$ 1 mM, ácido EDTA 1 mM, fluoreto de fenilmetilsulfonil (PMSF) 0,1 mM, β-mercaptoetanol 5 mM, CHAPS 0,5 %, glicerol 10 %). Em seguida, as amostras receberam vórtex a cada 10 minutos por 40 minutos e após foram centrifugadas por 1 hora a 4ºC e em 13000 rpm. O sobrenadante foi coletado e foi armazenado a -20ºC. As proteínas (20 µg) foram separadas por eletroforese em gel de poliacrilamida 10%. Em seguida as proteínas foram transferidas para uma membrana de nitrocelulose (GE Healthcare Life Sciences, Pensilvânia, EUA). A membrana foi bloqueada com BSA 5% em solução salina tamponada com Tris e Tween 20 a 0,05% por 30 minutos em temperatura ambiente. Após o bloqueio, a membrana foi incubada com os anticorpos primários anti-β-actina, anti-AKT total (1: 500 em BSA 5%, Cell signaling, Massachusetts, EUA) e anti-LC3B (1: 200 em BSA 5%, Thermo-Life Tecnology, Massachusetts, EUA) overnight a 4°C. Por fim, foi incubada com anticorpo secundário HRP *anti-rabbit* (1: 1000 em BSA 5%, Cell

signaling, Massachusetts, EUA). A intensidade das bandas foi normalizada pela proteína β-actina utilizando o programa Image J.[129]

5.3.22 Dosagem de proteínas

A mensuração da concentração de proteína no sobrenadante do tecido pulmonar foi realizada utilizando o Kit Qubit™ Protein Assay Kit (Invitrogen, Carlsbad, EUA) para citocinas. O método de Lowry e colaboradores foi utilizado para a mensuração das proteínas utilizadas nas técnicas de estresse oxidativo, metabolismo energético mitocondrial e Na^+,K^+-ATPase.[130] A técnica de Bradford foi utilizada para avaliar os níveis das proteínas utilizadas no Western Blot.[131]

5.3.23 Análise estatística

Os dados foram expressos através de média ± desvio padrão. O teste de *Shapiro-Wilk* foi utilizado para avaliar a normalidade dos dados. Utilizamos ANOVA de uma via seguida de pós-teste de Tukey e o nível de significância adotado foi de $p \leq 0,05$. A análise estatística e os gráficos foram realizados através do Software Graphpad Prism, versão 5 (GraphPad Software, San Diego, EUA).

6. CONCLUSÕES

Os resultados presentes nesta dissertação, de acordo com os artigos científicos, permitem concluir que:

6.1.1 Artigo científico 1

- ✓ A estimulação com o VSR *in vitro* teve a capacidade de aumentar a liberação de EETs do LBA de camundongos submetidos a um modelo experimental de asma;
- ✓ O aumento da estimulação da liberação de EETs induzida pelo VSR *in vitro* em eosinófilos do LBA não induz morte celular avaliada pelo Kit Anexina e PI;
- ✓ O VSR *in vitro* reduziu a produção de IFN-γ no sobrenadante da cultura de eosinófilos do LBA de camundongos submetidos a um modelo experimental de asma, mas não alterou os níveis de IL-4 e nem a atividade da enzima EPO.

6.1.2 Artigo Científico 2

- ✓ O tratamento com NAC reduziu a contagem total de células, o número absoluto de eosinófilos e linfócitos, diminuiu o infiltrado de células inflamatórias perivasculares e peribrônquicas do tecido pulmonar bem como reduziu a atividade da enzima EPO no LBA;
- ✓ Os tratamentos com DPI e NAC reduziram a hiperplasia de células caliciformes;
- ✓ Os tratamentos com DPI e NAC melhoraram parâmetros de mecânica ventilatória pulmonar;
- ✓ Os tratamentos com DPI e NAC diminuíram as citocinas IL-5, IFN-γ e IL-1β, bem como reduziram o imunoconteúdo da proteína NFκB p65 no pulmão;
- ✓ Os tratamentos com DPI e NAC reduziram a produção de EROs e somente o tratamento com NAC aumentou a atividade da enzima antioxidante CAT;
- ✓ O tratamento com NAC melhorou o metabolismo energético mitocondrial pelo aumento da atividade da SDH e do complexo IV no pulmão;

✓ Os tratamentos com DPI e NAC reduziram a liberação de EETs nas células do LBA de animais submetidos a um modelo experimental de asma, demonstrando que sua liberação é dependente de EROs;

✓ Os tratamentos com DPI e NAC não induziram morte celular em eosinófilos do LBA.

6.1.3 Artigo Científico 3

✓ O tratamento com 3-MA reduziu a contagem total de células, o número absoluto de eosinófilos e neutrófilos, bem como diminuiu o infiltrado de células inflamatórias perivasculares e peribrôquicas no tecido pulmonar bem como reduziu a atividade da enzima EPO no LBA;

✓ O tratamento com 3-MA reduziu hiperplasia de células caliciformes;

✓ O tratamento com 3-MA melhorou parâmetros de mecânica ventilatória pulmonar;

✓ O tratamento com 3-MA diminuiu os níveis das citocinas IL-5, IFN-γ e IL-13 no tecido pulmonar, bem como reduziu o imunoconteúdo da proteína NFκB p65;

✓ O tratamento com 3-MA promoveu uma redução na produção de EROs e aumentou a atividade da enzima antioxidante CAT;

✓ O tratamento com 3-MA melhorou o metabolismo energético mitocondrial pelo aumento da atividade da SDH e do complexo II no pulmão;

✓ O tratamento com 3-MA reduziu a liberação de EETs, demostrando que sua liberação é dependente de autofagia;

✓ O tratamento com 3-MA reduziu a presença de AVOs em eosinófilos do LBA, bem como reduziu o imunoconteúdo da proteína LC3B em eosinófilos do LBA e no tecido pulmonar;

✓ O tratamento com 3-MA aumentou o imunoconteúdo da proteína AKT no pulmão;

✓ O tratamento com 3-MA não induziram morte celular em eosinófilos do LBA.

6.2 Conclusão Geral

Demonstramos que o VSR *in vitro* estimulou a liberação de EETs no sobrenadante da cultura de eosinófilos do LBA de animais submetidos a um modelo experimental de asma com OVA, o que pode exacerbar as alterações clínicas e inflamatórias da doença. Além disso, podemos verificar que a inibição da formação de EROs com DPI e NAC, bem como a inibição da autofagia com 3-MA, promoveram uma redução da reposta inflamatória e do estresse oxidativo nas vias aéreas de animais asmáticos. Entretanto, somente os tratamentos com NAC e 3-MA foram capazes de melhorar alguns parâmetros do metabolismo energético mitocondrial no pulmão dos animais. Os tratamentos com o DPI, NAC e 3-MA foram capazes de reduzir a liberação de EETs no LBA de animais asmáticos. Por isso, acreditamos com nossos resultados que a exacerbação pelo VSR, bem como as EROs e a autofagia são mecanismos fundamentais na liberação das EETs na asma experimental, conforme demonstrado na Figura 7 que descreve nossas principais conclusões. Acreditamos que a identificação desses mecanismos possa contribuir para uma melhor compreensão da resposta imune nesta doença.

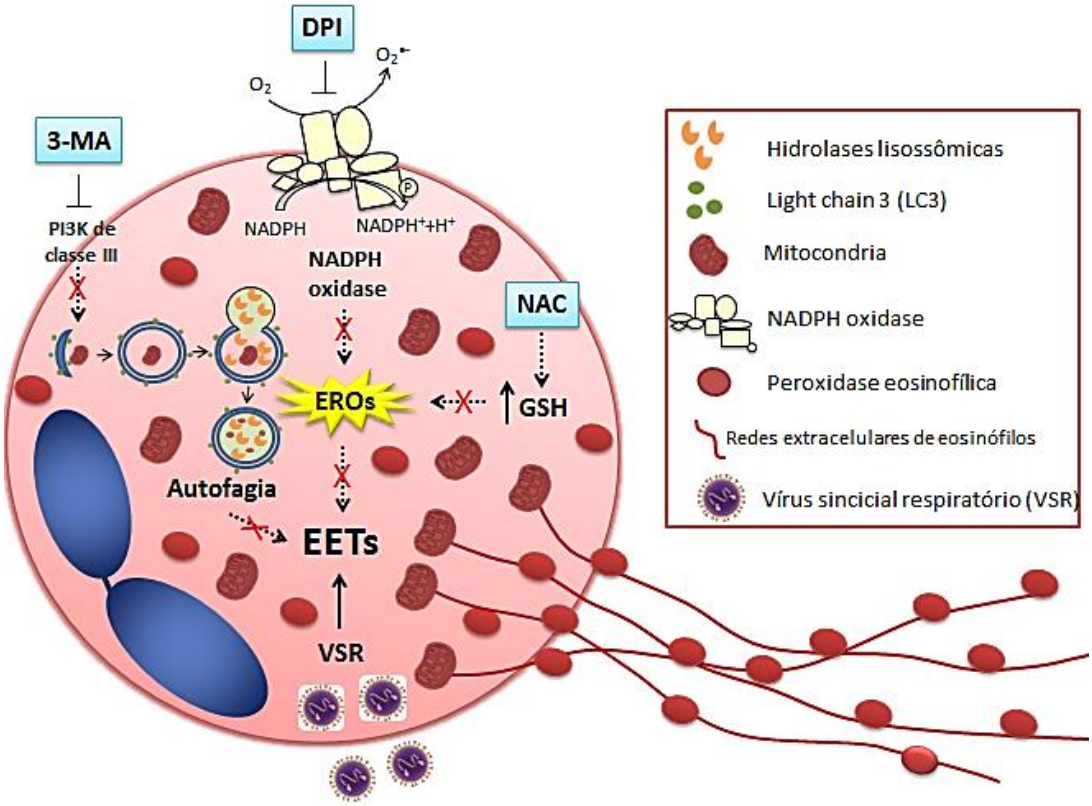

Figura 7: Resumo dos mecanismos de formação de redes extracelulares de eosinófilos na asma. DPI: difenileno-iodônio; EETs: redes extracelulares de eosinófilos, EROs: espécies reativas de oxigênio; GSH: glutationa; 3-MA: 3-metiladenina; NAC: N-acetilcisteína; NADPH: nicotinamida adenina dinucleotídeo fosfato oxidase; VSR: vírus sincicial respiratório.

REFERÊNCIAS

1. Global initiative for asthma. Global strategy for the asthma management and prevention. Global Initiative for Asthma, 2017.
   Disponível em: <http://ginasthma.org/2017-gina-reportglobal-strategy-for-asthma management-and-prevention/>. Acesso em 9 Ago. 2018.
2. Renauld JC. New insights into the role of cytokines in asthma. J Clin Pathol 2001;54(8):577-589.
3. Elias JA, Lee CG, Zheng T, Ma B, Homer RJ, Zhu Z. New insights into the pathogenesis of asthma. J Clin Invest 2003;111(3):291-297.
4. Comhair SA, Erzurum SC. Redox control of asthma: molecular mechanisms and therapeutic opportunities. Antioxid Redox Signal 2010;12(2):93-124.
5. Lambrecht BN, Persson EK, Hammad H. Myeloid Cells in Asthma. Microbiol Spectr 2017;5(1):MCHD-0053-2016.
6. Poon A, Eidelman D, Laprise C, Laprise C, Hamid Q. ATG5, autophagy and lung function in asthma. Autophagy 2012;8(4):694-695.
7. Dickinson JD, Alevy Y, Malvin NP, Patel KK, Gunsten SP, Holtzman MJ, et al. IL13 activates autophagy to regulate secretion in airway epithelial cells. Autophagy 2016;12(2):397-409.
8. Liu JN, Suh DH, Trinh HKT, Chwae YJ, Park HS, Shin YS. The role of autophagy in allergic inflammation: a new target for severe asthma. Exp Mol Med 2016; 48(7):e243.
9. Johnston SL, Pattemore PK, Sanderson G, Smith S, Lampe F, Josephs L, et al. Community study of role of viral infections in exacerbations of asthma in 9-11 year old children. BMJ 1995;310(6989):1225-1229.
10. Stein RT, Sherrill DL, Morgan, Wayne J, Holberg, Catherine J, et al. Respiratory Syncytial virus in early life and the subsequent risk of wheeze and allergy by age 13 years. The Lancet 1999;354(9178):541-545.
11. Hall CB. The burgeoning burden of respiratory syncytial virus among children. Infect Disord Drug Targets 2012;12(2):92-97.
12. Chang J, Srikiatkhachorn A, Braciale TJ. Visualization and characterization of respiratory syncytial virus F-specific CD8(+) T cells during experimental virus infection. J Immunol 2001;167(8):4254-4260.

13. Braciale TJ. Respiratory syncytial virus and t cells: interplay between the virus and the host adaptive immune system. Proc Am Thorac Soc 2005;2(2):141-146.
14. Fullmer JJ, Khan AM, Elidemir O, Chiappetta C, Stark JM, Colasurdo GN. Role of cysteinyl leukotrienes in airway inflammation and responsiveness following VSR infection in BALB/c mice. Pediatr Allergy Immunol 2005;16(7):593-601.
15. Yousefi S, Gold JA, Andina N, Lee JJ, KellyAM, Kozlowski E, Schmid I, Straumann A, Reichenbach J, Gleich GJ, Simon HU. Catapult-like release of mitochondrial DNA by eosinophils contributes to antibacterial defense. Nat Med 2008;14:949-53.
16. Morshed M, Yousefi S, Stöckle C, Simon HU, Simon D. Thymic stromal lymphopoietin stimulates the formation of eosinophil extracellular traps. Allergy 2012;67(9):1127-1137.
17. Muniz VS, Silva JC, Braga YAV, Melo RCN, Ueki S, Takeda M, et al. Eosinophils release extracellular DNA traps in response to Aspergillus fumigatus. J Allergy Clin Immunol 2017;141(2):571-585.
18. Ueki S, Melo RC, Ghiran I, Spencer LA, Dvorak AM, Weller PF. Eosinophil extracellular DNA trap cell death mediates lytic release of free secretion-competent eosinophil granules in humans. Blood 2013;121(11):2074-2083.
19. Simon D, Radonjic-Hösli S, Straumann A, Yousefi S, Simon HU. Active eosinophilic esophagitis is characterized by epithelial barrier defects and eosinophil extracellular trap formation. Allergy 2015;70(4):443-452.
20. Funchal GA, Natália J, Czepielewski RS, Machado MS, Stéfanie PM, Stein RT, et al. Respiratory Syncytial Virus Fusion Protein Promotes TLR-4-Dependent Neutrophil Extracellular Trap Formation by Human Neutrophils. PLoS One 2015;10(4):e0124082.
21. Cortjens B, de Jong R, Bonsing JG, van Woensel JBM, Antonis AFG, Bem RA. Local dornase alfa treatment reduces NETs-induced airway obstruction during severe RSV infection. Thorax 2018;73(6):578-580.
22. Dworski R, Simon HU, Hoskins A, Yousefi S. Eosinophil and neutrophil extracellular DNA traps in human allergic asthmatic airways. J Allergy Clin Immunol 2011;127(5):1260-1266.

23. Cunha AA, Porto BN, Nuñez NK, Souza RG, Vargas MH, Silveira JS, et al. Extracellular DNA traps in bronchoalveolar fluid from a murine eosinophilic pulmonary response. Allergy 2014;69(12):1696-1700.
24. Remijsen Q, Vanden BT, Wirawan E, Asselbergh B, Parthoens E, De Rycke R, et al. Neutrophil extracellular trap cell death requires both autophagy and superoxide generation. Cell Res 2011;21(2):290-304.
25. Cunha AA, Nuñez NK, Souza RG, Moraes Vargas MH, Silveira JS, Antunes GL, et al. Recombinant human deoxyribonuclease therapy improves airway resistance and reduces DNA extracellular traps in a murine acute asthma model. Exp Lung Res 2016;42(2):66-74.
26. Eder W, Ege MJ, von Mutius E. The asthma epidemic. N Engl J Med 2006;355(21):2226-35.
27. Solé D, Wandalsen GF, Camelo-Nunes IC, Naspitz CK; ISAAC - Grupo Brasileiro. Prevalence of symptoms of asthma, rhinitis, and atopic eczema among Brazilian children and adolescents identified by the International Study of Asthma and Allergies in Childhood (ISAAC) - Phase 3. J Pediatr 2006;82(5):341-346.
28. Solé D, Camelo-Nunes I, Wandalsen G, Pastorino AC, Jacob CM, Gonzalez C, et al. Prevalence of symptoms of asthma, rhinitis, and atopic eczema in Brazilian adolescents related to exposure to gaseous air pollutants and socioeconomic status. J Investig Allergol Clin Immunol 2007;17(1):6-13.
29. Sociedade Brasileira de Pneumologia e Tisiologia. Diretrizes Brasileiras para o Manejo da Asma. J Bras Pneumol 2012;38 (Suplemento 1):S1-S46.
30. Roncada C, de Oliveira SG, Cidade SF, Sarria EE, Mattiello R, Ojeda BS, et al. Burden of asthma among inner-city children from Southern Brazil. J Asthma 2016;53(5):498-504.
31. Sociedade Brasileira de Pneumologia e Tisiologia. IV Diretrizes Brasileiras para o Manejo da Asma. J Bras Pneumol 2006;32(Suplemento 7):S447-S474.
32. Lötvall J, Akdis CA, Bacharier LB, Bjermer L, Casale TB, Custovic A. Asthma endotypes: a new approach to classification of disease entities within the asthma syndrome. J Allergy Clin Immunol 2011;127(2):355-360.

33. Holt PG & Sly, PD. Prevention of allergic respiratory disease in infants: current aspects and future perspectives. Curr Opin Allergy Clin Immunol 2007;7(6):547-555.
34. Hamid Q, Tulic MK, Liu MC, Moqbel R. Inflammatory cells in asthma: mechanisms and implications for therapy. J Allergy Clin Immunol 2003 Jan;111(1 Suppl):S5-S12.
35. Moqbel RLP, Adamko DJ, Odemuyiwa SO. Biology of Eosinophils. Adv Immunol 2009;101:81-121.
36. McBrien CN, Menzies-Gow A. The Biology of Eosinophils and Their Role in Asthma. Front Med 2017;4:93.
37. Barnes PJ. The cytokine network in asthma and chronic obstructive pulmonary disease. J Clin Invest 2008;118(11):3546-3556.
38. Maneechotesuwan K, Xin Y, Ito K, Jazrawi E, Lee KY, Usmani OS, et al. Regulation of Th2 cytokine genes by p38 MAPK-mediated phosphorylation of GATA-3. J Immunol 2007;178(4):2491-2498.
39. Aujla SJ, Alcorn JF. T(H)17 cells in asthma and inflammation. Biochimica et biophysica acta 2011;1810(11):1066-79.
40. Vroman H, Blink VD, Kool M. Mode of dendritic cell activation: The decisive hand in Th2/Th17 cell differentiation. Implications in asthma severity?. J Immunol 2015;220(2):254-261.
41. Holgate ST. Innate and adaptive immune responses in asthma. Nat Med 2012;18(5):673-683.
42. Li BWS, Hendriks RW. Group 2 innate lymphoid cells in lung inflammation. J Immunol 2013;140(3):281-287.
43. Wenzel SE. Asthma phenotypes: the evolution from clinical to molecular approaches. Nat Med 2012;18(5):716-25.
44. Carroll KN, Wu P, Gebretsadik T, Griffin MR, Dupont WD, Mitchel EF, et al. The severity-dependent relationship of infant bronchiolitis on the risk and morbidity of early childhood asthma. J Allergy Clin Immunol 2009;123(5):1055-1061.
45. Nair H, Nokes DJ, Gessner BD, Dherani M, Madhi SA, Singleton RJ, et al. Global burden of acute lower respiratory infections due to respiratory syncytial

virus in young children: a systematic review and meta-analysis. Lancet 2010;375(9725):1545-1555.

46. Hacking D, Hull J. Respiratory syncytial virus-viral biology and the host response. J Infect 2002;45(1):18-24.
47. Harris J, Werling D. Binding and entry of respiratory syncytial virus into host cells and initiation of the innate immune response. Cell Microbiol 2003;5(10):671-680.
48. Kurt-Jones EA, Popova L, Kwinn L, Haynes LM, Jones LP, Tripp RA, et al. Pattern recognition receptors TLR4 and CD14 mediate response to respiratory syncytial virus. Nat Immunol 2000;1(5):398-401.
49. Tourdot S, Mathie S, Hussel T, Edwards L, Wang H, Openshaw PJM, et al. Respiratory syncytial virus infection provokes airway remodelling in allergen-exposed mice in absence of prior allergen sensitization. Clin Exp Allergy 2008;38:1016-24.
50. Janssen R, Pennings J, Hodemaekers H, Buisman A, van Oosten M, de Rond L, et al. Host transcription profiles upon primary respiratory syncytial virus infection. J Virol 2007;81(11):5958-5967.
51. Bueno SM, González PA, Pacheco R, Leiva ED, Cautivo KM, Tobar HE, et al. Host immunity during VSR pathogenesis. Int Immunopharmacol 2008;8(10):1320-1329.
52. Varga SM, Wang X, Welsh RM, Braciale TJ. Immunopathology in VSR infection is mediated by a discrete oligoclonal subset of antigen-specific CD4(+) T cells. Immunity 2001;15(4):637-646.
53. Bermejo-Martin JF, Garcia-Arevalo MC, De Lejarazu RO, Ardura J, Eiros JM, Alonso A, et al. Predominance of Th2 cytokines, CXC chemokines and innate immunity mediators at the mucosal level during severe respiratory syncytial virus infection in children. Eur Cytokine Netw 2007;18(3):162-167.
54. Martinez FD, Stern DA, Wright AL, Taussig LM, Halonen M. Differential immune responses to acute lower respiratory illness in early life and subsequent development of persistent wheezing and asthma. J Allergy Clin Immunol 1998;102(6 Pt 1):915-920.

55. Macaubas C, de Klerk NH, Holt BJ, Wee C, Kendall G, Firth M, et al. Association between antenatal cytokine production and the development of atopy and asthma at age 6 years. Lancet 2003;362(9391):1192-1197.
56. Bartz H, Buning-Pfaue F, Turkel O, Schauer U. Respiratory syncytial virus induces prostaglandin E2, IL-10 and IL-11 generation in antigen presenting cells. Clin Exp Immunol 2002;129(3):438-445.
57. Birben E, Sahiner UM, Sackesen C, Erzurum S, Kalayci O. Oxidative stress and antioxidant defense. World Allergy Organ J 2012;5(1):9-19.
58. Valko M, Rhodes CJ, Moncol J, Izakovic M, Mazur M. Free radicals, metals and antioxidants in oxidative stress-induced cancer. Chem Biol Interact 2006;160(1):1-40.
59. Halliwell B, Gutteridge JMC. Free Radicals in Biology and Medicine, 4rd ed. Oxford: Oxford University Press;2007.p.79-185.
60. Mokhtari V, Afsharian P, Shahhoseini M, Kalantar SM, Moioni A. A Review on Various Uses of N-Acetyl Cysteine. Cell J 2017;19(19):11-17.
61. Andreadis AA, Hazen SL, Comhair SA, Erzurum SC. Oxidative and nitrosative events in asthma. Free Radic Biol Med 2003;35(3):213-225.
62. Dozor AJ. The role of oxidative stress in the pathogenesis and treatment of asthma. Ann N Y Acad Sci 2010;1203:133-137.
63. Caramori G, Papi A. Oxidants and Asthma. BMG 2004;(59):170-173.
64. Henricks PA, Nijkamp FP. Reactive oxygen species as mediators in asthma. Pulm Pharmacol Ther 2001;14(6):409-420.
65. Henderson LM, Chappel JB. NADPH oxidase of neutrophils. Biochim Biophys Acta 1996; 1273(2):87-107.
66. O'donnell VB, Tew DG, Jones OT, England PJ. Studies on the inhibitory mechanism of iodonium compounds with special reference to neutrophil NADPH oxidase. Biochem J 1993;290(Pt 1):41-49.
67. Millar AH, Whelan J, Soole KL, Day DA. Organization and regulation of mitochondrial respiration in plants. Annual Review of Plant Biology 2011;62: 79-104.
68. Zmijewski JW, Lorne E, Zhao X, Tsuruta Y, Sha Y, Liu G, et al. Mitochondrial respiratory complex I regulates neutrophil activation and severity of lung injury. Am J Respir Crit Care Med 2008;178(2):168-179.

69. Zmijewski JW, Lorne E, Banerjee S, Abraham E. Participation of mitochondrial respiratory complex III in neutrophil activation and lung injury. Am J Physiol Lung Cell Mol Physiol 2009;296:624-634.
70. Aguilera-Aguirre L, Bacsi A, Saavedra-Molina A, Kurosky A, Sur S, Boldogh I. Mitochondrial dysfunction increases allergic airway inflammation. J Immunol 2009;183(8):5379-5387.
71. Cunha MJ, Cunha AA, Scherer EB, Machado FR, Loureiro SO, Jaenisch RB, et al. Experimental lung injury promotes alterations in energy metabolism and respiratory mechanics in the lungs of rats: prevention by exercise. Molecular Cell Biochemical 2014;389:(1-2)229-238.
72. Mabalirajan U, Dinda AK, Kumar S, Roshan R, Gupta P, Sharma SK, et al. Mitochondrial structural changes and dysfunction are associated with experimental allergic asthma. J Immunol 2008;181(5):3540-3548.
73. Schmitz F, Pierozan P, Rodrigues AF, Biasibetti H, Grings M, Zanotto B, et al. Methylphenidate decreases ATP levels and impairs glutamate uptake and Na+, K+-ATPase activity in juvenile rat hippocampus. Mol Neurobiol 2016;54(10):7796-7807.
74. Agrawal A, Agrawal KP, Ram A, Sondhi A, Chhabra SK, Gangal SV, et al. Basis of Rise in Intracellular Sodium in Airway Hyperresponsiveness and Asthma. Lung 2005;183(6):375-387.
75. Chideckel EW, Frost JL, Mike P, Fedan JS. The effect of ouabain on tension in isolated respiratory tract smooth muscle of humans and other species. Br J Pharmacol 1987;92:609-614.
76. Yoshimori T, Noda T. Toward unraveling membrane biogenesis in mammalian autophagy. Curr Opin Cell Biol 2008;20(4):401-407.
77. Dunn WA. Autophagy and related mechanisms of lysosome-mediated protein degradation. Trends Cell Bio 1994;4(4):139-143.
78. Liou W, Geuze HJ, Geelen MJ et al. The autophagic and endocytic pathways converge at the nascent autophagic vacuoles. J Cell Biol 1997;136(1):61-70.
79. Jing K, Lim K. Why is autophagy important in human diseases? Exp Mol Med 2012;44(2):69-72.
80. Bhattacharya A, Eissa NT. Autophagy and autoimmunity crosstalks. Front Immunol 2013;4:88.

81. Mihalache CC, Simon HU. Autophagy regulation in macrophages and neutrophils. Exp Cell Res 2012;318(11):1187-1192.
82. Paludan C, Schmid D, Landthaler M, Vockerodt M, Kube D, Tuschl T, et al. Endogenous MHC class II processing of a viral nuclear antigen after autophagy. Science 2005;307(5709):593-596.
83. Munz C. Enhancing immunity through autophagy. Annu Rev Immunol 2009; 27:423-449.
84. Ryter SW, Choi AMK. Autophagy in the Lung. Proc Am Thorac Soc 2010;7(1):13-21.
85. Murphy MP. How mitochondria produce reactive oxygen species. Biochem J 2009; 417(Pt 1):1-13.
86. Scherz-Shouval R, Elazar Z. ROS, mitochondria and the regulation of autophagy. Trends Cell Biol 2007;17(9):422-427.
87. Ban GY, Pham DL, Trinh TH, Lee SI, Suh DH, Yang EM, et al. Autophagy mechanisms in sputum and peripheral blood cells of patients with severe asthma: a new therapeutic target. Clin Exp Allergy 2016;46(1):48-59.
88. Takei H, Araki A, Watanabe H, Ichinose A, Sendo F, et al. Rapid killing of human neutrophils by the potent activator phorbol 12-myristate 13-acetate (PMA) accompanied by changes different from typical apoptosis or necrosis. J Leukoc Biol 1996;59(2):229-240.
89. Brinkman V, Reichard U, Goosmann C, Fauler B, Uhlemann Y, Weiss DS, et al. Neutrophil extracellular traps kill bacteria. Science 2004;303(5663):1532-1535.
90. Pilsczek FH, Salina D, Poon KKH, Fahey C, Yipp BG, Sibley CD, et al. A novel mechanism of rapid nuclear neutrophil extracellular trap formation in response to Staphylococcus aureus. J Immunol 2010;185(12):7413-7425.
91. Yipp BG, Petri B, Salina D, Jenne CN, Scott BN, Zbytnuik LD, et al. Infection-induced NETosis is a dynamic process involving neutrophil multi-tasking in vivo. Nat Med 2012; 18(9):1386-1393.
92. Ermert D, Urban CF, Laube B, Goosmann C, Zychlinsky A, Brinkmann V. Mouse neutrophil extracellular traps in microbial infections. J Innate Immun 2009;1(3):181-193.

93. Villanueva E, Yalavarthi S, Berthier CC, Hodgin JB, Khandpur R, Lin AM, et al. Netting neutrophils induce endothelial damage, infiltrate tissues, and expose immunostimulatory molecules in systemic lupus erythematosus. J Immunol 2011;187(1)538-552.
94. Saffarzadeh M, Juenemann C, Queisser MA, Lochnit G, Barreto G, Galuska SP, et al. Neutrophil extracellular traps directly induce epithelial and endothelial cell death: a pre-dominant role of histones. PLoS One 2012;7(2):e32366.
95. Manzenreiter R, Kienberger F, Marcos V, Schilcher K, Krautgartner WD, Obermayer A, et al. Ultrastructural characterization of cystic fibrosis sputum using atomic force and scanning electron microscopy. J Cyst Fibros 2012;11(2):84-92.
96. Pedrazza L, Cunha AA, Luft C, Nunes NK, Schimitz F, Gassen RB, et al. Mesenchymal stem cells improves survival in LPS-induced acute lung injury acting through inhibition of NETs formation. J Cell Physiol 2017;232(12):3552-3564.
97. Douda DN, Jackson R, Grasemann H, Palaniyar N. Innate immune collectin surfactant protein D simultaneously binds both neutrophil extracellular traps and carbohydrate ligands and promotes bacterial trapping. J Immunol 2011;187(4):1856-1865.
98. Bruns S, Kniemeyer O, Hasenberg M, Kniemeyer O, Aimanianda V, Nietzsche S,et al. Production of extracellular traps against Aspergillus fumigatus in vitro and in infected lung tissue is dependent on invading neutrophils and influenced by hydrophobin RodA. PLoS Pathog 2010;29;6(4):e1000873.
99. Narasaraju T, Yang E, Samy RP, Ng HH, Poh WP, Liew AA, et al. Excessive neutrophils and neutrophil extracellular traps contribute to acute lung injury of influenza pneumonitis. Am J Pathol 2011;179(1):199-210.
100. Wright TK, Gibson PG, Simpson JL, McDonald VM, Wood LG, Baines KJ. Neutrophil extracellular traps are associated with inflammation in chronic airway disease. Respirology 2016;21(3):467-475.
101. Hellenbrand KM, Forsythe KM, Rivera-Rivas JJ, Czuprynski CJ, Aulik NA, et al. Histophilus somni causes extracellular trap formation by bovine neutrophils and macrophages. Microb Pathog 2013;(54):67-75.

102. Lin AM, Rubin CJ, Khandpur R, Wang JY, Riblett MB, Yalavarthi S, et al. Mast Cells and Neutrophils Release IL-17 through Extracellular Trap Formation in Psoriasis. J Immunol 2011;187(1)490-500.
103. Yousefi S, Morshed M, Amini P, Stojkov D1, Simon D, von Gunten S, et al. Basophils exhibit antibacterial activity through extracellular trap formation. Allergy 2015;70(9):1184-1188.
104. Miyata T, Fan X. A second hit for TMA. Blood 2012; Blood 2012;120(6):1152-1154.
105. Ueki S, Konno Y, Takeda M, Moritoki Y, Hirokawa M, Matsuwaki Y, et al. Eosinophil extracellular trap cell death-derived DNA traps: Their presence in secretions and functional attributes. J Allergy Clin Immunol 2015;137(1):258-267.
106. Hatano Y, Taniuchi S, Masuda M, Tsuji S, Ito T, Hasui M, et al. Phagocytosis of heat-killed Staphylococcus aureus by eosinophils: comparison with neutrophils. APMIS 2009;117(2):115-123.
107. Ueki S, Tokunaga T, Fujieda S, Honda K, Hirokawa M, Spencer LA, et al. Eosinophil ETosis and DNA Traps: a New Look at Eosinophilic Inflammation. Curr Allergy Asthma Rep 2016;16(8):54.
108. Rosenberg HF, Phipps S, Foster PS. Eosinophils trafficking in allergy and asthma. J Allergy Clin Immunol 2007;119(6):1303-1310.
109. Fuchs TA, Abed U, Goosmann C, Hurwitz R, Schulze I, Wahn V, et al. Novel cell death program leads to neutrophil extracellular traps. J Cell Biol 2007;176(2): 231-241.
110. Bianchi M, Hakkim A, Brinkmann V, Siler U, Seger RA, Zychlinsky A, et al. Restoration of NET formation by gene therapy in CGD controls aspergillosis. Blood 2009;114(13):2619-2622.
111. Choi Y, Pham DL, Lee DH, Lee SH,1 Kim SH, Park HS. Biological function of eosinophil extracellular traps in patients with severe eosinophilic asthma. Exp Mol Med 2018;50(8):104.
112. Kenno S, Perito S, Mosci P, Vecchiarelli A, Monari C. Autophagy and Reactive Oxygen Species Are Involved in Neutrophil Extracellular Traps Release Induced by C. albicans Morphotypes. Front Microbiol 2016;8(7):879-893.

113. Maugeri N, Campana L, Gavina M, Covino C, De Metrio M, Panciroli C, et al. Activated platelets present high mobility group box 1 to neutrophils, inducing autophagy and promoting the extrusion of neutrophil extracellular traps. J Thromb Haemost 2014;12(12):2074-2088.
114. Mitroulis I, Kambas K, Chrysanthopoulou A, Skendros P, Apostolidou E, Kourtzelis I, et al. Neutrophil extracellular trap formation is associated with IL-1b and autophagy-related signaling in gout. PLoS One 2011;6(12):e29318.
115. Boone BA, Orlichenko L, Schapiro NE, Loughran P, Gianfrate GC, Ellis JT, et al. The receptor for advanced glycation end products (RAGE) enhances autophagy and neutrophil extracellular traps in pancreatic cancer. Cancer Gene Ther 2015;22(6):326-334.
116. Pham DL, Ban GY, Kim SH, Shin YS, Ye YM, Chwae YJ, et al. Neutrophil autophagy and extracellular DNA traps contribute to airway inflammation in severe asthma. Clin Exp Allergy 2016;47(1):57-70.
117. Strath M, Warren DJ, Sanderson CJ. Detection of eosinophils using an eosinophil peroxidase assay. Its use as an assay for eosinophil differentiation factors. J Immunol Methods 1985;83: 209-15.
118. Hantos Z, Daróczy B, Suki B, Nagy S, Fredberg JJ. Input impedance and peripheral inhomogeneity of dog lungs. J Appl Physiol 1992;72(1):168-178.
119. Zosky GR, Janosi TZ, Adamicza A, Bozanich EM, Cannizzaro V, Larcombe AN, et al. The bimodal quasi-static and dynamic elastance of the murine lung. J Appl Physiol 2008;105(2):685-692.
120. LeBel CP, Ali SF, M McKee. Evaluation of the probe 2’7’-dichlorofluorescin as an indicator of reactive oxygen species formation and oxidative stress. Toxicol Appl Pharmacol 1990;104(2):17-24.
121. Wendel A. Glutathione peroxidase. Method Enzymol 1981; 77:325-333.
122. Marklund SL. Pyrogallol autoxidation. In: Greenwald RA, Handbook for oxygen radical research. CRC Press, Boca Raton;1985.p243-247.
123. Aebi H. Catalase in vitro. Methods Enzymol 1984;105:121-126.
124. Fischer JC, Ruitenbeek W, Berden JA, Trijbels JMF, Veerkamp JH, Stadhouders, et al. Differential investigation of the capacity of succinate oxidation in human skeletal muscle. Clin Chim Acta 1985;153:23-36.

125. Rustin P, Chretien D, Bourgeron T, Gérard B, Rötig A, Saudubray JM, et al. Biochemical and molecular investigations in respiratory chain deficiencies. Clin Chim Acta 1994;228:35-51.
126. Wyse ATS, Streck EL, Barros SV, Brusque AM, Zugno AI, Wajner M. Methylmalonate administration decreases Na^{+},K^{+}-ATPase activity in cerebral cortex of rats. Neuro report 2000;11:2331-2334.
127. CHAN, K.M., DELFER, D. and JUNGER, K.D.. A direct colorimetric assay for Ca_2^{+}-stimulated ATPase activity. Anal. Biochem. v. 157,(1986) p.375-380.
128. Anderson RGW, Falck JR, Goldstein J, Brown MS. Visualization of acidic organelles in intact cells by electron microscopy. Proc Natl Acad Sci USA 1984;81(15):4838-4842.
129. Rueden, C. T., Schindelin, J., Hiner M. C., DeZonia, B. E., Walter, A. E. Arena, E. T., & Eliceiri, K. W. (2017). ImageJ2: ImageJ for the next generation of scientific image data. BMC Bioinformatics, 18, 529.
130. Lowry OH, Rosebrough NJ, Farr AL, Randall RJ. Protein measurement with the Folin phenol reagent. J Biol Chem 1951;193:265-75.
131. Bradford MM (1976) A rapid and sensitive method for the quantitation of microgram quantities of protein utilizing the principle of protein-dye binding. Anal Biochem 72:248-254.

ANEXO

Anexo A: Carta de aprovação do projeto pela Comissão de ética no uso de animais (CEUA)

SIPESQ

Sistema de Pesquisas da PUCRS

Código SIPESQ: 7910 Porto Alegre,22 de agosto de 2017

Prezado(a) Pesquisador(a),

A Comissão de Ética no Uso de Animais da PUCRS apreciou e aprovou o Projeto de Pesquisa "Envolvimento das espécies reativas de oxigênio e da autofagia na formação das redes extracelulares de eosinófilos na asma e na exacerbação da asma pelo vírus sincicial respiratório" coordenado por PAULO MARCIO CONDESSA PITREZ.

Sua investigação, respeitando com detalhe as descrições contidas no projeto e formulários avaliados pela CEUA, está autorizada a partir da presente data.

Informamos que é necessário o encaminhamento de relatório final quando finalizar esta investigação. Adicionalmente, ressaltamos que conforme previsto na Lei no. 11.794, de 08 de outubro de 2008 (Lei Arouca), que regulamenta os procedimentos para o uso científico de animais, é função da CEUA zelar pelo cumprimento dos procedimentos informados, realizando inspeções periódicas nos locais de pesquisa.

Duração do Projeto: 22/08/2017 - 22/02/2019

Nº de Animais	Espécie
120	Camundongo
Total de Animais: 120	

Atenciosamente,

Comissão de Ética no Uso de Animais(CEUA)

APÊNDICES

Apêndice A: Submissão do artigo científico 1

Revista: Asia Pacific Allergy

Fator de impacto: 1.366

Asia Pacific allergy

New submission (Complete submission)

Thank you for submitting your manuscript.

All manuscripts will first be reviewed to ensure compliance with the manuscript submission guidelines.
will receive the registration number or return notice via email.

For any questions, please contact editorial staff at

Asia Pacific allergy
The official journal of the Asia Pacific Association of Allergy, Asthma and Clinical Immunology

TEL : +82-2-3410-3787
FAX : +82-2-3410-0043
E-mail : editor.apallergy@gmail.com
Website : http://submit.apallergy.org/

Confirm

Educational & Teaching Material

Respiratory syncytial virus increases eosinophil extracellular traps in a murine model of asthma

Running Title: RSV induces eosinophil extracellular traps

Josiane Silva Silveira[1], Géssica Luana Antunes[1], Rodrigo Benedetti Gassen[2], Ricardo Vaz Breda[3], Renato Tetelbom Stein[1], Paulo Márcio Pitrez[4], Aline Andrea da Cunha[1*]

[1] Laboratory of Pediatric Respirology - Infant Center, Pontifical Catholic University of Rio Grande do Sul (PUCRS), Porto Alegre, Rio Grande do Sul, Brazil

[2] Laboratory of Cellular and Molecular Immunology, Pontifical Catholic University of Rio Grande do Sul (PUCRS), Porto Alegre, Rio Grande do Sul, Brazil

[3] Laboratory of Neuroscience - Brain Institute, Pontifical Catholic University of Rio Grande do Sul (PUCRS), Porto Alegre, Rio Grande do Sul, Brazil

[4] Infant Center, Pontifical Catholic University of Rio Grande do Sul (PUCRS), Institutional Research Coordinator, Hospital Moinhos de Vento, Porto Alegre, Rio Grande do Sul, Brazil

Correspondent author: Aline Andrea da Cunha, PhD, Laboratory of Pediatric Respirology, Infant Centre - PUCRS, 6690 Ipiranga Ave., 2nd floor, Room 13, Zip Code: 90610-000 - Porto Alegre, RS, Brazil. Tel: +55 51 3320-3015, Fax: +55 51 3320-3040, e-mail: alineacunha@hotmail.com

Word count: Main 1000 words and abstract 230 words

Tables and figures: Two figures

ABSTRACT

Backgroud: Respiratory viral infections are the leading cause of asthma exacerbations. Eosinophil activation results in the formation of eosinophil extracellular traps (EETs), which release web-like structures of DNA and proteins that bind, disarm and extracellularly kill pathogens.

Objective: We investigated whether the respiratory syncytial virus (RSV) *in vitro* could induce EETs in bronchoalveolar lavage fluid (BALF) eosinophils in a murine model of asthma.

Methods: BALB/cJ mice (6-8 weeks old) were sensitized with two subcutaneous injections of ovalbumin (20 µg) on days 0 and 7, followed by three intranasal challenges with OVA (100 µg) on days 14, 15 and 16 of the protocol. The control group received Dulbecco's phosphate-buffered saline (DPBS). BALF eosinophils of OVA group and control group were stimulated with RSV (10^3 PFU/mL) *in vitro* for 3 hours. After that, culture supernatant was collected in order to perform the analyses proposed in this study.

Results: We verified an increase in extracellular DNA concentration in BALF eosinophils from ovalbumin (OVA) group stimulated with RSV (10^3 PFU/mL) *in vitro*, which was confirmed by confocal microscopy. In addition, we demonstrated that most cells are negative for annexin-V and propidium iodide in all groups evaluated. In addition, RSV *in vitro* decreased IFN-ɣ in BALF cells when compared to the OVA group.

Conclusions: In this study, we demonstrated for the first time that RSV *in vitro* induces EETs formation in eosinophils from asthmatic mice.

Keywords: eosinophil extracellular traps; asthma; respiratory syncytial virus

INTRODUCTION

During episodes of asthma exacerbation, respiratory viral infection can be detected in nearly 80-85% of school-age children [1]. Respiratory syncytial virus (RSV) is a main cause of bronchiolitis in children and may increase susceptibility to the development asthma [2].

Eosinophil activation results in the eosinophil extracellular traps (EETs) formation which are capable of killing bacteria in the extracellular space [3]. In this context, our group described that EETs are released in bronchoalveolar lavage fluid (BALF) and lung tissue of asthmatic mice [4, 5]. Currently, there are no available data in the literature regarding the production of EETs induced by RSV. Therefore, we investigated whether RSV *in vitro* induces EETs in BALF cells in a murine model of asthma.

MATERIALS AND METHODS

Sensibilization and challenge

BALB/cJ mice were sensitized with two subcutaneous injections of ovalbumin (20 µg) (OVA - Grade V, Sigma, USA) on days 0 and 7, followed by intranasal challenges with OVA (100 µg) on days 14, 15 and 16 of the protocol [5]. The control group received only Dulbecco's phosphate-buffered saline (DPBS).

Virus culture and eosinophils stimulation

The production of RSV A2 strain (kindly donated by Dr. Fernando Polack Vanderbilt University School of Medicine, USA) was obtained in VERO cells with 2% FBS at 37°C under 5% CO_2. BALF cells (2 x 10^5/mL) were stimulated with RSV (10^3 PFU/mL) for 3 hours at 37°C under 5% CO_2 while others remained unstimulated. The mentioned RSV concentration was used because higher concentrations (10^4 - 10^6 PFU/mL) were cytotoxic to eosinophils.

Quantification of extracellular DNA traps

Extracellular DNA traps were quantified in BALF cells supernatants stimulated with RSV (10^3 PFU/mL) or unstimulated using Quant-iT ds DNA HS (Invitrogen, Carlsbad, USA).

Visualization of EETs by fluorescence microscopy

BALF cells (2 x 10^5/mL) were stimulated with phorbol-12-myristate-13-acetate (PMA) (50 nM). After that, cells stimulated with RSV (10^3 PFU/mL) and unstimulated ones were incubated for 3 hours, fixed with 4% paraformaldehyde (PFA) and stained with anti-EPO and anti-histone H2B. Later, both groups of cells were incubated with FITC and Alexa fluor 633 and stained with Hoechst 33342. Confocal images were taken in a Leica TCS-SP8 exciter microscope (Leica Microsystem, Wetzlar, Germany).

Determination of cell death

Cell death in BALF was analyzed by annexin-V and propidium iodide (PI) (BD Pharmingen).

Cytokine levels

IL-4 and IFN-ɣ levels were measured by the multiplex technique (MAGPIX® TECHNOLOGY, MILLIPLEX® MAP, USA).

Peroxidase eosinophil (EPO) activity

EPO activity was measured in BALF and was determined through colorimetric assay [6].

Statistical analysis

Data were expressed as mean ± SD. Results were analyzed using GraphPad Prism Software, version 5. One-way ANOVA was used, followed by the Tukey *post hoc* test, and $P \leq 0.05$ was considered statistically significant.

Ethics

This study was approved by the Animal Ethics Committee (CEUA) of our Institution (Protocol number: 14/00387).

RESULTS

Firstly, we investigated whether RSV in a concentration-dependent manner (10^3 - 10^6 PFU/mL) would induce the release of EETs in BALF eosinophils of asthmatic mice. RSV was able to stimulate EETs only in RSV 10^3 PFU/mL concentration (Figure 1A). Thus, we decided to stimulate BALF eosinophils from asthmatic mice with RSV 1 x 10^3 PFU/mL.

Eosinophils from BALF-asthmatic mice stimulated with RSV increased extracellular DNA in the culture supernatant when compared to the OVA group (Figure 1B). In confocal microscopy, we observed multiple extracellular DNA extrusions in eosinophils colocalized with EPO but not colocalized with histone H2B in BALF cells in the OVA group stimulated with RSV (Figure 1C). EETs release with RSV stimulation were not due to apoptosis showing that most cells were negative for Annexin-V and PI (Figure 1D).

Finally, we showed (Figure 2A) that in culture supernatant from BALF cells stimulated with RSV from asthmatic mice there was no alteration in IL-4 levels. On the other hand, we showed a decrease in IFN-ɣ levels when compared to the OVA group (Figure 2B). In BALF cells from the OVA group there was an increase in EPO activity but we could not see any alteration in this parameter when stimulated with RSV *in vitro* (Figure 2C).

DISCUSSION

EETs are web-like networks of expelled DNA covered with microbicidal and cytotoxic proteins [3] which are able to efficiently kill bacteria through DNA traps and may also contribute to lung dysfunction. The first evidence of EETs formation in asthma was in endobronchial biopsies from human atopic asthmatic patients [7]. Moreover, studies have demonstrated that viruses such as the RSV are capable of inducing neutrophil extracellular traps (NETs) formation [8]. Therefore, we

demonstrated for the first time that RSV *in vitro* can induce EETs colocalized with EPO in BALF cells from asthmatic mice.

Moreover, in previous studies of our group, we demonstrated that BALF cells produced EETs without showing sign of apoptosis [4, 5]. We showed that RSV stimulation *in vitro* did not induce cell death. Furthermore, we demonstrated that EETs were not colocalized with histone H2B, which suggests that DNA released by EETs is of mitochondrial origin.

RSV infection enhances T helper type 2 (Th2) cytokine in lung tissue [9]. IL-4 levels were elevated in the OVA group when compared to the control group while that RSV stimulation *in vitro* did not alter IL-4 levels in BALF cells in asthmatic mice. Moreover, RSV *in vitro* reduces IFN-ɣ levels, a T helper type 1 (Th1) cytokine when compared to the OVA group. Aberle and colleagues (1999) showed that severe RSV bronchiolitis is associated with decreased mRNA IFN-ɣ expression in peripheral blood [10]. Sanz and colleagues (1997) showed that EPO serum levels are significantly higher in asthmatic patients than in healthy controls [11]. In addition, EPO activity in BALF cells was elevated in the OVA group when compared to the control group, but the RSV stimulation *in vitro* did not alter this parameter. Taken together our results showed, for the first time, that RSV *in vitro* increases EETs release in BALF cells from asthmatic mice, which probably contributes to airway obstruction and tissue damage in asthma.

FINANCIAL SUPPORT

This study was financed in part by the Coordenação de Aperfeiçoamento de Pessoal de Nivel Superior (CAPES) and Conselho Nacional de Desenvolvimento Científico e Tecnológico (CNPq), Brazil.

CONFLICTS OF INTEREST

The authors declare no conflicts of interest.

AUTHOR CONTRIBUTIONS

JJS, GLA, RBG, RVB, PMP, and AAC designed the research. JJS and GLA performed the research. JJS, GLA, RBG and RVB analyzed the data. JJS, PMP and

AAC wrote the manuscript, and all authors commented on the manuscript and approved the final version.

REFERENCES

1. Jackson DJ, Sykes A, Mallia P, Johnston SL. Asthma exacerbations: origin, effect, and prevention. J Allergy Clin Immunol 2011;128:1165-74.
2. Psarras S, Papadopoulos NG, Johnston SL. Pathogenesis of respiratory syncytial virus bronchiolitis-related wheezing. Paediatr Respir Rev 2004;5:S179-S184.
3. Yousefi S, Gold JA, Andina N, Lee JJ, KellyAM, Kozlowski E, Schmid I, Straumann A, Reichenbach J, Gleich GJ, Simon HU. Catapult-like release of mitochondrial DNA by eosinophils contributes to antibacterial defense. Nat Med 2008;14:949-53.
4. Cunha AA, Porto BN, Nuñez NK, Souza RG, Vargas MHM, Silveira JS, Souza TT, Jaeger N, Pitrez PM. Extracellular DNA traps in bronchoalveolar fluid from a murine eosinophilic pulmonary response. Allergy 2014;69:1696-00.
5. Cunha AA, Nuñez NK, Souza RG, Vargas HMV, Silveira JS, Antunes GL,Durante LS, Porto BN, Marczak ES, Jones MH, Pitrez PM. Recombinant human deoxyribonuclease therapy improves airway resistance and reduces DNA extracellular traps in a murine acute asthma model. Exp Lung Res 2016;42:66-74.
6. Strath M, Warren DJ, Sanderson CJ. Detection of eosinophils using an eosinophil peroxidase assay. Its use as an assay for eosinophil differentiation factors. J Immunol Methods 1985;83: 209-15.
7. Dworski R, Simon HU, Hoskins A, Yousefi S. Eosinophil and neutrophil extracellular DNA traps in human allergic asthmatic airways. J Allergy Clin Immunol 2011;127:1260-66.
8. Funchal GA, Jaeger N, Czepielewski RS, Machado MS, Muraro SP, Stein RT, Bonorino CBC, Porto BN. Respiratory syncytial virus fusion protein promotes TLR-4–dependent neutrophil extracellular trap formation by human neutrophils. PLoS One 2015;10:1-14.
9. Tourdot S, Mathie S, Hussel T, Edwards L, Wang H, Openshaw PJM, Schwarze J, Lloyd CM. Respiratory syncytial virus infection provokes airway

remodelling in allergen-exposed mice in absence of prior allergen sensitization. Clin Exp Allergy 2008;38:1016-24.

10. Aberle JH, Aberle SW, Dworzak MN, Mandl CW, Rebhandl W, Vollnhofer G, Kundi M, Popow-Kraupp T. Reduced interferon-g expression in peripheral blood mononuclear cells of infants with severe respiratory syncytial virus disease. Am J Respir Crit Care Med 1999;160:1263-68.
11. Sanz ML, Parra A, Prieto I, Diéguez I, Oehling AK. Serum eosinophil peroxidase (EPO) levels in asthmatic patients. Allergy 1997;52:417-22.

LEGEND TO THE FIGURE

Figure 1. RSV *in vitro* induces EETs colocalized with EPO in BALF cells from asthmatic mice**.** (A) Effect of different concentrations of RSV (10^3-10^6 PFU/mL) *in vitro* in extracellular DNA concentration. (B) Extracellular DNA concentration in BALF cells from asthmatic and control mice stimulated with RSV (10^3 PFU/mL) *in vitro* or unstimulated. (C) EETs release in BALF cells from asthmatic and control mice stimulated with RSV (10^3 PFU/mL) *in vitro* or unstimulated (630x magnification, arrows indicate EETs formation). (D) Analysis of Annexin-V binding and PI uptake in BALF cells from all groups. Results are expressed as mean ± SD, for 7-10 animals in each group, of three independent experiments,*P < 0.05; **P < 0.01; ***P < 0.001. DPBS: dulbecco's phosphate-buffered saline; EPO: eosinophil peroxidase; OVA: ovalbumin; PFU: plaque-forming unit; RSV: Respiratory syncytial virus.

Figure 2. Effect of RSV in BALF cells from asthmatic mice in cytokines levels and eosinophil peroxidase (EPO) activity. (A) IL-4, (B) IFN-ɣ and (C) EPO activity in from BALF cells ($2x10^5$/mL) from asthmatic mice stimulated with RSV (10^3 PFU/mL) *in vitro* or unstimulated. Results are expressed as mean ± SD, for 5 animals in each group, of three independent experiments, **P < 0.01. EPO: eosinophil peroxidase; DPBS: dulbecco's phosphate-buffered saline; IFN-ɣ: interferon- ɣ; IL-4: interleukin-4; OVA: ovalbumin; RSV: Respiratory syncytial virus.

FIGURE 1

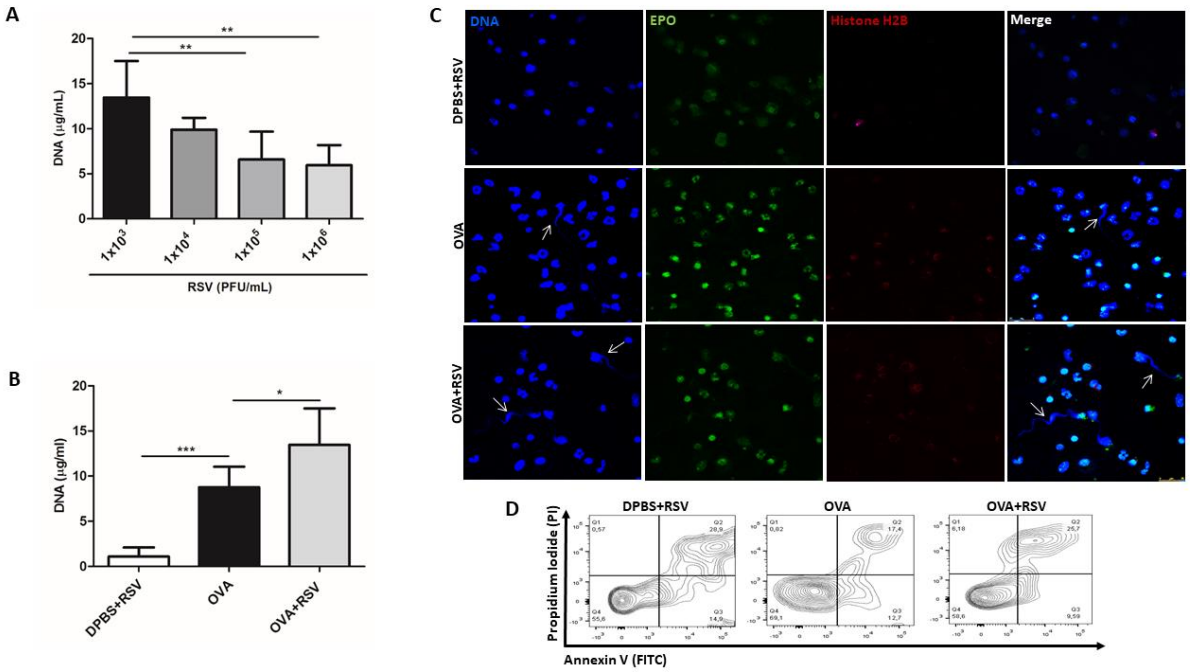

FIGURE 2

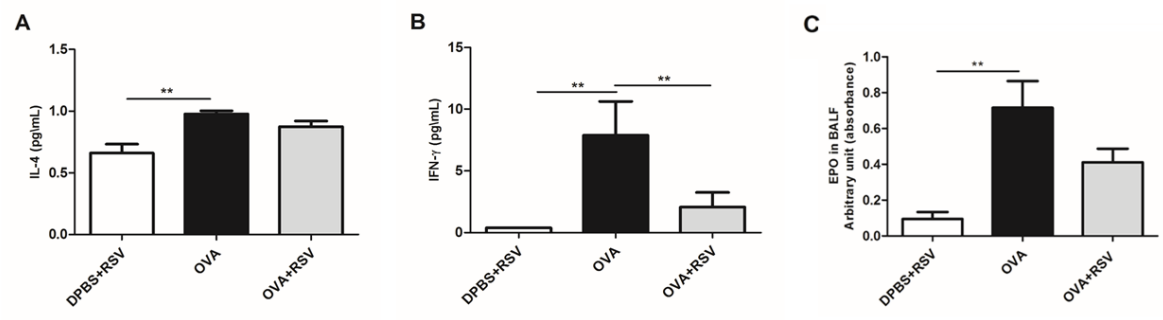

Apêndice B: Submissão do artigo científico 2

Revista: Allergy

Fator de impacto: 6,0 (Medicina II: A1)

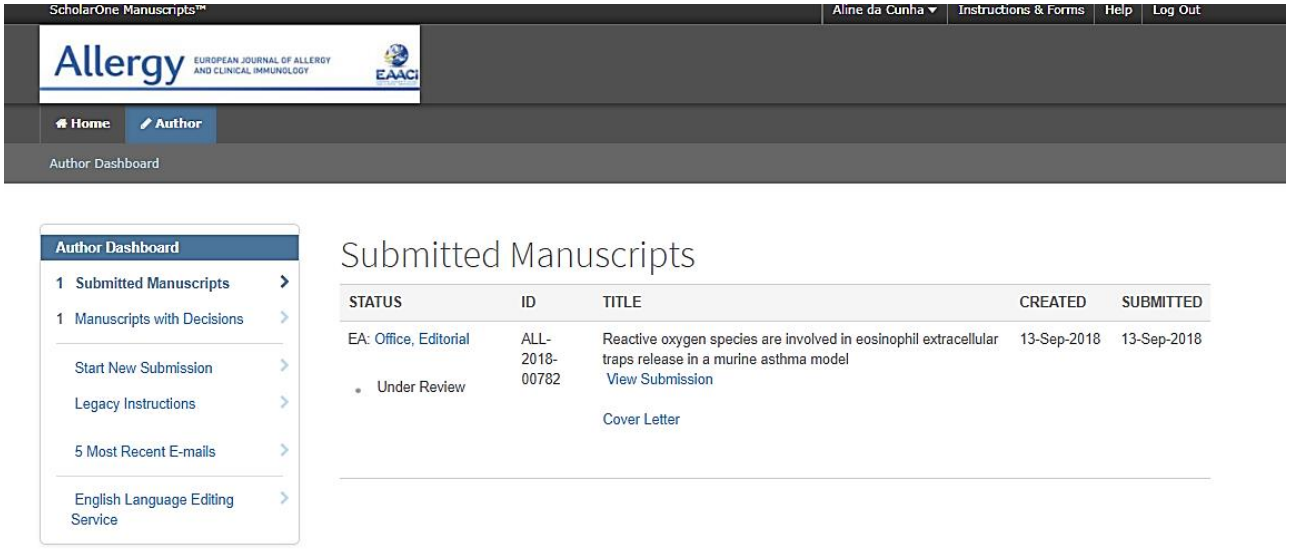

Reactive oxygen species are involved in eosinophil extracellular traps release in a murine asthma model

Short title: ROS-dependent EETs formation in an asthma model

J.S. Silveira[1] | G.L. Antunes[1] | D.B. Kaiber[1] | M. Severo[1] | E.P. Marques[2] | F. Ferreira[2] | R.B. Gassen[3] | R.V. Breda[4] | A.T. Wyse[2] | R.T.Stein[1] | P.M. Pitrez[1] | A.A. Cunha[1]

[1]Laboratory of Pediatric Respirology, Infant Center, Medicine School, Pontifícia Universidade Católica do Rio Grande do Sul (PUCRS), Porto Alegre, Brazil

[2]Laboratory of Neuroprotection and Neurometabolic Disease, Department of Biochemistry, Universidade Federal do Rio Grande do Sul, Porto Alegre, Brazil

[3]Laboratory of Cellular and Molecular Immunology, Science School, Pontifícia Universidade Católica do Rio Grande do Sul (PUCRS), Porto Alegre, Brazil

[4]Institute of the Brain (INSCER), Medicine School, Pontifícia Universidade Católica do Rio Grande do Sul (PUCRS), Porto Alegre, RS, Brazil

Address correspondence and reprint requests to Aline Andrea da Cunha, Laboratory of Pediatric Respirology, Infant Center - PUCRS, 6690 Ipiranga Ave., 2nd floor, Room 13, Zip Code: 90610-000 - Porto Alegre, RS, Brazil, e-mail: aline.cunha@pucrs.br.

Word count: 3441

Abstract

Background: Asthma is a complex disease characterized by secretion of elevated levels of cytokines, reactive oxygen species (ROS), lipid mediators and eosinophil extracellular traps (EETs) in airway. However, the mechanism of EETs formation and its pathophysiologic role in asthma are poorly understood. The aim of this study is to investigate the ROS involvement in EETs formation and airway inflammation in an experimental asthma model.

Methods: Mice were sensitized with ovalbumin (OVA), followed by OVA challenge. Before the challenge with OVA, mice were treated with ROS inhibitors, N-acetylcysteine (NAC) and diphenyleneiodonium (DPI). Bronchoalveolar lavage fluid (BALF) and lung tissue were obtained on day 17 in order to measure several inflammation markers and EETs formation.

Results: We showed that in NAC-treated OVA group there was a decrease in the inflammatory cells in lung tissue. DPI and NAC treatments reduced EPO activity, goblet cells hyperplasia, inflammatory cytokines, NFκB p65 immunocontent and oxidative stress in lung. However, only NAC treatment improved mitochondrial energy metabolism. We observed that BALF eosinophils from asthmatic mice released EETs colocalized with EPO, but not colocalized with histone H2B. Furthermore, the treatment with DPI and NAC reduced EETs formation in BALF. Thus, we were able to show that ROS are involved in EETs release in an experimental asthma model.

Conclusions: This is the first study to demonstrate that ROS is required for EETs formation in airway in asthma. In addition, NAC and DPI treatment can be an interesting alternative for reducing airway inflammation, mitochondrial damage and EETs release in asthma.

KEYWORDS

eosinophil extracellular traps, experimental asthma, inflammation, reactive oxygen species

1 | INTRODUCTION

Asthma is a chronic inflammatory disease that is highly prevalent with high morbidity and mortality worldwide. Also, asthma is a complex disease characterized by secretion in the lung of elevated levels of immunoglobulin E (IgE), proinflammatory cytokines and increased levels of reactive oxygen species (ROS) causing airway hyperresponsiveness (AHR), mucus overproduction, airway wall remodeling and airway narrowing.[1-3] In asthmatic patients and in the asthma model in mice, eosinophils are recruited to the airway in order to generate ROS such as hydrogen peroxide (H_2O_2), superoxide ($O_2^{\bullet-}$) and hydroxyl radical (HO^-) which may cause airway damage.[3-5] Under physiological conditions, ROS are maintained in balance with appropriate production of protective antioxidant mechanisms, including superoxide dismutase (SOD), catalase (CAT) and glutathione peroxidase (GPx). Furthermore, the exposure of cells to ROS can result in oxidative damage to mitochondria and to inactivate the electron transport chain causing the significant increase in ROS production.[6,7]

Extracellular DNA traps released by leukocytes have been described as an important mechanism of the innate immune response in infectious and noninfectious diseases, including allergic diseases.[8-10] Stimulated eosinophils rapidly release extracellular DNA fibers, decorated with intact eosinophil granules forming eosinophil extracellular traps (EETs), that trapping and killing various microorganisms.[8] Moreover, EETs contain granule proteins with antimicrobial activity such as eosinophil peroxidase (EPO), major basic protein (MBP) and eosinophil cationic protein (ECP).[8-10] In 2011, Dworski *et al.* provided the first evidence that EETs and NETs are present in the airways of allergic asthmatics patients.[11] Besides that, Cunha *et al.* demonstrated that in a murine asthma model, there was a significant increase in EETs formation in bronchoalveolar lavage fluid (BALF).[12] EETs can be pathogenic when they are produced in excess.[4,13] Nevertheless, the persistence of EETs can be proinflammatory, but their role in immune responses in respiratory disease is unclear.

ROS participation in extracellular DNA traps formation depends on stimulus. Many studies have reported that ROS production is essential for extracellular DNA traps formation; *other studies have shown* that they can also be *formed* independently of ROS.[9,10,14] However, the mechanism of EETs formation

and the pathophysiologic function in allergic asthma are poorly understood. Therefore, the aim of this study is to investigate the effect of a precursor of glutathione, N-acetylcysteine (NAC), and an inhibitor of nicotinamide adenine dinucleotide phosphate-oxidase (NADPH oxidase), diphenyleneiodonium (DPI), in the EETs formation and in the airway inflammation in an experimental asthma model.

2 | MATERIALS AND METHODS

Further details can be found in Methods S1.

2.1 | Animals

Female BALB/cJ mice were used for all experiments. All studies were conducted with approval of the Pontifícia Universidade Católica do Rio Grande do Sul Animal Ethics Committee (7910).

2.2 | Sensitization and challenge

Mice were sensitized with subcutaneous injections of 20 μg of ovalbumin (OVA), on days 0 and 7 of protocol. Followed three intranasal challenges with 100 μg of OVA on days 14, 15 and 16.[4] Control group received subcutaneous and intranasal only with DPBS (Figure 1A).

2.3 | Treatment protocol

In this study in order to investigate ROS participation in EETs release and asthma physiopathology, we utilized two ROS inhibitors, NAC and DPI. Besides NAC being an antioxidant thiol and a glutathione precursor, it is a mucolytic and anti-inflammatory drug. In contrast, DPI is a NADPH oxidase inhibitor which reduces $O2^{\bullet-}$ production. Mice were treated intranasally with DPI 1 mg/Kg or NAC 15 mg/100 g of body weight 45 minutes before the three intranasal OVA administrations (Figure 1A).

2.4 | Total and differential cells count from BALF

Twenty-four hours after the last challenge intranasal, BALF was collected. Total cells count and cells viability was realized, and differential cells count slides were stained with H&E.

2.5 | Analysis of the EPO activity enzyme in BALF

EPO activity was measured by the colorimetric assay based on the oxidation of O-phenylenediamine (OPD) in the presence of H_2O_2.[15]

2.6 | Lung histopathologic analysis

In order to evaluate inflammatory infiltrate and morphometric analysis, lung sections were stained with H&E. For evaluation of goblet cell hyperplasia and mucus-production, lung sections were stained with alcian blue.

2.7 | Assessment of lung function

Animals were anesthetized, the trachea was cannulated and the animal was connected to the ventilator (flexiVent). Four-parameter model with constant phase tissue impedance was fitted to the Zrs data to obtain Resistance (Rn), tissue damping (G) and H (tissue elastance).[16]

2.8 | Cytokine levels in lung

Interleukin (IL)-5, IL-13, interferon (IFN)-γ, IL1-β, tumor necrosis factor (TNF)-α and IL-10 levels in lung were measured by multiplex assay using magnetic beads according to the manufacturer's recommendations.

2.9 | Analysis of NFκB p65 by immunofluorescence in lung

For immunofluorescence analyses, formalin-fixed lungs sections were incubated with primary antibody, anti-NFκB p65 (1:500), followed for secondary antibody, FITC anti-rabbit (1:250) and Hoechst 33342 (1:2000).

2.10 | ROS assay in lung

ROS production in lung was analyzed by technique based on the oxidation of the 2'7' dichlorofluorescein (H2DCF) described by Lebel et al.[17]

2.11 | SOD assay in lung

SOD activity in lung was based in the technique of self-oxidizing ability of pyrogallol, a highly $O_2^{\bullet-}$dependent process, which is a substrate for SOD.[18]

2.12 | CAT assay in lung

CAT activity in the lung was based on the measurement of the decrease in the H_2O_2 consumption.[19]

2.13 | GPx activity in lung

GPx activity was analyzed in lung according to Wendel and tert-butylhydroperoxide was utilized as substrate.[20]

2.14 | Complex II, succinate dehydrogenase (SDH) and complex IV activity in lung

The enzymatic activity of complex II in lung was measured after to decrease the absorbance by reduction of 2, 6-dichloroindophenol (DCIP). The enzymatic activity of SDH was measured after reduction of the absorbance by reduction of the DCIP in the presence of phenazine methasulfate.[21] The enzymatic activity of complex IV in the lung was measured by decrease in absorbance due to oxidation of reduced cytochrome.[22]

2.15 | NA^+, K^+-ATPase activity in lung

In NA^+, K^+-ATPase in lung was determined by decreasing the absorbance by cytochrome oxidation and reduction.[23]

2.16 | Quantification and immunofluorescence microscopy confocal of EETs in BALF eosinophils

Extracellular DNA traps were quantified in BALF supernatant using the Quant-iT dsDNA HS kit, according to the manufacturer's recommendations. To visualize the EETs formation, eosinophils obtained in BALF ($2x10^5$/mL) were plated and incubated with primary antibodies, anti-EPO and anti-histone H2B (1: 250) followed by secondary antibodies, FITC anti-goat (1:100) and alexa fluor 633 anti-goat (1: 100) and stained with Hoechst 33342 DNA.

2.17 | Electron microscopy of BALF eosinophils

BALF eosinophils (2 x 10^5/mL) were placed and fixed with 2.5% glutaraldehyde. Followed for post-fixation with osmium tetroxide 2% and dehydration in graded acetone. The critical point technique with CO_2 was performed and the samples were covered with a thin layer of gold (metallization).

2.18 | Analysis of cell death in BALF eosinophils

BALF eosinophils were analyzed for apoptosis by Annexin V and necrosis by propidium iodide (PI), according to the manufacturer's instructions and analyzed by flow cytometry.

2.19 | Statistical analysis

Data are expressed as mean ± standard deviation. We used one-way ANOVA followed by Tukey pos-hoc and the significance level adopted was $p \leq 0.05$. Statistical analysis and graphs were performed using the GraphPad Prism Software, version 5 (GraphPad Software, San Diego, USA).

3 | RESULTS

3.1 | NAC reduces inflammatory cells in airway while NAC and DPI decrease EPO activity and goblet cells hyperplasia

We observed that OVA group had a significant increase in the total cells count, as well as an increase in eosinophils, neutrophils, macrophages and lymphocytes cells count compared to the control group. After that, we showed that the NAC-treated OVA decreased total cells count as well as eosinophils and lymphocytes cells count in BALF compared to the OVA group. On the other hand, the DPI-treated OVA group did not have an alteration in BALF inflammation (Figure 1C-H). In EPO granular protein analysis, we demonstrated that OVA significantly increased EPO activity while NAC and DPI significantly decreased EPO in BALF (Figure 1B). Histopathological examination showed an increase in inflammatory cells located in the peribronchial and perivascular areas in OVA-challenge mice, and NAC-treated OVA group had a decrease in the pulmonary influx of cells (Figure 1I-K). On the other hand, DPI treatment did not change the influx of cells for the airway (Figure 1I-K). We demonstrated that OVA-challenge mice had an increase in goblet cells and

mucus production compared to the control group while NAC and DPI reduced goblet cells hyperplasia and mucus production compared to the OVA group (Figure 1L).

3.2 | NAC and DPI improve lung function

Tissue damping and tissue elastance were significantly increased in the OVA-challenged mice compared to the DPBS group. DPI-treated OVA group we showed significantly decreased in tissue damping and tissue elastance when compared to the OVA group. In addition, NAC-treated OVA we showed significantly decreased only in tissue elastance. On the other hand, we did not observe differences between the groups in airway resistance (Figure 2A-C).

3.3 | NAC and DPI decrease inflammatory cytokines and NFκB p65 immunocontent in lung

In cytokines analyses in lung, we showed that OVA challenge mice increased IL-5, IL-13, IFN-Y, TNF-α and IL-1β when compared to the control group. Other on the hand, NAC and DPI treatment reduced IL-5, IFN-γ and IL-1β. Meanwhile, only DPI reduced TNF-α. We did not observe differences between the groups in IL-10 concentration (Figure 2D-I). Moreover, we observe that OVA challenge mice increased NFκB p65 immunocontent while that NAC and DPI treatments decreased NFκB p65 immunocontent in lung tissue (Figure 2J).

3.4 | NAC and DPI decrease ROS production while that only NAC improves antioxidant defenses in lung

We demonstrate that OVA significantly increased the levels of ROS in lung when compared to the control group. In addition, we showed that NAC and DPI decreased ROS production in lung when compared to the OVA group (Figure 3A). We observed significant decrease in CAT and GPx activity in the OVA group compared to the control group (Figure 3C,D). We verified that only NAC treatment significantly increases in the CAT activity compared to the OVA group (Figure 3C). In addition, we did not observe any significant difference in SOD activity between the groups (Figure 3B). We also showed that OVA group significantly increases SOD/CAT ratio when compared to the control group. On the other hand, we verified that only NAC decreased significantly SOD/CAT compared to the OVA group (Figure 3E).

3.5 | NAC improves energy metabolism in lung

We observed that OVA group significantly decreases complex II, SDH and complex IV activity when compared to the control group (Figure 3F-H). In addition, we demonstrated that only NAC-treated OVA group increased SDH and complex IV activities in lung when compared to the OVA group (Figure 3F,H). In NA^+, K^+-ATPase analysis, we showed that OVA group significantly decrease NA^+, K^+-ATPase activity when compared with the control group. On the other hand, DPI and NAC were not effective in restoring the levels of this enzyme (Figure 3I).

3.6 | EETs release depends on ROS production in an active process without cell death

OVA-challenged mice had an increase in extracellular DNA concentration in BALF when compared to the DPBS group (Figure 4C). In immunofluorescence microscopy confocal, we observed that eosinophils from asthmatic mice released EETs colocalized with EPO, but not colocalized with histone H2B (Figure 4A). After that, we investigated whether ROS would be necessary for EETs formation in the airway in OVA-challenged mice. NAC and DPI treatments decreased extracellular DNA concentrations in the BALF from OVA-challenged mice compared to the OVA group (Figure 4C). In confocal immunofluorescence microscopy and electron microscopy analyses, NAC and DPI abrogated OVA-induced EETs formation (Figure 4A,B). In addition, EETs release was not due to apoptosis or necrosis as shown in BALF since cell viability remained high between the groups, showing that most cells present negative staining for annexin-V and PI (Figure 4D).

4 | DISCUSSION

Infiltration of eosinophils to lungs is one of the hallmark characteristics of asthma and play an important role in the development of allergic airway inflammation. In lungs, eosinophils can produce ROS, cytokines, chemokines, lipid mediators, cytotoxic granules and EETs.[3,4] This study provides the first evidence that ROS is required for EETs formation in airway in a murine model of asthma. Moreover, we showed that ROS inhibition improves airway inflammation, lung function, oxidative stress, and reduces EETs release in an asthma model.

Evidences have shown that oxidative stress plays an important role in the pathogenesis of asthma, associated with damage to biological molecules, inflammation increase and AHR.[24] We showed that in the OVA group there was a significant increase in inflammatory cells with a high influx of eosinophils in airway as well as an increase in goblet cells hyperplasia, a typical pathological feature of asthma. In NAC-treated OVA mice, we observed a decrease in inflammatory cells mainly in eosinophils number as well as a reduction in goblet cells hyperplasia. On the other hand, we demonstrated that the treatment with DPI did not inhibit airway inflammation, but DPI decreased goblet cells hyperplasia. In this study, we showed that OVA-challenged mice increased eosinophil migration into airway and only NAC decreased lung eosinophilia. So, we decided to evaluate EPO activity in BALF, which is a granular protein of the eosinophils. We observed that OVA increased EPO release in airway while that DPI and NAC decreased significantly EPO activity. In according to our result, studies showed that ROS plays a crucial role in the release of granular proteins from eosinophils.[25,26] Later, in lung function evaluation, we demonstrated an increase in tissue damping and tissue elastance in OVA-challenged mice. Other on the hand, we did not observe differences between the groups in airway resistance. In agreement to our result, Mori and colleagues (2017) also demonstrated that for resistance, there are not significant differences between an acute asthma model and control group.[27] Moreover, NAC and DPI improved lung function in the OVA-induced asthma model and that occurred probably because a decrease in mucus viscosity and inflammation airway. Asthma is characterized by secretion of elevated levels of inflammatory mediators such as proinflammatory cytokines.[28] In OVA-group we observed an increase of IL-5, IL-13, IFN-γ, TNF-α and IL-1β levels in lung tissue, contributing to airway inflammation and AHR, mucus hypersecretion and airway remodeling. On the other hand, DPI and NAC decreased IL-5, IFN-γ and IL-1β levels in lung without modifying the concentration of IL-10. In this context, we hypothesized that ROS inhibition could reduce inflammatory cytokines in lung via NFκB p65 inhibition. In active NFκB, subunits p65 and p50 translocate to the nucleus and increase production of inflammatory cytokines but can also regulate ROS production.[29] We observe that OVA challenge mice increased NFκB p65 immunocontent while that DPI and NAC significantly decreased NFκB p65 in lung when compared to the OVA-group, demonstrating that ROS inhibition

modulates NFκB p65 activity. In this context, NAC is a precursor of glutathione and studies have shown that glutathione repletion suppresses transcription factors such as NFκB, which are involved in allergic airway inflammation and AHR.[30] Furthermore, NAC is a thiol that breaks mucus, by substituting sulfhydryl groups by disulfide bonds, reducing mucus viscosity and improving lung function.[31] In addition, DPI is a NADPH oxidase inhibitor which is an enzyme responsible for ROS production. Furthermore, proinflammatory stimuli induce ROS via activation of NADPH oxidase, and consequently, increase activation of NFκB.[32]

It is well known that oxidative stress involved in the pathogenesis of asthma.[5] We showed that DPI and NAC decrease ROS production in lung analyzed by the technique based on the oxidation of H2DCF. Furthermore, OVA-group had significant decrease in CAT and GPx and did not alter SOD in lung, suggesting disbalance in oxidant-antioxidant status. SOD enzyme catalyzes the dismutation of $O2^{\bullet-}$, and CAT and GPx catalyze the reduction of H_2O_2.[33] In this context, we suggest that increase in ROS formation did not increase the consumption of the SOD that catalyzes the dismutation of $O_2^{\bullet-}$ in H_2O_2. Thus, normal levels of SOD increase H_2O_2 formation while insufficient levels of CAT and GPx enhance H_2O_2 accumulation, increasing oxidative stress in lung. Moreover, we verified that only NAC increased CAT activity in lung. NAC is a scavenger of ROS and consequently decreased the consumption of CAT, reducing H_2O_2 accumulation in OVA-challenged mice and decreased oxidative stress in lung. NAC is metabolically converted to glutathione precursors that is essential for the antioxidant defenses and it may be used as a therapeutic alternative.[34] On the other hand, DPI inhibits NADPH oxidase and consequently decreases $O^{2\bullet-}$ formation. NADPH oxidase catalyzes the production of $O^{2\bullet-}$ by the one-electron reduction of oxygen, using NADPH as a reducing agent.[35]

Studies have shown an association between mitochondrial dysfunction and pulmonary inflammatory diseases.[36] Furthermore, cells exposition to ROS can inactivate the mitochondrial electron transport chain and consequently decrease ATP production and increase ROS formation.[6,7] In addition, the high flux of electrons through the mitochondrial electron transport chain predisposes $O^{2\bullet-}$generation. The most important sources of mitochondrial $O^{2\bullet-}$ generation are complex I, complex II and complex III.[37] In this study, we showed that in OVA-challenged mice ROS production increased and, consequently, decreased SDH, complex II and complex

IV. Moreover, we demonstrated that only NAC-treated OVA group there was an increase of SDH and complex IV activities which significantly improved mitochondrial energy metabolism in lung. In this context, NAC protects mitochondrial function by promoting cysteine donation and maintaining glutathione levels. Furthermore, glutathione is a critical component which prevents or repairs oxidative damage generated during aerobic metabolism.[38]

Na^+, K^+-ATPase activity controls cellular ionic gradient and its activity is susceptible to an increase in ROS formation and to ATP depletion.[39] In consequence to damage of the electron transport chain and oxidative stress, we observed that the OVA group had significant decrease in the NA^+,K^+-ATPase activity while DPI and NAC treatments did not alter this enzyme. Consequences of reduction in Na^+,K^+-ATPase activity include alteration of electrical membrane potential, increased activation of leukocytes, downregulation of responses to β-agonists in β-adrenergic receptors and bronchoconstriction.[40-42]

EETs formation is related to various pathologies, including allergic diseases.[11] In this context, studies have shown that EETs are present in the airways of allergic asthmatic patients and in a murine asthma model.[11,12] We showed in confocal immunofluorescence microscopy analysis that BALF eosinophils from asthmatic mice released EETs colocalized with EPO. Increase in EETs production in asthma may contribute to airway obstruction by increasing the viscosity of mucus and it, consequently, may damage lung function in asthma. Moreover, studies have shown that ROS production is essential for EETs release.[8,9] We showed that NAC and DPI treatments reduce EETs formation in BALF eosinophils in a murine model of asthma. Thus, our result demonstrate that ROS is required for EETs release in airway in an experimental asthma model. Scavenger NAC is a glutathione precursor and decreased ROS formation in lung and consequently, it decreased EETs formation. In contrast, DPI inhibits NADPH oxidase and decreases ROS formation and consequently, it abrogated EETs formation suggesting that NADPH oxidase is required to EETs formation. In contrast with our results, Muniz and colleagues (2017) demonstrated that EETs release, after *Aspergillus fumigatus* fungus stimulation, is ROS independent.[10]

In EETs formation it is not clear whether DNA is of mitochondrial or nuclear origin. In this study, we demonstrated that EETs were not colocalized with histone

HB2, which suggests that the DNA released by EETs is of mitochondrial origin. Histones compact and protect nuclear DNA, in contrast, in mitochondrial DNA there are no histones.[43] In this context, Yousefi and colleagues (2008), by using Polymerase Chain Reaction (PCR), showed that EETs contained sequences of mitochondrial DNA.[8] Furthermore, in 2004, Brinkmann and colleagues showed that NETs formation is a process that involves cell death.[44] Subsequent studies have shown that DNA extracellular traps are not formed by cell death or lysis.[8,9] We observed that EETs release was not due to apoptosis or necrosis in BALF since cell viability remained high in all groups, showing a negative staining for annexin-V and PI. In agreement to our result, previous studies of our group demonstrated that EETs release in asthma model was not due to apoptosis or necrosis either.[4,12] Thus, to summarize our results, Figure 5 shows the effects of DPI and NAC in EETs formation in OVA-challenged mice.

In conclusion, this is the first study to demonstrate that viable eosinophils release EETs dependent of ROS in airway of a murine model of asthma. DPI and NAC treatments improved airway inflammation, lung function, oxidative stress, and energy metabolism, and also reduced EETs formation in lung from asthmatic mice. Therefore, a decrease in ROS production due to DPI or NAC treatments reduces EETs release in BALF, showing that ROS regulate the activation process of eosinophils extracellular DNA traps release in asthma.

ACKNOWLEDGEMENTS

We thank Carolina Luft, Rodrigo Godinho de Souza, Krist Helen Antunes Fernandes e Betânia Souza Freitas for your technical assistance. This work was supported by grant from the Conselho Nacional de Desenvolvimento Científico e Tecnológico (CNPq).

CONFLICTS OF INTEREST

The authors declare no commercial or financial conflict of interest.

AUTHOR CONTRIBUTIONS

JSS and AAC designed the studies. JSS, AAC, GLA, DBK, MS, EPM, FF, RBG and RVB contributed to the data collection. JSS, AAC, PMP and ATW analysed and

interpreted the work. JSS and AAC wrote the manuscript. All authors have read, revised and approved the final version of this manuscript.

SUPPORTING INFORMATION

Additional Supporting Information may be found in the online version of this article: **Methods S1.** Materials and methods.

REFERENCES

1. Renauld JC. New insights into the role of cytokines in asthma. J Clin Pathol 2001;**54**:577-589.
2. Elias JA, Lee CG, Zheng T, Ma B, Homer RJ, Zhu Z. New insights into the pathogenesis of asthma. J Clin Invest 2003;**111**:291-297.
3. Comhair SA, Erzurum SC. Redox control of asthma: molecular mechanisms and therapeutic opportunities. Antioxid Redox Signal 2010;**12**:93-124.
4. Cunha AA, Nuñez NK, Souza RG, Vargas HMV, Silveira JS, Antunes GL, et al. Recombinant human deoxyribonuclease therapy improves airway resistance and reduces DNA extracellular traps in a murine acute asthma model. Exp Lung Res 2016;**42**:66-74.
5. Henricks PA, Nijkamp FP. Reactive oxygen species as mediators in asthma. Pulm Pharmacol Ther 2001;**14**:409-420.
6. Zmijewski JW, Lorne E, Zhao X, Tsuruta Y, Sha Y, Liu G, et al. Mitochondrial respiratory complex I regulates neutrophil activation and severity of lung injury. Am J Respir Crit Care Med 2008;**178**:168-179.
7. Zmijewski JW, Lorne E, Banerjee S, Abraham E. Participation of mitochondrial respiratory complex III in neutrophil activation and lung injury. Am J Physiol Lung Cell Mol Physiol 2009;**296**:624-634.
8. Yousefi S, Gold JA, Andina N, Lee JJ, Kelly AM, Kozlowski E, et al. Kozlowski, Catapult- like release of mitochondrial DNA by eosinophils contributes to antibacterial defense. Nat Med 2008;**14**:949-953.
9. Morshed M, Yousefi S, Stockle C, Simon HU, Simon D. Thymic stromal lymphopoietin stimulates the formation of eosinophil extracellular traps. Allergy 2012;**67**:1127-1137.

10. Muniz VS, Silva JC, Braga YAV, Melo RCN, Ueki S, Takeda M, et al. Eosinophils release extracellular DNA traps in response to Aspergillus fumigatus. J Allergy Clin Immunol 2017;**141**:571-585.
11. Dworski R, Simon HU, Hoskins A, Yousefi S. Eosinophil and neutrophil extracellular DNA traps in human allergic asthmatic airways. J Allergy Clin Immunol 2011;**127**:1260-1266.
12. Cunha AA, Porto BN, Nuñez NK, Souza RG, Vargas MH, Silveira JS, et al. Extracellular DNA traps in bronchoalveolar fluid from a murine eosinophilic pulmonary response. Allergy 2014;**69**:1696-1700.
13. Ueki S, Tokunaga T, Fujieda S, Honda K, Hirokawa M, Spencer LA, et al. Eosinophil extracellular trap cell death-derived DNA traps: Their presence in secretions and functional attributes. J Allergy Clin Immunol 2016;**137**:258-267.
14. Barth CR, Funchal GA, Luft C, de Oliveira JR, Porto BN, Donadio MV. Carrageenan-induced inflammation promotes ROS generation and neutrophil extracellular trap formation in a mouse model of peritonitis. Eur J Immunol 2016;**46**:964-970.
15. Strath M, Warren DJ, Sanderson CJ. Detection of eosinophils using an eosinophil peroxidase assay. Its use as an assay for eosinophil differentiation factors. J Immunol Methods 1985;**83**:209-215.
16. Hantos Z, Daróczy B, Suki B, Nagy S, Fredberg JJ. Input impedance and peripheral inhomogeneity of dog lungs. J Appl Physiol 1992;**72**:168-178.
17. LeBel CP, Ischiropoulos H, Bondy SC. Evaluation of the probe 2',7'-dichlorofluorescin as an indicator of reactive oxygen species formation and oxidative stress. Chem Res Toxicol 1992;**5**:227-231.
18. Marklund SL. Pyrogallol auto oxidation. In: Greenwald RA. Handbook of Methods for Oxygen Radical Research. Boca Raton, CRC Press,1985;243-247.
19. Aebi H. Catalase, in vitro. Methods Enzymol 1984;**105**:121-126.
20. Wendel A. Glutathione peroxidase. Methods Enzymol 1981;**77**:325-332.
21. Fischer JC, Ruitenbeek W, Berden JA, Trijbels JMF, Veerkamp JH, Stadhouders, et al. Differential investigation of the capacity of succinate oxidation in human skeletal muscle. Clin Chim Acta 1985;**153**:23-36.

22. Rustin P, Chretien D, Bourgeron T, Gérard B, Rötig A, Saudubray JM, et al. Biochemical and molecular investigations in respiratory chain deficiencies. Clin Chim Acta 1994;**228**:35-51.
23. Wyse ATS, Streck EL, Barros SV, Brusque AM, Zugno AI, Wajner M. Methylmalonate administration decreases Na^+, K^+-ATPase activity in cerebral cortex of rats. Neuro report 2000;**11**:2331-2334.
24. Andreadis AA, Hazen SL, Comhair SA, Erzurum SC. Oxidative and nitrosative events in asthma. Free Radic Biol Med 2003;**35**:213-225.
25. Lee YC, Lee KS, Park SJ, Park HS, Lim JS, Park KH, et al. Blockade of airway hyperresponsiveness and inflammation in a murine model of asthma by a prodrug of cysteine, L-2-oxothiazolidine-4-carboxylic acid. Faseb J 2004;**18**:1917-1919.
26. Nesi RT, Barroso MV, Muniz VS, de Arantes AC, Martins MA, Brito Gitirana L, et al. Pharmacological modulation of reactive oxygen species (ROS) improves the airway hyperresponsiveness by shifting the Th1 response in allergic inflammation induced by ovalbumin. Free Radic Res 2017;**51**:708-722.
27. Mori V, Oliveira MA, Vargas MHM, da Cunha AA, de Souza RG, Pitrez PM, et al. Input respiratory impedance in mice: comparison between the flow-based and the wavetube method to perform the forced oscillation technique. Physiol Meas 2017;**38**:992-1005.
28. Kudo M, Ishigatsubo Y, Aoki Ichiro. Pathology of asthma. Front Microbiol 2013;**4**:263.
29. Oka S, Kamata H, Kamata K, Yagisawa H, Hirata H. N-acetylcysteine suppresses TNF-induced NF-kappaB activation through inhibition of IkappaB kinases. FEBS Lett 2000;**472**:196-202.
30. Lee KS, Kim SR, Park HS, Park SJ, Min KH, Lee KY, et al. A novel thiol compound, N-acetylcysteine amide, attenuates allergic airway disease by regulating activation of NF-kappaB and hypoxia-inducible factor-1alpha. Exp Mol Med 2007;**39**:756-768.
31. Dodd S, Dean O, Copolov DL, Malhi GS, Berk M. N-acetylcysteine for antioxidant therapy: pharmacology and clinical utility. Expert Opin Biol Ther 2008;**8**:1955-1962.

32. Chen CC, Chow MP, Huang WC, Lin YC, Chang YJ. Flavonoids inhibit tumor necrosis factor-alpha-induced up-regulation of intercellular adhesion molecule-1 (ICAM-1) in respiratory epithelial cells through activator protein-1 and nuclear factor-kappaB: structure–activity relationships. Mol Pharmacol 2004;**66**:683-693.
33. da Cunha AA, Ferreira AG, da Cunha MJ, Pederzolli CD, Becker DL, Coelho JG, et al.Chronic hyperhomocysteinemia induces oxidative damage in the rat lung. Mol Cell Biochem 2011;**358**:153-160.
34. Mokhtari V, Afsharian P, Shahhoseini M, Kalantar SM, Moioni A. A Review on Various Uses of N-Acetyl Cysteine. Cell J 2017;**19**:11-17.
35. Babior BM. NADPH oxidase: an update. Blood 1999;**93**:1464-1476.
36. Aguilera-Aguirre L, Bacsi A, Saavedra-Molina A, Kurosky A, Sur S, Boldogh I. Mitochondrial dysfunction increases allergic airway inflammation. J Immunol 2009;**183**:5379-5387.
37. Quinlan CL, Orr AL, Perevoshchikova IV, Treberg JR, Ackrell BA, Brand MD. Mitochondrial complex II can generate reactive oxygen species at high rates in both the forward and reverse reactions. J Biol Chem 2012;**287**:27255-27264.
38. Marí M, Morales A, Colell A, García-Ruiz C, Kaplowitz N, Fernández-Checa JC.Mitochondrial glutathione: features, regulation and role in disease. Biochim Biophys Acta 2013;**1830**:3317-3328.
39. Schweinberger BM, Schwieder L, Scherer E, Sitta A, Vargas CR, Wyse ATS. Development of an animal model for gestational hypermethioninemia in rat and its effect on brain Na^+,K^+-ATPase/Mg2+-ATPase activity and oxidative status of the offspring. Metab Brain Dis 2014;**29**:153-160.
40. Agrawal A, Agrawal KP, Ram A, Sondhi A, Chhabra SK, Gangal SV, et al. Basis of Rise in Intracellular Sodium in Airway Hyperresponsiveness and Asthma. Lung 2005;**183**:375-387
41. Lichtstein D Samuelov S. Membrane potential changes induced by the ouabain-like compound extracted from mammalian brain. Proc Natl Acad Sci USA 1982;**79**:1453-1456.
42. Scheid CR, Honeyman TW, Fay FS. Mechanism of β-adrenergic relaxation of smooth muscle. Nature 1979;**277**:32-36.

43. Alexeyev M, Shokolenko I, Wilson G, et al. The Maintenance of Mitochondrial DNA Integrity-Critical Analysis and Update The unfolded protein response in lung disease. Proc Am Thorac Soc 2010;**7**:356-362.
44. Brinkmann V, Reichard U, Goosmann C, et al. Neutrophil extracellular traps kill bacteria. Science 2004;**303**:1532-1535.

LEGEND TO THE FIGURE

FIGURE 1: Protocol used to induce a murine asthma model in BALB/cJ mice and treatments with DPI and NAC (A). Analysis of the activity of the EPO enzyme (B). Total and differential cells count in BALF (C-G). Representative illustration of BALF cells (400× magnification, arrows indicate eosinophils) (H). Histopathological analysis in lung. Representative photomicrographs of stained sections with H&E (200x and 1000x magnification, arrow indicate inflammatory infiltrate) (I). Morphometric analysis perivascular and peribronchial with H&E staining (J,K). Representative photomicrographs of stained sections with alcian blue (200× and 1000x magnification, arrows indicate goblet cells) (L). Data represent the mean ± SD, n = 20 animals per group. * $p < 0.05$, ** $p < 0.01$ and *** $p < 0.001$ (One-way ANOVA followed by Tukey test). OVA: ovalbumin; DPBS: dulbecco phosphate buffered saline; DPI: diphenyleneiodonium; NAC: N-acetylcysteine; EPO: eosinophil peroxidase; BALF: bronchoalveolar lavage fluid; TCC: total cell count.

FIGURE 2: Assessment of lung function: resistance (Rn), tissue damping (G) and tissue elastance (H) (A-C). Cytokine levels in lung (IL-5, IL-13, IFN-γ, IL1-β, TNF-α and IL-10) (D-I). Analysis of the NFκB p65 protein by immunofluorescence in lung sections (J). Data represent the mean ± SD, n = 10 animals per group. * $p < 0.05$, ** $p < 0.01$ and *** $p < 0.001$ (One-way ANOVA followed by Tukey test). OVA: ovalbumin; DPBS: dulbecco phosphate buffered saline; DPI: diphenyleneiodonium; NAC: N-acetylcysteine; IL: interleukin, IFN: interferon; TNF: tumor necrosis factor.

FIGURE 3: ROS production in lung (A). Activity of antioxidant enzymes (SOD, CAT and GPx) in lung (B-E). Mitochondrial energy metabolism (Complex II, SDH, complex IV) in lung (F-H). NA^+, K^+-ATPase activity analyses in lung (F-I). Data represent the mean ± SD, n = 10 animals per group. * $p < 0.05$, ** $p < 0.01$ and *** $p < 0.001$ (One-way ANOVA followed by Tukey test). OVA: ovalbumin; DPBS: dulbecco phosphate buffered saline; DPI: diphenyleneiodonium; NAC: N-acetylcysteine; DCF: dichlorofluorescein; SOD: superoxide dismutase; CAT: catalase; GPx: glutathione peroxidase; SDH: succinate dehydrogenase.

FIGURE 4: Immunofluorescence microscopy confocal of EETs in BALF eosinophils (630x magnification, arrows indicate EETs formation) (A). Electron microscopy of EETs in BALF eosinophils (Scale bars = 10 and 30 μm) (B). Quantification of

extracellular DNA traps in BALF (C). Analysis of cell death in BALF cells by Annexin V and PI (D). Data represent the mean ± SD, n = 20 animals per group. *** $p < 0.001$ (One-way ANOVA followed by Tukey test). OVA: ovalbumin; DPBS: dulbecco phosphate buffered saline; DPI: diphenyleneiodonium; NAC: N-acetylcysteine; EPO: eosinophil peroxidase; BALF: bronchoalveolar lavage fluid; PI: propidium iodide.

FIGURE 5: Summary of the effect of DPI and NAC in EETs formation in OVA-challenge mice. DPI: diphenyleneiodonium; NAC: N-acetylcysteine; NADPH oxidase: nicotinamide adenine dinucleotide phosphate-oxidase; ROS: reactive oxygen species; EETs: eosinophil extracellular traps; GSH: glutathione.

FIGURE 1

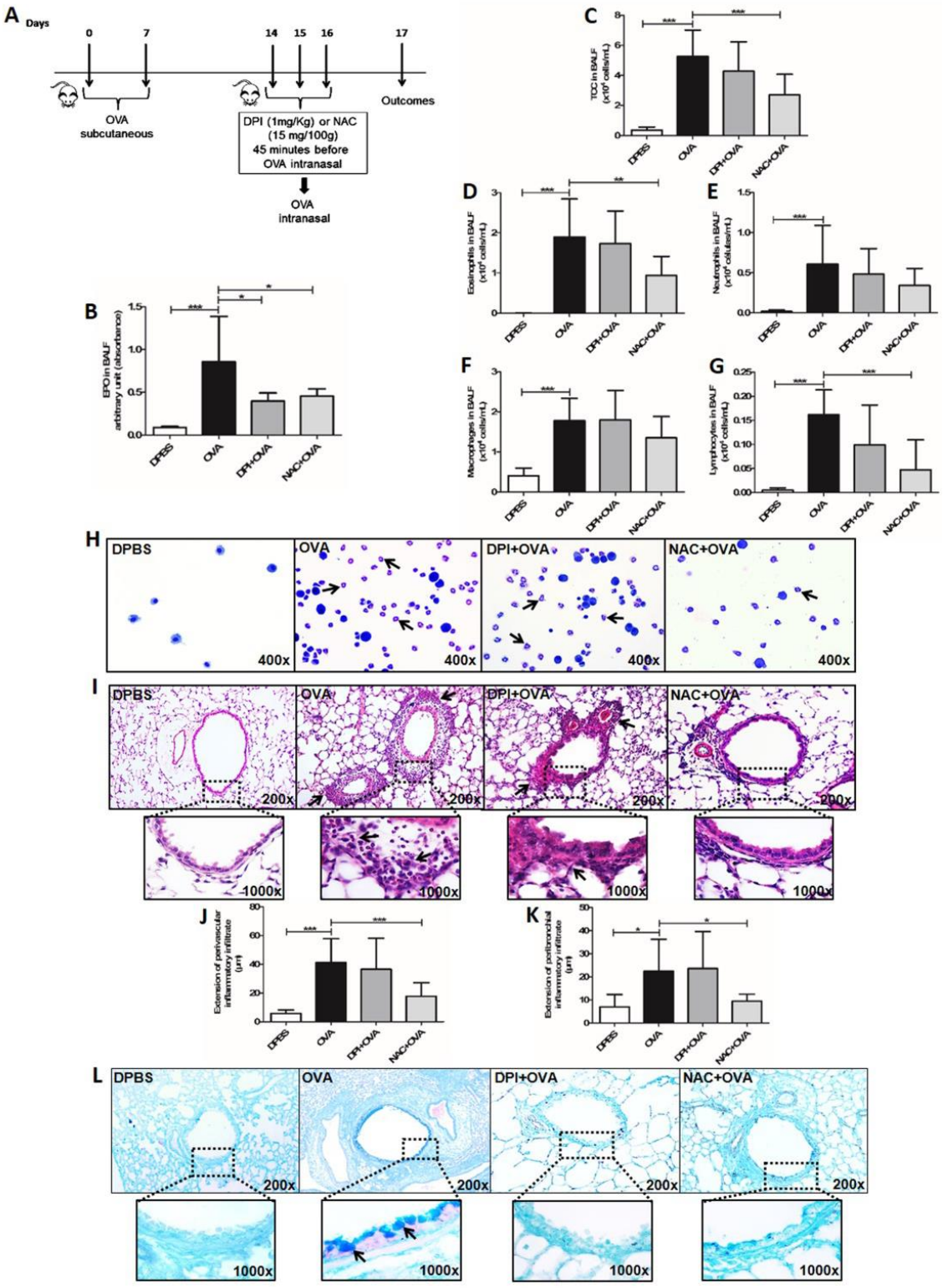
A
Days
0
7
14
15
16
17
OVA
subcutaneous
DPI (1mg/Kg) or NAC
(15 mg/100g)
45 minutes before
OVA intranasal
OVA
intranasal
Outcomes
B
EPO in BALF
arbitrary unit (absorbance)
C
TCC in BALF
(x10⁴ cells/mL)
D
Eosinophils in BALF
(x10⁴ cells/mL)
E
Neutrophils in BALF
(x10⁴ cells/mL)
F
Macrophages in BALF
(x10⁴ cells/mL)
G
Lymphocytes in BALF
(x10⁴ cells/mL)
DPBS
OVA
DPI+OVA
NAC+OVA
H
I
400x
200x
1000x
J
Extension of perivascular
inflammatory infiltrate
(u.a)
K
Extension of peribronchial
inflammatory infiltrate
(u.a)
L

FIGURE 2

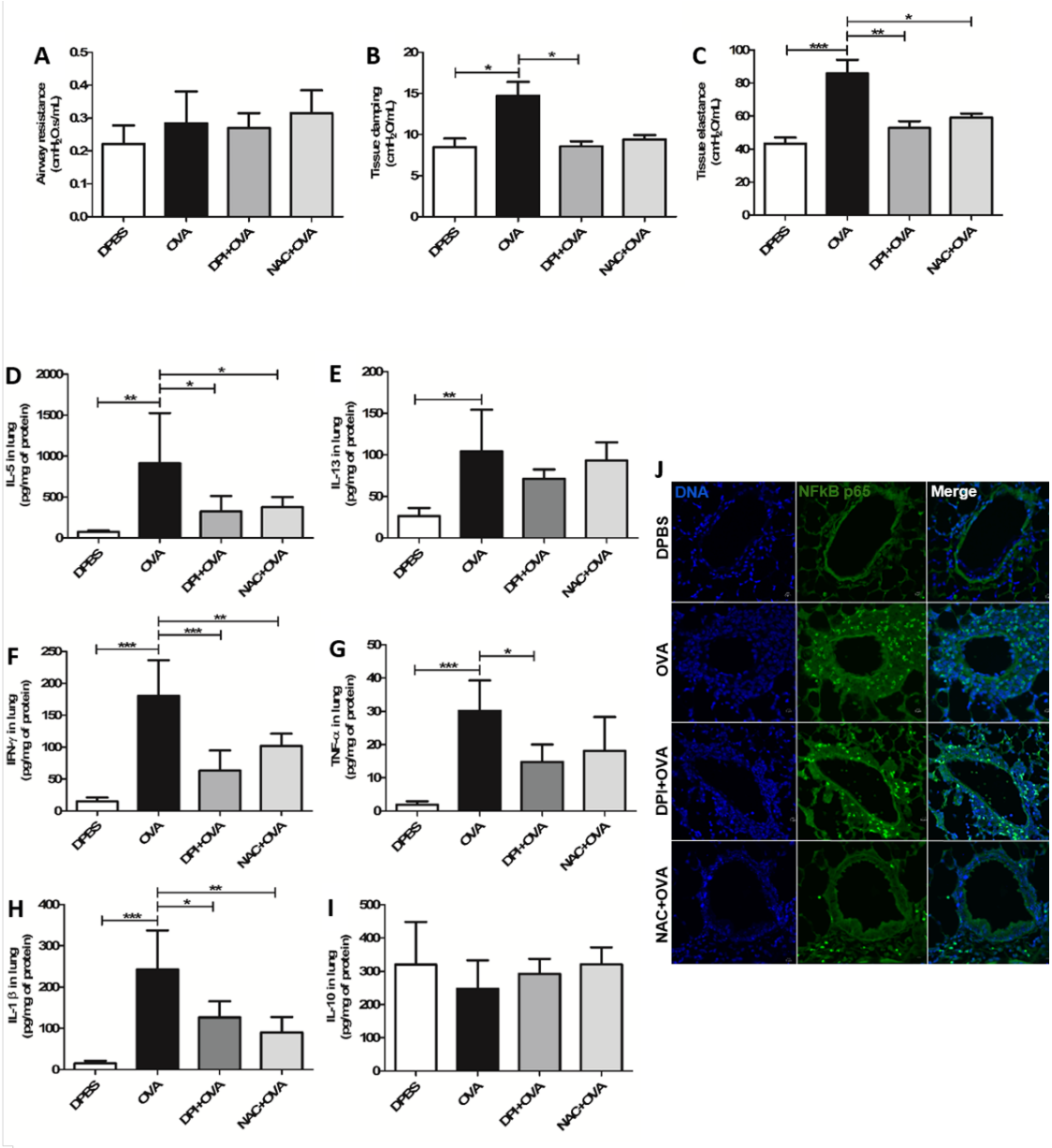
A
Airway resistance (cmH2Os/mL)
B
Tissue damping (cmH2O/mL)
C
Tissue elastance (cmH2O/mL)
D
IL-5 in lung (pg/mg of protein)
E
IL-13 in lung (pg/mg of protein)
F
IFN-γ in lung (pg/mg of protein)
G
TNF-α in lung (pg/mg of protein)
H
IL-1β in lung (pg/mg of protein)
I
IL-10 in lung (pg/mg of protein)
DPBS
OVA
DPI+OVA
NAC+OVA
J
DNA
NFkB p65
Merge

FIGURE 3

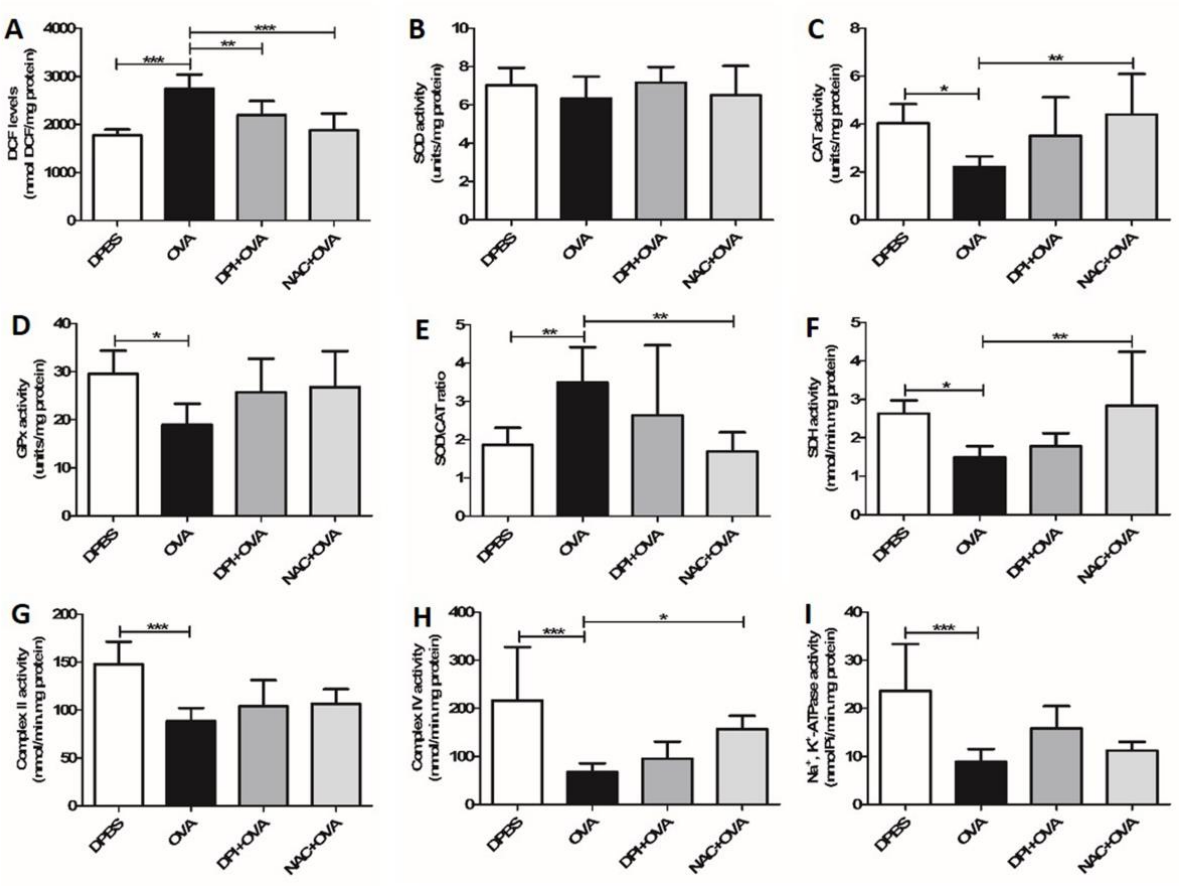
A
DCF levels (nmol DCF/mg protein)
B
SOD activity (units/mg protein)
C
CAT activity (units/mg protein)
D
GPx activity (units/mg protein)
E
SOD/CAT ratio
F
SDH activity (nmol/min.mg protein)
G
Complex II activity (nmol/min.mg protein)
H
Complex IV activity (nmol/min.mg protein)
I
Na+, K+-ATPase activity (nmolPi/min.mg protein)
DPBS
OVA
DPH+OVA
NAC+OVA

FIGURE 4

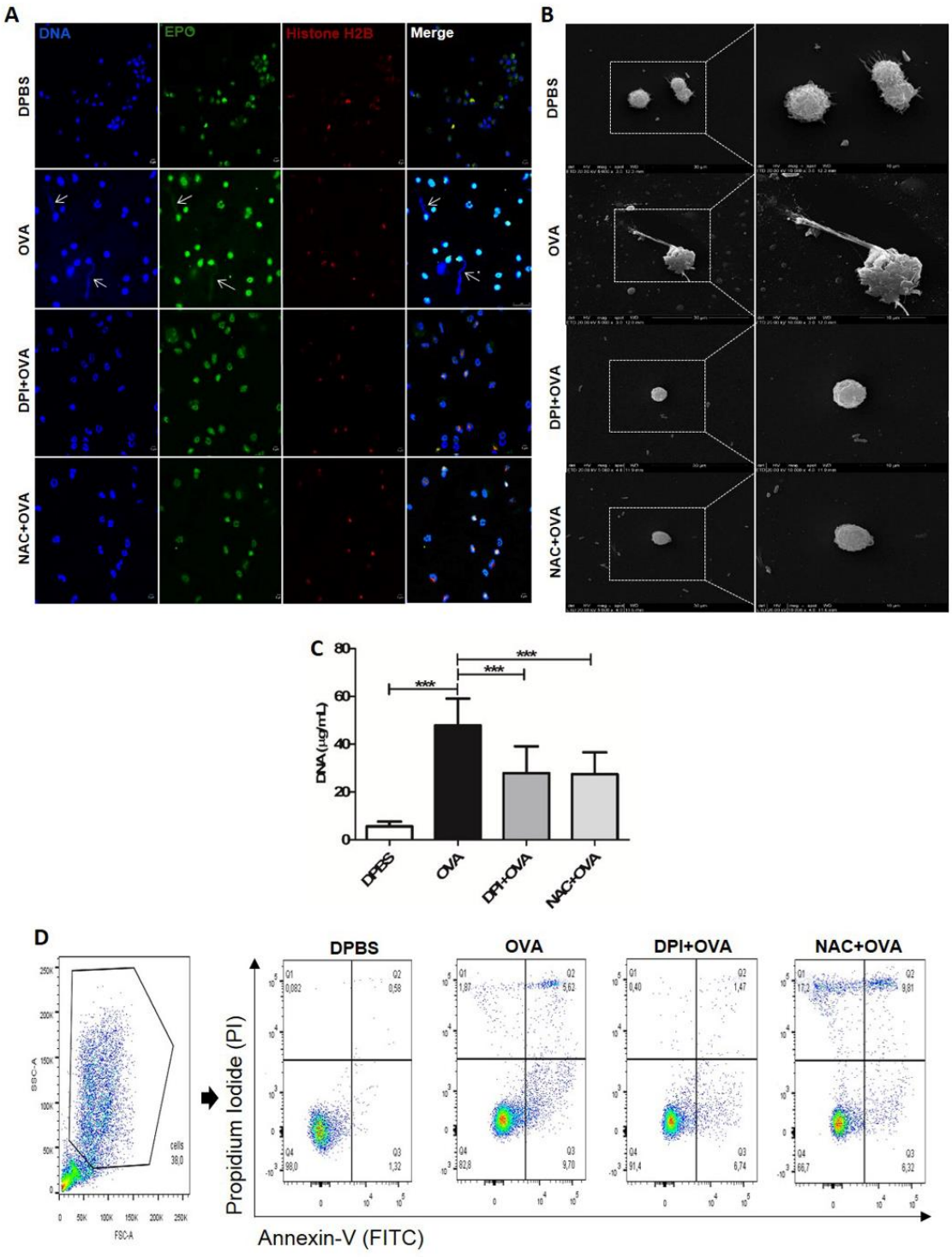
A
DNA
EPO
Histone H2B
Merge
DPBS
OVA
DPI+OVA
NAC+OVA
B
DPBS
OVA
DPI+OVA
NAC+OVA
C
DNA (µg/mL)
***
***
***
DPBS
OVA
DPI+OVA
NAC+OVA
D
SSC-A
FSC-A
cells
38,0
Propidium Iodide (PI)
Annexin-V (FITC)
DPBS
OVA
DPI+OVA
NAC+OVA

Figure 5

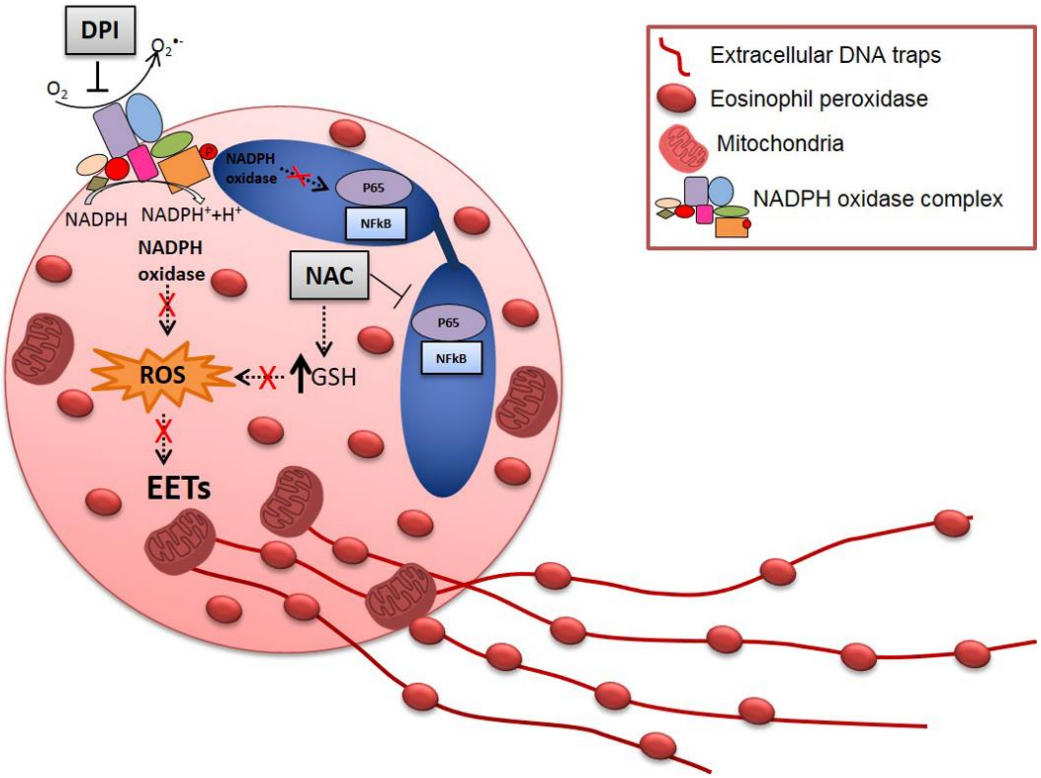
DPI
$O_2^{\bullet-}$
O_2
NADPH
$NADPH^+ + H^+$
NADPH oxidase
P65
NFkB
NADPH oxidase
NAC
P65
NFkB
ROS
GSH
EETs
Extracellular DNA traps
Eosinophil peroxidase
Mitochondria
NADPH oxidase complex

Supporting Information

Methods S1

Animals

Female BALB/cJ mice, specific pathogen-free (SPF), 6-8 weeks of age, weighing approximately 20 g from the Center for Experimental Biological Models (CeMBE, PUCRS) were used for all experiments. The animals were fed standard ration for rodents and access to water ad libitum, housed in cages and kept in a 12/12 h light/dark cycle. All studies were conducted with the approval of the Pontifícia Universidade Católica do Rio Grande do Sul Animal Ethics Committee (7910).

Sensitization and challenge

Mice were sensitized with subcutaneous injections of 20 µg of ovalbumin (OVA; Grade V, Sigma, Missouri, USA), diluted in 200 µl of Dulbecco phosphate buffered saline (DPBS, Gibco, Massachusetts, USA), on days 0 and 7 of the protocol. Followed three intranasal challenges with 100 µg of OVA, diluted in 50 µL of DPBS, on days 14, 15 and 16 of the protocol.[1] Control group received subcutaneous and intranasal only DPBS.

Treatment protocol

To evaluate the involvement of reactive oxygen species (ROS) in airway inflammation and in eosinophil extracellular traps (EETs) formation in an asthma model, animals were pretreated intranasally with diphenyleneiodonium (DPI) (Sigma, Missouri, USA), 1 mg/Kg or N-acetylcysteine (NAC), 15 mg/100 g of body weight (União Química, São Paulo, Brazil), 45 minutes before of the three intranasal with OVA.

Total and differential cells count in BALF

Twenty-four hours after the last challenge, bronchoalveolar lavage fluid (BALF) was collected. The animals were anesthetized (ketamine 0.4 mg/g and xylazine 0.2 mg/g), after the trachea was cannulated with a 20 gauge needle and 1 mL of PBS (phosphate buffered saline) 2 % fetal bovine serum (FBS) was instilled for the BALF collection. BALF was centrifuged and the supernatant was used for the quantification

of extracellular DNA and measurement of the activity of the enzyme eosinophil peroxidase (EPO). The pellet was resuspended in PBS 2% FBS for performing total and differential cells count in the BALF. The total cells count and cell viability were determined by trypan blue exclusion test were performed in the Neubauer chamber (BOECO, Hamburg, Germany). For the differential cell count, the slides were performed through cytospin in a cytocentrifuge (Eppendorf, Wesseling, Germany) and stained with H&E (Newprov, Paraná, Brazil). Four hundred cells were counted under an optical microscope (Olympus, Tokyo, Japan).

Analysis of the activity of EPO enzyme in BALF

EPO activity was measured by the colorimetric assay based in the oxidation of O-phenylenediamine (OPD) (Sigma, Missouri, USA) in the presence of H_2O_2. For the implementation of the protocol, 50 µL of the BALF supernatant was transferred to a 96-well plate and working reagent was added (0.1 mM OPD, 0.05 M Tris pH = 8.0, Triton X -100 and 1 mM H_2O_2). The plate was incubated protected from light for 1 hour at room temperature (RT). After this period the reaction was stopped with 50 µL of H_2SO_4 1.0 M. The absorbance was measured at a wavelength of 492 nm.[2]

Lung Histopathologic analysis

After euthanasia, left lung was perfused with 10 % buffered formalin in a gravity column (20 cmH_2O). Tissue specimens were embedded in paraffin and histological sections of 5 micrometers (µm) were performed. For evaluation the inflammatory infiltrate the sections were stained with H&E. For evaluation of the extent of peribronchial and perivascular inflammatory infiltrate in µm, 10 measurements were performed starting from the end of the bronchial or vessel epithelium to the end of the inflammatory infiltrate using Olympus CellSens Standart software (Olympus, Tokyo, Japan). At least 5 fields were evaluated to obtain the average for each mouse. For evaluation of goblet cell hyperplasia and mucus-production, the slides were stained with alcian blue.

Assessment of lung function

Twenty-four hours after the last challenge, the animals were anesthetized with ketamine (0.4 mg/ g) and xylazine (0.2 mg/g). Pulmonary function test was performed

after cannulation of the trachea through a tracheostomy. The animal was maintained in the flexiVent system (flexiVent, SCIREQ, Montreal, Canada) for 5 minutes prior of to start the test to a respiratory rate of 150 movements per minute, after was administered pancuronium (1mg/kg) intraperitoneal. Three measurements of forced oscillation technique (FOT) were performed during a pause of the respirator (3 seconds). During the ventilation pauses, a frequency oscillatory signal (4-38 Hz) was generated by a loudspeaker and passed through the tracheal cannula of the animal. A four-parameter model with constant phase tissue impedance was fitted to the Zrs data to obtain Resistance (Rn) measurements, the Newtonian resistance which equates to airway resistance in mouse due to complacency of the chest wall, G (tissue damping), which represents the resistance of small airways where air movement occurs mainly by diffusion and H (tissue elastance). The data were analyzed in specific software (flexiWare, SCIREQ, Montreal, Canada), where airway resistance and elastic properties (viscosity and elasticity) of the lung were measured through a pulmonary impedance (Rn, G and H).[3]

Cytokine levels in lung

Lungs were prepared by homogenization in PBS 1x and the levels of IL-5, IL-13, interferon (IFN)-γ, IL1-β, tumor necrosis factor (TNF)-α and IL-10 were measured by multiplex assay using magnetic beads using a Milliplex MAP mouse kit (MILLIPLEX®, Millipore, Germany) and ProcartaPlex Multiplex immunoassay (Thermo-Life Technology, Massachusetts, USA) according to the manufacturer's recommendations. Analyzes were performed on the Magpix® equipment (Millipore, Germany). Results were analyzed using the software xPONENT® Solutions software (Luminex Corporation, Texas, EUA).

Analysis of NFkB p65 by immunofluorescence in lung

Analysis of the NFκB p65 protein by immunofluorescence was performed in formalin-fixed lungs. Firstly, tissue specimens were embedded in paraffin and histological sections of 5 µm were performed. Sections were dewaxed in xylol and rehydrated in water. After the sections were incubated with 9 mM citrate pH = 9.0 for 10 minutes and with 0.3 % H_2O_2 in methanol for 20 minutes. Next, sections were blocked with 10% bovine serum albumin (BSA) in PBS for 30 minutes. The sections were

incubated for 40 minutes with primary antibody, anti-NFkB p65 (1: 500, Thermo-Life Technology, Massachusetts, USA) followed for secondary antibody, FITC anti-rabbit (1: 250, Thermo-Life Technology, Massachusetts, USA) for 30 minutes. The sections were incubated with Hoechst 33342 (1: 2000; Invitrogen, Carlsbad, USA) for 4 minutes. The images were performed in a confocal immunofluorescence microscope (Zeiss LSM5).

Lung Preparation

For determination of oxidative stress parameters, the lungs were homogenized (1:10, *w/v*) in 20 mM sodium phosphate buffer pH = 7.4, containing 140 mM KCl. For mitochondrial energy metabolism analyses (complex II, succinate dehydrogenase (SDH) and complex IV), lungs were frozen and thawed three times to disrupt the mitochondrial membranes. After, lungs were homogenized (1:20, *w/v*) in SETH buffer (250 mM sucrose, 2 mM EDTA, 10 mM Trizma base, 50 UI/mL heparin), pH = 7.4. For NA^+, K^+-ATPase activity analyses, lungs were homogenized (1:10, *w/v*) in 0.32 mM sucrose solution containing 5.0 mM HEPES and 1.0 mM EDTA, pH= 7.5. After the homogenates were centrifuged at 800 ×g for 10 min at 4°C and the supernatants were collected and used for the analyses.

ROS assay in lung

ROS production was analyzed by the method described by Lebel et al. The technique is based on the oxidation of the 2'7' dichlorofluorescein (H2DCF). The lung sample was incubated in medium containing 100 µM 2'7'-dichlorofluorescein diacetate (H2DCF-DA). Then the reaction produces a fluorescent compound, dichlorofluorescein (DCF), which was measured in a spectrophotometer at 488 nm of excitation and 525 nm of emission. The results were expressed as nmol DCF/mg protein.[4]

Superoxide dismutase (SOD) activity in lung

SOD activity in lung was based in the technique of the self-oxidizing ability of pyrogallol, a highly $O2^{\bullet-}$ dependent process, which is a substrate for SOD. Inhibition of the self-oxidation of this compound occurs in the presence of SOD, the activity of which can be indirectly measured in a spectrophotometer at 412 nm. A calibration

curve was performed with purified SOD as standard, to calculate the SOD activity present in the samples. SOD activity was expressed in units of SOD/mg protein.[5]

Catalase (CAT) activity in lung

CAT activity in lung was determined according to Aebi. The lung sample was incubated in medium containing 20 mM H_2O_2 with 0.1 % of Triton X-100 and 10 mM potassium phosphate pH = 7.4. CAT activity was based on the measurement of the decrease in H_2O_2 consumption at 240 nm. A CAT unit is defined as H_2O_2 1 μM consumed per minute. CAT activity was expressed in units of CAT/mg protein.[6]

Glutathione peroxidase (GPx) activity in lung

GPx activity was analyzed in lung sample according to Wendel and tert-butylhydroperoxide was utilized as substrate. The lung sample was incubated in medium contained 2 mM glutathione, 0.15 U/ml glutathione reductase, 0.4 mM azide, 0.5 mM tert-butylhydroperoxide and 0.1 mM NADPH. One GPx unit was defined as 1 μMol of NADPH consumed per minute. The decay of the NADPH was monitored at 340 nm in a spectrophotometer at 25°C. GPx activity was expressed in GPx units/mg of protein.[7]

Complex II, SDH and complex IV activity in lung

Complex II activity and SDH was determined according to Fischer et al. Lung samples were mixtures in buffer containing 40 mM potassium phosphate pH= 7.4, 16 mM sodium succinate and 8 mM 2, 6-dichloroindophenol (DCIP) and incubated at 30°C for 20 minutes. Thereafter, 4 mM sodium azide, 7 mM rotenone and 40 mM DCIP were added. The enzymatic activity of complex II in lung was measured after decrease of the absorbance by reduction of DCIP. The reaction was monitored for 5 min and the results were reported as nmol/min mg of protein. The enzymatic activity of SDH was measured after depletion of the absorbance by reduction of the DCIP in the presence of phenazine methasulfate (PMS) at 600 nm. The reaction was started by the addition of 1 mM PMS, monitored for 5 min and e the results were reported as nmol/min.mg of protein.[8] Complex IV activity in lung was determined according to Rustin et al. Lung homogenate was added the reaction buffer containing 10 mM potassium phosphate pH = 7.0 and 0.6 mM n-dodecyl-α-D-maltoside. The reaction

will be initiated by the addition of 70 µL of reduced cytochrome c and the reaction is monitored for 10 min. The enzymatic activity of complex IV in lung was measured by decrease in absorbance due to oxidation of reduced cytochrome to 550 nm. The results were expressed as nmol/min mg of protein.[9]

NA^+, K^+-ATPase activity in lung

NA^+, K^+-ATPase activity in lung was determined according to Wyse et al. Tissue homogenate was added the reaction buffer containing 5.0 mM $MgCl_2$, 80.0 mM NaCl, 20.0 mM KCl and 40.0 mM Tris-HCl, pH= 7.4. The reaction was initiated by addition of ATP to a final concentration of 3.0 mM. Controls were added 1.0 mM ouabain. The enzymatic activity was measured by decreasing of the absorbance by cytochrome oxidation and reduced to 550 nm. The results were expressed as nmol P_i released per min per mg of protein.[10]

Quantification and immunofluorescence microscopy confocal of EETs in BALF

Extracellular DNA was quantified in BALF supernatant using the Quant-iT dsDNA HS kit (Invitrogen, Carlsbad, USA) and measured in the Quibit 2.0 fluorimeter (Invitrogen, Carlsbad, USA), according to the manufacturer's recommendations. To visualize the EETs formation, cells obtained in BALF (2 x 10^5/mL) were plated in 8-chamber culture slides (BD Falcon, New Jersey, USA) and incubated at 37°C with 5% CO_2 for 1 hour. After that, the cells were fixed with 4 % paraformaldehyde (PFA) for 45 minutes and incubated with primary antibodies, anti-EPO and anti-histone H2B (1: 250, Santa Cruz Biotechnology, Dallas, USA) for 45 minutes at RT. After this time, were incubated for 30 minutes with the secondary antibodies, FITC anti-goat (1: 100, Santa Cruz Biotechnology, Dallas, USA) and alexa fluor 633 anti-goat (1: 100, Invitrogen, Carlsbad, USA) at RT. Next, the cells were incubated with Hoechst 33342 DNA dye (1: 2000, Invitrogen, Carlsbad, USA) for 4 minutes at RT. Images were performed on a Zeiss LSM 5 Exciter confocal microscope (Zeiss LSM5, Oberkohen, Germany).

Electron microscopy of BALF cells

BALF cells (2 x 10^5/mL) were placed in a 6 wells plate with coverslips pre-treated with 0.0005% poly-*L*-lysine (Sigma, Missouri, USA) and incubated for 1 hour at 37°C,

5% CO_2. Next, the culture medium was removed and coverslips were fixed with 2.5 % glutaraldehyde. After three washes in PBS, the samples were post-fixed with osmium tetroxide solution 2 % for 45 minutes. Next, the samples were washed three times in PBS, followed by dehydration in graded acetone: 30 %, 50 %, 70 %, 2x 95 % and 2x 100 % for 10 minutes each. The critical point technique with CO_2 was performed, followed by mounting on a metallic support with carbon tape. The samples were covered with a thin layer of gold (metallization). The images were performed in an electron microscope Inspect F50 (FEI, Oregon, EUA).

Analysis of cell death in BALF cells

BALF cells were analyzed for apoptosis by Annexin V and necrosis by propidium iodide (PI), according to the manufacturer's instructions (BD Pharmingen). Cells were incubated with Annexin V-FITC and PI for 15 minutes at RT and analyzed by flow cytometry (FACS Canto II, BD Bioscience). Data were analyzed using FlowJo software version X.0.7 (TreeStar, Oregon, USA). This analysis allows the discrimination between the necrotic cells (Annexin V+/PI+), late apoptotic or necrotic cells (Annexin V +/PI +) and early apoptotic cells (Annexin V +/PI-).

Protein Determination

The proteins content in lungs were determined using Qubit™ Protein Assay Kit (Invitrogen, Carlsbad, USA) for cytokines. Lowry assay for proteins of oxidative stress, energy metabolism mitochondrial and Na^+, K^+-ATPase proteins. Bradford method for western blot proteins.[11,12]

Statistical analysis

Data are expressed as mean ± standard deviation. The Shapiro-Wilk normality test was used to evaluate the normal distribution of the data. We used one-way ANOVA followed by Tukey pos-hoc and the significance level adopted was $p \leq 0.05$. Statistical analysis and graphs were performed using the GraphPad Prism Software, version 5 (GraphPad Software, San Diego, USA).

REFERENCES

1. Cunha AA, Nuñez NK, Souza RG, Vargas HMV, Silveira JS, Antunes GL, et al. Recombinant human deoxyribonuclease therapy improves airway resistance and reduces DNA extracellular traps in a murine acute asthma model. Exp Lung Res 2016;**42**:66-74.
2. Strath M, Warren DJ, Sanderson CJ. Detection of eosinophils using an eosinophil peroxidase assay. Its use as an assay for eosinophil differentiation factors. J Immunol Methods 1985;**83**:209-215.
3. Hantos Z, Daróczy B, Suki B, Nagy S, Fredberg JJ. Input impedance and peripheral inhomogeneity of dog lungs. J Appl Physiol 1992;**72**:168-178.
4. LeBel CP, Ischiropoulos H, Bondy SC. Evaluation of the probe 2',7'-dichlorofluorescin as an indicator of reactive oxygen species formation and oxidative stress. Chem Res Toxicol 1992;**5**:227-231.
5. Marklund SL. Pyrogallol auto oxidation. In: Greenwald RA. Handbook of Methods for Oxygen Radical Research. Boca Raton, CRC Press, 1985; 243-247.
6. Aebi H. Catalase, in vitro. Methods Enzymol 1984;**105**:121-126.
7. Wendel A. Glutathione peroxidase. Methods Enzymol 1981;77:325-332.
8. Fischer JC, Ruitenbeek W, Berden JA, Trijbels JMF, Veerkamp JH, Stadhouders, et al. Differential investigation of the capacity of succinate oxidation in human skeletal muscle. Clin Chim Acta 1985;**153**:23-36.
9. Rustin P, Chretien D, Bourgeron T, Gérard B, Rötig A, Saudubray JM, et al. Biochemical and molecular investigations in respiratory chain deficiencies. Clin Chim Acta 1994;**228**:35-51.
10. Wyse ATS, Streck EL, Barros SV, Brusque AM, Zugno AI, Wajner M. Methylmalonate administration decreases Na+, K+-ATPase activity in cerebral cortex of rats. Neuro report 2000;**11**:2331-2334.
11. Lowry OH, Rosebrough NJ, Farr AL, Randall RJ. Protein measurement with the Folin phenol reagent. J Biol Chem 1951;**193**:265-75.
12. Bradford MM (1976) A rapid and sensitive method for the quantitation of microgram quantities of protein utilizing the principle of protein-dye binding. Anal Biochem **72**:248-254.

Apêndice C: Submissão do artigo científico 3

Revista: Journal of cellular physiology

Fator de impacto: 3,9 (Medicina II: A2)

Submission Confirmation

Thank you for your submission

Submitted to	Journal of Cellular Physiology
Manuscript ID	JCP-18-1695
Title	Autophagy induces eosinophil extracellular traps formation and allergic airway inflammation in a murine asthma model
Authors	Silveira, Josiane Antunes, Géssica Kaiber, Daniela da Costa, Mariana Ferreira, Fernanda Marques, Eduardo Schmitz, Felipe Gassen, Rodrigo Breda, Ricardo Wyse, Angela Terezinha Stein, Renato Pitrez, Paulo Marcio Cunha, Aline
Date Submitted	24-Sep-2018

Autophagy induces eosinophil extracellular traps formation and allergic airway inflammation in a murine asthma model

Short title: Autophagy-dependent EETs formation in an asthma model

Josiane Silva Silveira[1] | Géssica Luana Antunes[1] | Daniela Benvenutti Kaiber[1] | Mariana Severo da Costa[1] | Fernanda Ferreira[2] | Eduardo Peil Marques[2] | Felipe Schmitz[2] | Rodrigo Benedetti Gassen[3] | Ricardo Vaz Breda[4] | Angela Terezinha Wyse[2] | Renato Tetelbom Stein[1] | Paulo Márcio Pitrez[1] | Aline Andrea da Cunha[1]

[1]Laboratory of Pediatric Respirology, Infant Center, Medicine School, Pontifícia Universidade Católica do Rio Grande do Sul (PUCRS), Porto Alegre, Brazil

[2]Laboratory of Neuroprotection and Neurometabolic Disease, Department of Biochemistry, Universidade Federal do Rio Grande do Sul, Porto Alegre, Brazil

[3]Laboratory of Cellular and Molecular Immunology, Science School, Pontifícia Universidade Católica do Rio Grande do Sul (PUCRS), Porto Alegre, Brazil

[4]Institute of the Brain (INSCER), Medicine School, Pontifícia Universidade Católica do Rio Grande do Sul (PUCRS), Porto Alegre, RS, Brazil

Address correspondence and reprint requests to Aline Andrea da Cunha, Laboratory of Pediatric Respirology, Infant Centre - PUCRS, 6690 Ipiranga Ave., 2nd floor, Room 13, Zip Code: 90610-000 - Porto Alegre, RS, Brazil, e-mail: alineacunha@hotmail.com.

ABSTRACT

Studies have shown autophagy participation in physiopathology of inflammatory diseases such as asthma. However, autophagy role in asthma pathogenesis and in EETs release is poorly understood. The aim of this study is to investigate the autophagy involvement in EETs formation and airway inflammation in an experimental asthma model. Mice were sensitized with ovalbumin (OVA), followed by OVA challenge. Before the challenge with OVA, mice were treated with an autophagy inhibitor, 3-methyladenine (3-MA). We showed that in 3-MA-treated OVA group there was a decrease in the inflammatory cells, EPO activity, goblet cells hyperplasia, inflammatory cytokines, NFκB p65 immunocontent, and oxidative stress in airway. Moreover, 3-MA was able to improve mitochondrial energy metabolism and increase Na^+,K^+ATPase activity. We demonstrated that treatment with autophagy inhibitor 3-MA reduced EETs formation in bronchoalveolar lavage fluid (BALF). Thus, 3-MA treatment can be an interesting alternative for reducing airway inflammation, mitochondrial damage and EETs release in asthma.

KEY WORDS

Asthma, autophagy, eosinophils, eosinophil extracellular traps, inflammation

1 | INTRODUCTION

Asthma is a highly prevalent chronic airway inflammatory disease characterized by an increase in inflammatory cells, remodeling, airway hyperresponsiveness (AHR), mucus overproduction, and pro-inflammatory cytokines in lung which may cause decrease in lung function (Lambrecht et al., 2015). Eosinophils are key inflammatory cells that play an important role in asthma immunopathology. Eosinophil granule proteins such as eosinophil peroxidase (EPO), major basic protein (MBP), eosinophil cationic protein (ECP), and eosinophil-derived neurotoxin (EDN) are involved in airway inflammation and damage (Sanz et al., 1997). Besides, asthma increases oxidative stress in lung due to increase in reactive oxygen species (ROS) production and decrease in antioxidant defense mechanisms being associated to damage to biologic molecules (Comhair et al., 2010; Cunha et al., 2016). Oxidative stress is also involved in important mitochondrial dysfunction and in inactivation of electron transport chain in airway (Mabalirajan et al., 2008).

Autophagy is a critically important intracellular process, by which damaged organelles and proteins are sequestered to autophagosomes and delivered to lysosomes for degradation to maintain cell survival during starvation and cellular stress (Mizushima, 2007). Moreover, autophagy plays an important role in immunity and in inflammatory disease (Jyothula et al., 2013). Studies have shown autophagy participation in physiopathology of inflammatory diseases such chronic obstructive pulmonary disease (COPD), acute lung injury (ALI), and asthma (Chen et al., 2008; Li et al., 2009, Ban et al., 2015). Ban and colleagues found high levels of autophagy in sputum granulocytes, peripheral blood cells (PBCs), and peripheral blood eosinophils (PBEs) in patients with severe asthma as compared to non-severe asthma and healthy controls (Ban et al., 2015). Recently, some studies suggest association between genetic polymorphisms of autophagy-related gene 5 (ATG5) and asthma (Poon et al., 2012; Martin et al., 2012). Furthermore, Liu and colleagues showed that autophagy inhibition significantly decreased eosinophilia, inflammation, AHR, and IL-5 levels in airway in an asthma experimental model (Liu et al., 2016). However, autophagy role in asthma pathogenesis is poorly understood.

In 2008, Shida and colleagues provided the first evidence that eosinophils generate eosinophil extracellular traps (EETs) capable of killing bacteria in the extracellular space (Shida et al., 2008). Eosinophil extracellular traps (EETs) are

composed by extracellular DNA fibers and intact eosinophil granules that trap and kill microorganisms (Shida et al., 2008; Ueki et al., 2016). EETs release has been described as an important mechanism of innate immune response in allergic diseases (Simon et al., 2011; Ueki et al., 2016). In this context, Dworski and colleagues showed that EETs are present in the airways of asthmatic patients (Dworski et al., 2011). Furthermore, Cunha and colleagues demonstrated that there was a significant increase in EETs formation from bronchoalveolar lavage fluid (BALF) in a murine asthma model (Cunha et al., 2014; Cunha et al., 2016). Increase in EETs formation may contribute to the inflammatory response of asthma, even though, EETs release mechanisms are poorly understood. Studies have shown that autophagy regulates neutrophil extracellular DNA traps (NETs) formation (Kenno et al., 2011; Remijsen et al., 2011). In this context, Pham and colleagues showed positive correlations between NETs release and autophagy in peripheral blood neutrophils in severe asthma patients (Pham et al., 2016). However, autophagy participation in mechanism of eosinophil EETs formation in asthma has not been elucidated.

The present study hypothesized that high levels of autophagy in eosinophils increase EETs formation and enhance airway inflammation in asthma. Therefore, the aim of this study is to investigate the effect of an autophagy inhibitor, 3-methyladenine (3-MA), in EETs formation and in airway inflammation in an experimental asthma model.

2 | MATERIAL AND METHODS

2.1 | Animals

Six-8 week old specific pathogens-free (SPF) female BALB/cJ mice weighing approximately 20 g from the Center for Experimental Biological Models (CeMBE, PUCRS) were used in the experiments. The animals were fed standard ration for rodents and water *ad libitum.* The animals were maintained on a 12-hour light/dark cycle in accordance with the Guiding Principles in the Care and Use of Animals approved by the Council of the American Physiological Society. The experimental protocol was approved by Pontifícia Universidade Católica do Rio Grande do Sul Animal Ethics Committee (protocol number 7910).

2.2 | Experimental asthma protocol and 3-MA treatment

Mice were sensitized subcutaneously with 20 µg of ovalbumin (OVA) (Grade V, Sigma, Missouri, USA) on days 0 and 7. Afterwards, mice were challenged intranasally with 100 µg of OVA on days 14, 15 and 16 (Cunha et al., 2016). The negative control group received subcutaneous and intranasal Dulbecco phosphate buffered saline (DPBS; Gibco, Massachusetts, USA). To investigate the participation of autophagy in EETs release, we used an autophagy inhibitor, 3-MA (Sigma, Missouri, USA). Autophagy inhibitor 3-MA blocks a crucial protein, type III Phosphatidylinositol 3-kinases (PI3K), for the onset of autophagy. The treatment was performed 45 minutes before the three intranasal challenges, with 15 mg/kg of 3-MA intranasal administration (Liu et al., 2016).

2.3 | Total and differential cell counts in BALF

On day 17 of the protocol, the animals were anesthetized with ketamine (0. 4 mg/g) and xylazine (0.2 mg/g), and BALF was collected with 1 mL of phosphate buffered saline (PBS) with 2% fetal bovine serum (FBS). BALF was centrifuged and pellet was resuspended in PBS with 2% FBS for performing total and differential cells count in BALF. The total cells count and cell viability were determined in Neubauer chamber (BOECO, Hamburg, Germany). Differential cells count was done by cytospin preparations (Eppendorf, Wesseling, Germany) and stained with H&E (Newprov, Paraná, Brazil). Four hundred cells were counted under an optical microscope (Olympus, Tokyo, Japan).

2.4 | Analysis of the activity of EPO in BALF

EPO activity was determined by the colorimetric assay according to Strath and colleagues. For the implantation of the protocol, BALF supernatant was incubated with working reagent (0.1 mM O-phenylenediamine (OPD), 0.05 M Tris pH= 8.0, Triton X-100 and 1mM hydrogen peroxide). After that, the reaction was stopped with sulfuric acid 1.0 M. The absorbance was measured at a wavelength of 492 nm (Strath et al., 1985).

2.5 | Lung histology

Lungs were fixed in 10% buffered formalin. Tissue was embedded in paraffin blocks and cut into 5 μm sections. In order to evaluate the inflammatory infiltrate, sections were stained with H&E staining. For evaluating the extent of peribronchial and perivascular inflammatory infiltrate in μm, 10 measurements were performed starting from the beginning of the bronchial or vessel epithelium to the end of the inflammatory infiltrate using Olympus CellSens Standart software (Olympus, Tokyo, Japan). Goblet cells hyperplasia and mucus production were evaluated by alcian blue dye.

2.6 | Assessment of respiratory system mechanics

The animals were anesthetized with ketamine (0.4 mg/g) and xylazine (0.2 mg/g) on day 17 of the protocol. Respiratory system mechanics testing was performed after cannulation of the trachea and the animals were connected to a ventilator (flexiVent, SCIREQ, Montreal, Canada). Three measurements of forced oscillation technique (FOT) were performed during a pause of the respirator (3 seconds). During the ventilation pauses, a frequency oscillatory signal (4-38 Hz) was generated by a loudspeaker and passed through the tracheal cannula of the animal. A four parameter model of tissue impedance with constant phase was fitted to Zrs data to obtain newtonian resistance (Rn) measurements, which is equivalent to airway resistance in mice due to complacency of the chest wall. Tissue damping (G) represents the resistance of small airways where air movement occurs mainly by diffusion while that tissue elastance (H) reflects the energy conservation in the alveolus. The data were analyzed in specific software (flexiWare, SCIREQ, Montreal, Canada), where airway resistance and elastic properties (viscosity and elasticity) of the lung were measured through a pulmonary impedance (Hantos et al., 1997; Zosky et al., 2012).

2.7 | Cytokine levels in lung

Lungs were homogenized in PBS 1x and interleukin (IL)-5, IL-13, interferon (IFN)-γ, tumor necrosis factor (TNF)-α, IL-1-β, and IL-10 levels were measured by multiplex assay using a Milliplex MAP mouse kit (MILLIPLEX®, Millipore, Germany) and Procarta Plex Multiplex immunoassay (Thermo-Life Technology, Massachusetts,

USA) according to the manufacturer's recommendations. Results were analyzed using the xPONENT® Solutions software (Luminex Corporation).

2.8 | Lung preparation

For determination of oxidative stress parameters, the lungs were homogenized (1:10, w/v) in 20 mM sodium phosphate buffer pH=7.4, containing 140 mM potassium chloride. For mitochondrial energy metabolism analyses (complex II, succinate dehydrogenase (SDH) and complex IV), lungs were frozen and thawed three times to disrupt the mitochondrial membranes. After, lungs were homogenized (1:20, w/v) in SETH buffer (250 mM sucrose, 2 mM EDTA, 10 mM trizma base, 50 UI/mL heparin), pH=7.4. For NA^+,K^+-ATPase activity analyses, lungs were homogenized (1:10, w/v) in 0.32 mM sucrose solution containing 5.0 mM HEPES and 1.0 mM EDTA, pH= 7.5. After the lungs were homogenized they were centrifuged at 800 ×g for 10 min at 4°C and the supernatants were collected and used for the analyses.

2.9 | ROS assay in lung

ROS production was measured by the colorimetric assay based in the oxidation of the 2'7' dichlorofluorescein (H2DCF-DA). The samples were incubated in 100 μM H2DCF-DA. At the end of the reaction, dichlorofluorescein (DCF) was formed and measured in a spectrophotometer at 488 nm of excitation and 525 nm of emission. The levels of ROS were expressed as DCF nmol/mg protein (LeBel et al., 1990).

2.10 | Glutathione peroxidase (GPx) activity in lung

GPx activity was measured by using tert-butylhydroperoxide as substrate. The samples were incubated in 2 mM glutathione, 0.15 U/ml glutathione reductase, 0.4 mM azide, 0.5 mM tert-butylhydroperoxide, and 0.1 mM nicotinamide adenine dinucleotide phosphate (NADPH). One GPx unit was defined as 1 μmol of NADPH consumed per minute. The decay of the NADPH was monitored at 340 nm in a spectrophotometer. GPx activity was plotted in GPx units/mg of protein (Wendel, 1981).

2.11 | Superoxide dismutase (SOD) assay in lung

SOD activity was analyzed by the method described by Marklund. Inhibition of the pyrogallol autoxidation occurs in the presence of SOD, and its activity can be indirectly measured in a spectrophotometer at 412 nm. A calibration curve was performed with purified SOD as standard. SOD activity was expressed in units of SOD/mg protein (Marklund, 1985).

2.12 | Catalase (CAT) assay in lung

CAT activity was based on the measurement of the disappearance in hydrogen peroxide consumption at 240 nm in a reaction containing 20 mM hydrogen peroxide, 0.1 of Triton X-100, 10 mM potassium phosphate at pH=7.4. One CAT unit is defined as hydrogen peroxide 1 μM consumed per minute. CAT activity was represented in units of CAT/mg protein (Aebi, 1984).

2.13 | Complex II, SDH and complex IV activity in lung

Lung samples were incubated in buffer containing 40 mM potassium phosphate pH =7.4, 16 mM sodium succinate and 8 mM 2, 6-dichloroindophenol (DCIP). After that, 4 mM sodium azide, 7 mM rotenone and 40 mM DCIP were added. The enzymatic activity of complex II in lung was measured after a decrease in the absorbance by the reduction of DCIP at 600 nm. The enzymatic activity of SDH was measured after depletion of the absorbance by the reduction of the DCIP in the presence of phenazinemethasulfate (PMS) at 600 nm. The results were reported as nmol/min/mg of protein (Fischer et al., 1985). Complex IV activity was measured by decreasing of absorbance due to oxidation and reduction of cytochrome c at 550 nm. Samples were added to a buffer containing 10 mM potassium phosphate, pH 7.0 and 0.6 mM n-dodecyl-β-D-maltoside. The reaction was initiated by the addition of 7 μg of cytochrome C. The results were expressed as nmol/min/mg of protein (Rustin et al., 1994).

2.14 | NA^+, K^+-ATPase activity in lung

NA^+,K^+-ATPase activity was determined according to the method of Wyse and colleagues. Samples were added to a buffer containing 5.0 mM magnesium chloride, 80.0 mM sodium chloride, 20.0 mM potassium chloride and 40.0 mM Tris-

hydrochloric acid, pH 7.4. The reaction was initiated by the addition of adenosine triphosphate (ATP) to a final concentration of 3.0 mM. Controls were added 1.0 mM of ouabain. The results were expressed as nmol inorganic phosphate released per min/mg of protein (Wyse et al., 2000).

2.15 | Quantification of extracellular DNA traps and immunofluorescence in BALF eosinophils

Extracellular DNA concentration was measured in LBA supernatant using the Quant-iT dsDNA HS kit (Invitrogen, Carlsbad, USA) and measured in Quibit 2.0 fluorimeter (Invitrogen, Carlsbad, USA), according to the manufacturer's recommendations. To visualize the EETs formation by immunofluorescence microscopy, BALF eosinophils (2×10^5/mL) were plated in 8-chamber culture slides (BD Falcon, New Jersey, USA) and incubated at 37°C with 5% carbon dioxide for 1 hour. Afterwards, cells were fixed with 4% paraformaldehyde (PFA) for 45 minutes and incubated with primary antibodies, anti-EPO and anti-histone H2B (1:250, Santa Cruz Biotechnology, Dallas, USA) for 45 minutes. After this time, cells were incubated for 30 minutes with secondary antibodies, FITC anti-goat (1:100, Santa Cruz Biotechnology, Dallas, USA) and Alexa fluor 633 anti-goat (1:100 in PBS, Invitrogen, Carlsbad, USA). Finally, the cells were stained with Hoechst 33342 DNA dye (1: 2000, Invitrogen, Carlsbad, USA) for 4 minutes. Images were performed in Zeiss LSM 5 Exciter confocal microscope (Zeiss LSM5, Oberkohen, Germany).

2.16 | Analysis of cell death in BALF eosinophils

BALF eosinophils were analyzed for apoptosis by Annexin V/Propidium Iodide (PI), according to the manufacturer's instructions (BD Pharmingen). Cells were incubated with Annexin V-FITC and PI and analyzed by flow cytometry (FACS Canto II, BD Bioscience). Data were analyzed using FlowJo software version X.0.7 (TreeStar, Oregon, USA).

2.17 | Analysis of light chain 3B (LC3B) and protein kinase B (AKT) in lung by Western blot

Lungs were lysed in CHAPS lysis buffer (10 mM Tris-HCl pH 7.5, 1 mM magnesium chloride, 2.1 mM EDTA, 0.1 mM PMSF, 5 mM β-mercaptoethanol, 0.5% Chaps, 10%

glycerol). Proteins (20 µg) were separated by electrophoresis on 10% polyacrylamide gel. Proteins were then transferred to a nitrocellulose membrane (GE Healthcare Life Sciences, Pennsylvania, USA). The membrane was blocked with BSA 5% in tris buffered saline (TBST) for 30 minutes. After blocking, the membrane was incubated with primary antibodies anti-LC3B (1:200 in BSA, Thermo-Life Technology, Massachusetts, USA), anti-AKT (1:500 in BSA 5%, Cell Signaling Technology, Massachusetts, USA) and anti-β-Actin (1:1000 in BSA 5%, Cell Signaling Technology, Massachusetts, USA) overnight. Finally, it was incubated with secondary antibody, HRP anti-rabbit (1:1000 in BSA 5%, Cell signaling, Massachusetts, USA). The quantification was performed using Chemiluminescent photo finder (Kodak/Carestream, model Gel Logic 2200 PRO Imaging System). The intensity of the bands was normalized by β-Actin using Image J (Rueden et al., 2017).

2.18 | Detection and quantification of acidic vesicle organelles (AVOs) in BALF eosinophils

For the detection of acid compartments of the cell, we used acridine orange (AO; Sigma, Missouri, USA) dye, which emits red fluorescence in acidic vesicles and green fluorescence in the cytoplasm and nucleus. To visualize the formation of AVOs, BALF eosinophils (2 x 10^5/mL) were plated in 8-chamber culture slides and incubated at 37°C with 5% CO_2 for 1 hour. After this period the cells were incubated with the AO dye at the final concentration of 1µg/mL for 15 minutes and visualized by Zeiss LSM 5 Exciter confocal microscope (Zeiss LSM5, Oberkohen, Germany). To quantify the formation of AVOs, BALF cells were incubated with AO in the final concentration of 1µg/mL and were analyzed by flow cytometry (FACS Canto II, BD Bioscience). Data were analyzed using FlowJo software version X.0.7 (TreeStar, Oregon, USA).

2.19 | Analysis of nuclear factor kappa B (NFκB) p65 and LC3B proteins in lung by immunofluorescence

The histological sections were dewaxed in xylol and rehydrated in water. After, the antigen recovery was performed with 10 mM citrate (pH=9.0) for 10 minutes then the endogenous peroxidases were blocked with 0.3% hydrogen peroxide in methanol for

20 minutes. After this period, slices were blocked with 10% bovine serum albumin (BSA) in PBS for 30 minutes. After that, sections were incubated for 40 minutes with primary antibodies, anti-NFκB p65 or anti-LC3B (1:500, Santa Cruz Biotechnology, Dallas, USA), followed by secondary antibody, FITC anti-rabbit (1:250, Santa Cruz Biotechnology, Dallas, USA) for 30 minutes. After, sections were stained with Hoechst 33342 (1:2000, Invitrogen, Carlsbad, USA) for 4 minutes. Images were performed on a Zeiss LSM 5 Exciter confocal microscope (Zeiss LSM5, Oberkohen, Germany).

2.20 |Analysis of LC3B in BALF cells by immunofluorescence

BALF cells (2 x 10^5/mL) were plated in 8-chamber culture slides (BD Falcon, New Jersey, USA) and incubated at 37°C at 5% CO_2 for 1 hour. After this period, the cells were fixed with 4% PFA for 15 minutes and the cells were permeabilized with 0.1% triton X-100 in PBS for 15 minutes. The cells were then incubated with primary antibody, anti-LC3B (0.5 µg/ml, Invitrogen, Carlsbad, USA) for 1 hour, followed by incubation for 40 minutes with secondary antibody, FITC anti-rabbit (1:100, Thermo-Life Technology, Waltham, USA). Afterwards, cells were stained with Hoechst 33342 (1:2000; Invitrogen, Carlsbad, USA) for 4 minutes and visualized by confocal microscope Zeiss LSM 5 Exciter (Zeiss LSM5, Oberkohen, Germany).

2.21 | Protein levels determination in lung

The proteins content in lungs was determined using Qubit™ Protein Assay Kit (Invitrogen, Carlsbad, USA) for cytokines analyses. Lowry assay for proteins from oxidative stress, mitochondrial energy metabolism and Na^+,K^+-ATPase (Lowry et al., 1951). In accordance to Bradford for western blot proteins analyses (Bradford, 1976).

2.22 |Statistical analysis

Data were expressed as mean ± standard deviation. The Shapiro-Wilk normality test was used to evaluate the normal distribution of the data. We used ANOVA followed by Tukey pos-hoc and the adopted significance level was $p \leq 0.05$. Statistical analysis and graphs were performed using the Graphpad Prism Software, version 5 (GraphPad Software, San Diego, USA).

3 | RESULTS

3.1 | 3-MA reduces inflammation, EPO activity and goblet cells hyperplasia in airways

Firstly, we observed that OVA group had a significant increase in the total cells count, as well as an increase in eosinophils, neutrophils, macrophages and lymphocytes cells count compared to the control group. In addition, we showed that the 3-MA-treated OVA group had a decrease in total cells count as well as a decrease in eosinophils and neutrophils cells count in BALF compared to the OVA group (Figure 1A-E,G). In EPO granular protein analysis, we demonstrated that OVA significantly increased the levels of EPO in BALF while 3-MA administration decreased significantly EPO activity (Figure 1F). In histopathological analysis we demonstrated an increase in inflammatory cells infiltration located in peribronchial and perivascular areas in OVA-challenged mice when compared to the control group. On the other hand, we observed that 3-MA-treated OVA group had a reduction in pulmonary influx of cells located peribronchial and perivascular areas compared to the OVA group (Figure 1H-J). In addition, we demonstrated that OVA challenge mice had an increase in goblet cells and mucus production compared to the control group. In contrast, we demonstrated that 3-MA-treated OVA group had a reduction in goblet cells and mucus production compared to the OVA group (Figure 1K).

3.2 | 3-MA improves respiratory system mechanics

Tissue damping and tissue elastance were significantly increased in the OVA-challenged mice compared to the DPBS group. In contrast, 3-MA treatment was able to reduce significantly tissue damping and tissue elastance compared to the OVA group. We did not observe differences between the groups in airway resistance (Figure 2A-C).

3.3 | 3-MA decreases inflammatory cytokines and NFκB p65 in lung

In cytokines analyses in lung, we showed that OVA-challenged mice had an increase in IL-5, IL-13, IFN-Y, TNF-α and IL-1β when compared to the control group. On the other hand, administration of 3-MA attenuated the levels of IL-5, IFN-Y and IL-13 in the lung compared to the OVA group (Figure 2D-I). We did not observe differences

between the groups in IL-10 levels. In addition, we observed that OVA group had a significantly increased in NFκB p65 when compared to the control group while 3-MA treatment decreased NFκB p65 in lung (Figure 2J).

3.4 | 3-MA decreases ROS production and increases catalase activity in lung

After that, we evaluated the effect of 3-MA in oxidative stress in OVA-challenged mice. We demonstrated that OVA group had a significantly increase in ROS production in lung when compared to the control group. In addition, ROS formation in the 3-MA-treated OVA group had a decrease compared to the OVA group (Figure 3A). Afterwards, we also evaluated the effect of 3-MA in the enzymatic antioxidant defenses. We showed that OVA group promoted a significant decrease in CAT and GPx activity when compared to the control group (Figure 3C,D). On the other hand, 3-MA was able to increase CAT activity in lung compared to the OVA group (Figure 3C). In addition, we did not observe any significant difference in SOD activity between groups (Figure 3B). We also showed that the OVA group had a significant increase in SOD/CAT ratio when compared to the control group while 3-MA decreased SOD/CAT ratio in lung (Figure 3E).

3.5 | 3-MA improves mitochondrial energy metabolism and NA^+,K^+-ATPase activity in lung

We investigated OVA effect in parameters of the mitochondrial energy metabolism (SDH, complex II, complex IV) in lung. We observed that the OVA group had a significant decrease in SDH, complex II and complex IV activity when compared to the control group, suggesting that OVA-challenged mice compromise electron transport chain function in lung. In addition, administration of 3-MA was able to increase significantly SDH and complex II activity in lung compared to the OVA group (Figure 3F-H). Moreover, we showed that OVA group had a decrease in NA^+,K^+-ATPase when compared to the control group while 3-MA significantly increased NA^+,K^+-ATPase activity in lung (Figure 3I).

3.6 | EETs release in airway of OVA-challenged mice depend on autophagy without cell death

OVA-challenged mice had an increase in extracellular DNA concentrations in BALF compared to the DPBS group. In immunofluorescence microscopy, we showed that eosinophils from asthmatic mice released EETs colocalized with EPO, but did not colocalized with histone H2B (Figure 4A-B). Furthermore, autophagy inhibitor 3-MA decreased extracellular DNA concentrations in BALF from OVA-challenged mice. Similarly, in immunofluorescence microscopy we did not observe EETs formation in BALF eosinophils in 3-MA-treated OVA group, confirming our findings (Figure 4A-B). In addition, EETs release was not due to cell death since cell viability remained high between the groups, showing that most cells present negative staining for annexin-V and PI (Figure 4C).

3.7 | 3-MA decreases AVOs formation and LC3B immunocontent in airway

We showed that OVA-challenged mice had an increase in AVOs formation in BALF eosinophils stained with AO by immunofluorescence analysis. In addition, 3-MA was able to reduce AVOs in BALF eosinophils when compared to the OVA group (Figure 5A). Similarly, in cytometry analysis, we observed that in OVA-challenged mice there was an increase in AVOs while 3-MA decreased AVOs formation in BALF cells (Figure 5B-C). After that, we analyzed LC3B protein that is an indicator of autophagosome formation. We showed that in OVA-challenged mice there was an increase in LC3B in BALF eosinophils and lung tissue by immunofluorescence and Western blot analysis. In contrast, we showed that autophagy inhibitor 3-MA was able to reduce LC3B in BALF eosinophils and lung tissue when compared to the OVA group (Figure 5D-F).

3.8 | 3-MA decreases AKT immunocontent in lung

We demonstrated that OVA group had a significantly decrease in AKT immunocontent in lung when compared to the control group. In addition, 3-MA-treated OVA group had an increase in AKT when compared to the OVA group (Figure 5G).

4 | DISCUSSION

Asthma is a chronic inflammatory disease characterized by an increase in airway eosinophil infiltration (Lambrecht et al., 2015). Although, there is an increase in DNA extracellular traps formation by eosinophils, mechanism of EETs release and their pathophysiologic role in asthma is poorly understood (Dworski et al., 2011; Cunha et al., 2014). Recently, studies have demonstrated the role of autophagy in asthma immunopathology. Our study provides the first evidence that autophagy is required for EETs formation in airway in a murine model of asthma. Furthermore, we demonstrated that autophagy inhibition improves significantly airway inflammation, respiratory system mechanics, oxidative stress, mitochondrial energy metabolism, Na^+, K^+ATPase activity and reduces EETs release.

Evidence has demonstrated that high levels of autophagy increase physiopathology in asthma (Liu et al., 2016; Jiang et al., 2017). Studies suggest association between genetic polymorphisms of ATG5 and airway remodeling as well as in decrease in lung function in asthma (Poon et al., 2012; Martin et al., 2012). Ban and colleagues demonstrated high levels of autophagy in sputum granulocytes of patients with severe asthma as compared with non-severe asthma and healthy controls (Ban et al., 2015). Poon and colleagues showed in transmission electron microscopy an increase of autophagosomes in fibroblasts and epithelial cells from bronchial biopsy tissue of asthmatic patients (Poon et al., 2012). Moreover, studies have shown that autophagy play an important role in differentiation and survival of cells of the immune system (Conwayet al., 2013). In this study, in order to evaluate the role of autophagy in asthma, an allergic asthma model was established. We showed that in the OVA group there was a significant increase in airway inflammatory cells, goblet cells hyperplasia, EPO activity and a decrease in respiratory system mechanics, a typical pathologic feature of asthma. In this model there is a significant high influx of eosinophils in airway. We showed that autophagy inhibition with 3-MA decreased total cells count as well as eosinophils and neutrophils cells count in BALF when compared to the OVA group. Moreover, we observed that the 3-MA-treated OVA group had a reduction in pulmonary influx of cells when compared to the OVA group. Our results are corroborated by studies which show that autophagy inhibition decrease inflammatory cells especially the amount of eosinophils in airway in an asthma model (Liu et al., 2016, Jiang et al.,

1997). In this study, we showed that in OVA group there was an increase in eosinophil migration into airway and 3-MA was able to decrease lung eosinophilia. So, we decided to evaluate EPO activity in BALF, which is a cytotoxic granular protein of the eosinophils (Sanz et al, 1997). In EPO granular protein analysis, we demonstrated that OVA significantly increased the levels of EPO in BALF while the administration of 3-MA decreased significantly EPO activity. In this context, Ban and colleagues showed that autophagy inhibition decreased the expression of ECP in human eosinophil-like cells (HL-60) stimulated with IL-5 (Ban et al., 2015). After that, we decided to evaluate autophagy role in airway goblet cells. We demonstrated that in the 3-MA-treated OVA group there was a reduction in goblet cells and mucus production compared to the OVA group. In agreement to our result, studies showed that autophagy inhibition decreases goblet cells and mucus hypersecretion in airway from an asthma model (Pham et al., 2016; Jiang et al., 2017). Moreover, Poon and colleagues showed an association between ATG polymorphism and asthma as well as the reduction of forced expiratory volume in 1 second (FEV1) (Poon et al., 2012). To assess whether autophagy inhibition has an effect in respiratory system mechanics in OVA-challenged mice, we measured airway resistance, tissue damping and tissue elastance. We showed that 3-MA was able to significantly reduce tissue damping and tissue elastance, but did not alter airway resistance when compared to the OVA group. In accordance to our results, Liu and colleagues observed an improve in lung function in an autophagy-related gene 5 (Atg5) knockdown murine asthma model (Liu et al., 2016). It probably occurred because of a decrease in mucus hypersecretion and in airway inflammation. Thus, 3-MA treatment can be an important alternative to decrease airway inflammation, goblet cells hyperplasia, and improve respiratory system mechanics in asthma via suppression of autophagy.

Inflammatory cytokines play a key role in airway inflammation, hyperresponsiveness, mucus hypersecretion and airway remodeling in asthma (Barnes, 2008). Recently, autophagy function has been widely investigated in adaptive and innate immunity, more specifically in Th2 immune response. Furthermore, autophagy is essential for lymphocyte development and survival (Puleston et al., 2014). We showed that in OVA-challenged mice there was an increase in IL-5, IL-13, IFN-Y, TNF-α and IL-1β cytokines when compared to the control group. On the other hand, autophagy inhibition with 3-MA attenuated the level

of IL-5, IFN-Y and IL-13 in the lung when compared to the OVA group. In this context, studies showed that IL-5, IFN-Y and IL-13 cytokines enhances autophagy (Jyothula et al., 2013; Ban et al., 2015). In agreement to our results, studies have showed that autophagy inhibition decreases inflammatory cytokines in lung (Liu et al., 2016; Jiang et al., 2017). In this context, we hypothesized that autophagy inhibition could reduce inflammatory cytokines in lung via NFκB p65 inhibition. In active NFκB, p65 and p50 subunits translocate to the nucleus and increase the production of inflammatory cytokines (Oka et al., 2000). Moreover, autophagy is required for the activation of NFκB (Criollo et al., 2012). We observed that in the OVA group there was an increase in NFκB p65 while the 3-MA treatment decreased NFκB p65 in lung. We suggested that in asthma 3-MA treatment can decrease NFκB p65 and, consequently, reduce inflammatory cytokines in lung.

Evidence has shown that oxidative stress plays an important role in the pathogenesis of asthma (Andreadis et al., 2003; Cunha et al., 2016). Moreover, mitochondrial ROS is a main source for signalling autophagy (Filomeni et al., 2015). In contrast, antioxidant defenses serve as natural down regulators of autophagy (Scherz-Shouval et al., 2011). We evaluated whether autophagy inhibition affects oxidative stress in OVA-challenged mice. We demonstrated that in the OVA group there was a significant increase in ROS production in lung when compared to the control group. We showed that in the OVA group there was a significant decrease in CAT and GPx activity, but there was not an alteration in SOD in lung, suggesting a disbalance in oxidant-antioxidant status. SOD catalyzes the dismutation of superoxide, and CAT and GPx catalyze the reduction of hydrogen peroxide (Cunha et al, 2011). In this context, we suggested that an increase in ROS formation did not increase the consumption of the SOD that catalyzes the dismutation of superoxide in hydrogen peroxide. However, normal levels of SOD increase hydrogen peroxide formation while insufficient levels of CAT and GPx enhance hydrogen peroxide accumulation, increasing oxidative stress in lung. In addition, ROS formation in the 3-MA-treated OVA group had a decrease when compared to the OVA group. In this context, Dickinson and colleagues showed that autophagy activity was required for the increase in intracellular superoxide production in airway epithelial cells (Dickinson et al., 2018). Moreover, we showed that autophagy inhibition with 3-MA was able to increase CAT activity in lung when compared to the OVA group. We demonstrated

that in the OVA group there was a significant decrease in AKT immunocontent in lung while in the 3-MA-treated OVA group we could observe an increase in AKT. Studies have shown that ROS production activates AKT, deactivates glycogen synthase kinase 3β (GSK-3β), and consequently, activates nuclear factor erythroid 2-related factor 2 (Nrf2). Nrf2 translocates to the nucleus and binds to the antioxidant response element (ARE) activating the transcription of antioxidant enzymes (Ma et al., 2016). Thus, we demonstrated that autophagy inhibition with 3-MA reduces oxidative stress in lung in an asthma model.

The high flux of electrons through the mitochondrial electron transport chain predisposes ROS generation. Exposition of cells to ROS may result in oxidative damage to the mitochondria which may inactivate the electron transport chain (Reddy et al, 2006). In this context, studies have shown an association between mitochondrial dysfunction and pulmonary inflammatory diseases (Cunha et al., 2014; Aguilera-Aguirre et al., 2009). We observed that in the OVA group there was a significant decrease in SDH, complex II and complex IV activity when compared to the control group, suggesting that in OVA-challenged mice there may be a damage in the respiratory chain function in lung. Aguilera-Aguirre and colleagues demonstrated that mitochondrial dysfunction is involved in the inflammation of the airways in allergic patients (Aguilera-Aguirre et al, 2009). Moreover, Mabalirajan and colleagues showed a decrease in complex IV activity as well as reducton in ATP levels in the lungs of asthmatic mice (Mabalirajan et al., 2008). We showed that autophagy inhibition with 3-MA was able to increase significantly SDH and complex II activity in lung. We suggested that 3-MA improved mitochondrial energy metabolism due to a decrease in oxidative stress in lung, and consequently, reduced the damage in the electron transport chain.

Na^+, K^+-ATPase controls cellular ionic gradient and its activity is susceptible to an increase in ROS formation and to ATP depletion (Schweinberger et al., 2014). Reduction in Na^+, K^+-ATPase activity alters electrical membrane potential, increases activation of leukocytes, downregulates the responses to β-agonists in β-adrenergic receptors, and increases bronchoconstriction (Agrawal et al., 2005). In consequence to the damage of the electron transport chain and ATP reduction, we observed that in the OVA group there was a significant decrease in the NA^+,K^+-ATPase activity. In accordance to our result, Agrawal and colleagues showed a decrease in Na^+,K^+-

ATPase activity in leucocytes in asthmatic patients (Agrawal et al., 2005). Moreover, we showed that 3-MA treatment significantly increased NA^+,K^+-ATPase activity in lung. We suggested that autophagy inhibition with 3-MA increased Na^+,K^+ATPase due to the improvement of mitochondrial energy metabolism in lung, and consequently, restored ATP levels.

Studies have shown an increase in EETs formation in airway in asthmatic patients as well as in asthma model in mice (Dworski et al., 2011; Cunha et a., 2014). EETs formation in airway may increase airway damage and mucus viscosity, and consequently, decrease lung function in asthma. We showed that OVA-challenged mice presented an increase in extracellular DNA concentrations. Moreover, in immunofluorescence microscopy, we showed that eosinophils from asthmatic mice released EETs colocalized with EPO. We demonstrated that EETs were not colocalized with histone HB2, which suggests that the DNA released by EETs is of mitochondrial origin. Histones compact and protect nuclear DNA, however, in mitochondrial DNA there are no histones (Alexeyev et al, 2013). Afterwards, we investigated whether autophagy would be necessary for EETs formation in the airway in OVA-challenged mice. Administration of autophagy inhibitor, 3-MA, decreased extracellular DNA concentrations in BALF from OVA-challenged mice. Similarly, in immunofluorescence microscopy we did not observe EETs formation in BALF eosinophils in the 3-MA-treated OVA group, which corrobarates our findings. Altogether, these data indicate that autophagy is indispensable for EETs formation in airway in OVA-challenged mice. Moreover, autophagy inhibition with 3-MA may reduce airway immunopathology in asthma through the decrease in EETs release. Some studies have reported that EETs release is due to eosinophil death; others have shown that they can remain viable (Yousefi et al., 2008; Cunha et al., 2016; Ueki et al., 2016). We observed that EETs release was not due to cell death once we have demonstrated that BALF cell viability remained high in control, asthmatic, and treated mice groups. Thus, we demonstrated that EETs release in asthma is dependent of autophagy in an active process without cell death.

Autophagy induces the cytoplasmic sequestration of proteins from the lytic component and it is characterized by the formation of AVOs, such as autolysosomes (Anderson et al, 1984). We observed that OVA-challenged mice had an increase in AVOs formation while that autophagy inhibition with 3-MA was able to reduce AVOs

in BALF eosinophils when compared to the OVA group. Studies have shown an increased in autophagosomes number in cells from asthmatic patients and in experimental asthma models (Ban et al., 2013; Liu et al., 2016; Pham et al., 2016). Typical feature of autophagy is the formation of double-membrane autophagosomes. LC3 is a protein needed for autophagosome formation and is an indicator of autophagosome (Cheng et al., 2017). Ban and colleagues showed an increase in expression of LC3-II in sputum granulocytes from patients with severe asthma in relation to patients with non-severe asthma and healthy controls (Ban et al., 2013). Similarly, we showed that LC3B immunocontent was significantly higher in BALF eosinophils and lung tissue in OVA-challenged mice than in the control group. We showed that 3-MA treatment decreased LC3B in BALF eosinophils and lung tissue when compared to the OVA group. Moreover, we demonstrated that in the OVA group there was a significant decrease in AKT immunocontent in lung while the 3-MA-treated OVA group showed an increase in AKT when compared to the OVA group. In this context, AKT promotes mammalian target of rapamycin (mTOR) activation, and consequently, suppress autophagy (Degtyarev et al., 2008). Altogether, these data indicate that 3-MA treatment was able to reduce autophagy in BALF eosinophils and lung tissue in OVA-challenged mice.

In summary, this is the first study to demonstrate that viable eosinophils release EETs dependent of autophagy in airway of a murine model of asthma. Autophagy inhibition with 3-MA improved airway inflammation, respiratory system mechanics, oxidative stress, mitochondrial energy metabolism, and NA^+,K^+ATPase activity, and also reduced EETs formation in lung from asthmatic mice. Therefore, we could show that modulation of eosinophils autophagy regulate the activation process of EETs release in asthma.

ACKNOWLEDGEMENTS

We thank Carolina Luft, Rodrigo Godinho de Souza, Betânia Souza Freitas and Krist Helen Antunes Fernandes for their technical assistance. This study was financed in part by the Coordenação de Aperfeiçoamento de Pessoal de Nível Superior (CAPES) and Conselho Nacional de Desenvolvimento Científico e Tecnológico (CNPq) - Brazil.

CONFLICTS OF INTEREST

The authors declare no commercial or financial conflict of interest.

AUTHOR CONTRIBUTIONS

JSS and AAC designed the studies. JSS, AAC, GLA, DBK, MS, EPM, FF, RBG and RVB contributed to the data collection. JSS, AAC, PMP and ATW analysed and interpreted the work. JSS and AAC wrote the manuscript. All authors have read, revised and approved the final version of this manuscript.

REFERENCES

Aebi, H. Catalase, in vitro. (1984). Methods Enzymology, 105, 121-126.
DOI: https://doi.org/10.1016/S0076-6879(84)05016-3

Agrawal, A., Agrawal, K. P., Ram, A., Sondhi, A., Chhabra, S. K., Gangal, S. V., & Dolly, M. (2005). Basis of Rise in Intracellular Sodium in Airway Hyperresponsiveness and Asthma. Lung, 183, 375-387.
DOI: 10.1007/s00408-005-2549-0

Aguilera-Aguirre L, Bacsi A, Saavedra-Molina A, Kurosky A, Sur S, & Boldogh I. (2009). Mitochondrial dysfunction increases allergic airway inflammation. Journal Immunology, 183, 5379-5387.
DOI: 10.4049/jimmunol.0900228

Alexeyev, M., Shokolenko, I., Wilson, G., & LeDoux, S. (2010). The Maintenance of Mitochondrial DNA Integrity-Critical Analysis and Update The unfolded protein response in lung disease. Proceedings of the American Thoracic Society, 7, 356-362.
DOI: 10.1101/cshperspect.a012641

Andreadis, A. A., Hazen, S. L., Comhair, S. A., & Erzurum, S. C. (2003). Oxidative and nitrosative events in asthma. Free Radical Biology and Medicine, 35, 213-225.
DOI: https://doi.org/10.1016/S0891-5849(03)00278-8

Barnes, P. J. (2008). The cytokine network in asthma and chronic obstructive pulmonary disease. The Journal of Clinical Investigation, 118, 3546-3456.
DOI: 10.1172/JCI36130

Bradford, M. M. (1976) A rapid and sensitive method for the quantitation of microgram quantities of protein utilizing the principle of protein-dye binding. Analytical Biochemistry, 72, 248-254.

DOI: https://doi.org/10.1016/0003-2697(76)90527-3

Chen, Z. H., Kim, H. P., Sciurba, F. C., Lee, S. J., Feghali-Bostwick, C., Stolz, D. B., … Choi, A. M. (2008). Egr-1 regulates autophagy in cigarette smoke-induced chronic obstructive pulmonary disease. PLoS One, 3, e3316.

DOI: 10.1371/journal.pone.0003316

Comhair, S. A., & Erzurum, S. C. (2010). Redox control of asthma: molecular mechanisms and therapeutic opportunities. Antioxidants & Redox Signaling, 12, 93-124.

DOI: 10.1089/ars.2008.2425

Conway, K.L., Kuballa, P., Khor, B., Zhang, M., Shi, H. N., Virgin, H. W., & Xavier, R. J. (2013). ATG5 regulates plasma cell differentiation. Autophagy, 9, 528-537.

DOI: 10.4161/auto.23484

Criollo, A., Chereau, F., Malik, S. A., Niso-Santano, M., Mariño, G., Galluzzi, L., … Kroemer, G. (2012). Autophagy is required for the activation of NFκB. Cell Cycle, 11, 194-199.

DOI: 10.4161/cc.11.1.18669.

Cunha, A. A., Nuñez, N. K., Souza, R. G., Vargas, H. M. V., Silveira, J. S., Antunes, G. L., … Pitrez, P. M. (2016). Recombinant human deoxyribonuclease therapy improves airway resistance and reduces DNA extracellular traps in a murine acute asthma model. Experimental Lung Research, 42, 66-74.

DOI: https://doi.org/10.3109/01902148.2016.1143537

Cunha, A. A., Porto, B. N., Nuñez, N. K., Souza, R. G., Vargas, M. H., Silveira, J. S., … Pitrez, P. M. (2014). Extracellular DNA traps in bronchoalveolar fluid from a murine eosinophilic pulmonary response. Allergy, 69, 1696-1700.

DOI: 10.1111/all.12507.

Cunha, M. J., Cunha, A. A., Scherer, E. B., Machado, F. R., Loureiro, S. O., Jaenisch, R. B., ... Wyse, A. T. (2014). Experimental lung injury promotes alterations in energy metabolism and respiratory mechanics in the lungs of rats: prevention by exercise. Molecular Cell Biochemical, 389, 229-238.

DOI: 10.1007/s11010-013-1944-8

Degtyarev, M., De Mazière, A., Orr, C., Lin, J., Lee, B. B., Tien, J. Y., … Lin, K. (2008). Akt inhibition promotes autophagy and sensitizes PTEN-null tumors to lysosomotropic agents. Journal Cell Biology, 183, 101-116.

DOI: 10.1083/jcb.200801099.

Dworski, R., Simon, H. U., Hoskins, A., & Yousefi, S. (2011). Eosinophil and neutrophil extracellular DNA traps in human allergic asthmatic airways. Journal Allergy Clinical Immunology, 127, 1260-1266.

DOI: 10.1016/j.jaci.2010.12.1103.

Filomeni, G., Zio D. D., & Cecconi F. (2015). Oxidative stress and autophagy: the clash betweendamage and metabolic needs. Cell Death & Differentiation, 22, 377–388.

DOI: 10.1038/cdd.2014.150

Fischer, J. C., Ruitenbeek, W., Berden, J. A., Trijbels, J. M. F, Veerkamp, J. H., Stadhouders, … Janssen, A. J. M. (1985). Differential investigation of the capacity of succinate oxidation in human skeletal muscle. Clinical Chemical Acta, 153, 23-36.

DOI: https://doi.org/10.1016/0009-8981(85)90135-4

Hantos, Z., Daróczy, B., Suki, B., Nagy, S., & Fredberg, J. J. (1992). Input impedance and peripheral inhomogeneity of dog lungs. J Applied Physiol, 72, 168-178.

DOI: https://doi.org/10.1152/jappl.1992.72.1.168

Jyothula, S. S., & Eissa, N. T. (2013). Autophagy and role in asthma. Current Opinion in Pulmonary Medicine, 19, 30-35.

DOI: 10.1097/MCP.0b013e32835b1150

Kenno, S., Perito, S., Mosci, P., Vecchiarelli, A., & Monari C. (2016). Autophagy and Reactive Oxygen Species Are Involved in Neutrophil Extracellular Traps Release Induced by C. albicans Morphotypes. Frontier Microbiology, 8, 879-893.

DOI: 10.3389/fmicb.2016.00879.

Lambrecht, B. N., Hammad, H. (2015). The immunology of asthma. Nature Immunology, 16, 45-56.

doi: 10.1038/ni.3049

LeBel, C. P., Ischiropoulos, H., & Bondy, S. C. (1992). Evaluation of the probe 2',7'-dichlorofluorescin as an indicator of reactive oxygen species formation and oxidative stress. Chemical Research Toxicology, 5, 227-231.

DOI: 10.1021/tx00026a012

Li, C., Liu, H., Sun, Y., Wang, H., Guo, F., Rao, S., Deng, J., Zhang, Y., Miao, Y., Guo, C., … Jiang C. (2009). PAMAM nanoparticles promote acute lung injury by

inducing autophagic cell death through the Akt-TSC2-mTOR signaling pathway. Journal Molecular Cell Biology, 1, 37-45.
DOI: 10.1093/jmcb/mjp002

Liu, J. N., Suh, D. H., Trinh, H. K., Chwae, Y. J., Park, H. S., & Shin, Y. S. (2016). The role of autophagy in allergic inflammation: a new target for severe asthma. Experimental Molecular Medicine, 48, e243.
DOI: 10.1038/emm.2016.38

Lowry, O. H., Rosebrough, N. J., Farr, A. L., & Randall, R. J. (1951). Protein measurement with the Folin phenol reagent. Journal of Biological Chemistry, 193, 265-75.

Ma, Q. (2013). Role of Nrf2 in Oxidative Stress and Toxicity. Annu Rev Pharmacol Toxicol, 53, 401-26.
DOI: 10.1146/annurev-pharmtox-011112-140320.

Mabalirajan, U., Dinda, A. K., Kumar, S., Roshan, R., Gupta, P., Sharma, S.K., & Ghosh, B. (2008). Mitochondrial structural changes and dysfunction are associated with experimental allergic asthma. Journal Immunology, 181, 3540-3548.
DOI: http://sci-hub.tw/10.4049/jimmunol.181.5.3540

Marklund S, L. (1985). Pyrogallol auto oxidation. In: Greenwald RA. Handbook for oxygen radical research. Boca Raton: CRC Press.

Martin, L. J., Gupta, J., Jyothula, S. S., Butsch, K. M., Biagini, M. J. M., Patterson, T. L., … Hershey GK. (2012). Functional variant in the autophagy-related 5 gene promotor is associated with childhood asthma. PLoS One, 7, e33454.
DOI: 10.1371/journal.pone.0033454.

Mizushima, N. (2007). Autophagy: process and function. Genes & Development, 21, 2861-2873.
DOI: 10.1101/gad.1599207

Oka, S., Kamata, H., Kamata, K., Yagisawa, H., & Hirata, H. (2000). N-acetylcysteine suppresses TNF-induced NF-kappaB activation through inhibition of IkappaB kinases. Federation of European Biochemical Societies Letter, 472, 196-202.
DOI: https://doi.org/10.1016/S0014-5793(00)01464-2

Pham, D. L., Ban G. Y., Kim S. H., Shin Y. S., Ye Y. M., Chwae Y. J., & Park H. S. (2017). Neutrophil autophagy and extracellular DNA traps contribute to airway inflammation in severe asthma. Clinical Experimental Allergy, 47, 57-70.

DOI: 10.1111/cea.12859.

Pham, D. L., Kim, S. H., Losol, P., Yang, E. M., Shin, Y. S., Ye, W. M., & Park, H. S. (2016). Association of autophagy related gene polymorphisms with neutrophilic airway inflammation in adult asthma. The Korean Journal of Internal Medicine, 31, 375-385. DOI: 10.3904/kjim.2014.390

Poon, A., Eidelman, D., Laprise, C., & Hamid. Q. (2012). ATG5, autophagy and lung function in asthma. Autophagy, 8, 694-695.

DOI: 10.4161/auto.19315

Puleston, D. J., & Simon, A. K. (2014). Autophagy in the immune system. Immunology, 141, 1-8.

DOI: 10.1111/imm.12165.

Reddy, P. H. (2006). Mitochondrial oxidative damage in aging and Alzheimer's disease: implications for mitochondrially targeted antioxidant therapeutics Journal of Biomedicine and Biotechnology, 3, 1-13.

DOI: 10.1155/JBB/2006/31372

Remijsen, Q., Vanden, B. T., Wirawan, E., Asselbergh, B., Parthoens, E., De Rycke, R., … Vandenabeele, P. (2011). Neutrophil extracellular trap cell death requires both autophag and superoxide generation. Cell Research, 21, 290-304.

DOI: 10.1038/cr.2010.150

Rueden, C. T., Schindelin, J., Hiner M. C., DeZonia, B. E., Walter, A. E. Arena, E. T., & Eliceiri, K. W. (2017). ImageJ2: ImageJ for the next generation of scientific image data. BMC Bioinformatics, 18, 529.

DOI: 10.1186/s12859-017-1934-z

Rustin, P., Chretien, D., Bourgeron, T., Gérard, B., Rötig, A., Saudubray, J. M., & Munnich, A. (1994). Biochemical and molecular investigations in respiratory chain deficiencies. Clinical Chemical Acta, 228, 35-51.

DOI: https://doi.org/10.1016/0009-8981(94)90055-8

Sanz, M. L., Parra, A., Prieto, I., Dieguez, I. & Oehling, A. K. (1997). Serum eosinophil peroxidase (EPO) levels in asthmatic patients. Allergy, 52, 417-422.

DOI: https://doi.org/10.1111/j.1398-9995.1997.tb01021.x

Scherz-Shouval, R., & Elazar, Z. (2011). Regulation of autophagy by ROS: physiology and pathology. Trends Biochemical Sciences, 36, 30-38.

DOI: 10.1016/j.tibs.2010.07.007.

Schweinberger, B. M., Schwieder, L., Scherer, E., Sitta, A., Vargas, C. R., & Wyse, A. T. S. (2014). Development of an animal model fore gestational hypermethioninemia in rat and its effect on brain Na^+,K^+-ATPase/$Mg2^+$-ATPase activity and oxidative status of the offspring. Metabolic Brain Disease, 29, 153-160.
DOI: 10.1007/s11011-013-9451-x

Simon, D., Hoesli, S., Roth, N., Staedler, S., Yousefi, S., & Simon HU. (2011). Eosinophil extracellular DNA traps in skin diseases. Journal Allergy Clinical Immunology, 127, 194-199.
DOI: 10.1016/j.jaci.2010.11.002

Strath, M., Warren, D. J., & Sanderson, C. J. (1985). Detection of eosinophils using an eosinophil peroxidase assay. Its use as an assay for eosinophil differentiation factors. Journal Immunology Methods, 83, 209-215.
DOI: https://doi.org/10.1016/0022-1759(85)90242-X

Ueki, S., Konno, Y., Takeda, M., Moritoki, Y., Hirokawa, M., Matsuwaki, Y., … Weller, P. F. (2016). Eosinophil extracellular trap cell death-derived DNA traps: Their presence in secretions and functional attributes. Journal Allergy Clinical Immunology, 137, 258-267.
DOI: 10.1016/j.jaci.2015.04.041

Wendel, A. (1981). Glutathione peroxidase. Methods Enzymology, 77, 325-332.
DOI: https://doi.org/10.1016/S0076-6879(85)13063-6

Wyse, A. T. S., Streck, E. L., Barros, S. V., Brusque, A. M., Zugno, A. I., & Wajner, M. (2000). Methylmalonate administration decreases Na^+, K^+-ATPase activity in cerebral cortex of rats. Neuro report, 11, 2331-2334.
DOI: 10.1097/00001756-200007140-00052

Yousefi, S., Gold, J. A., Andina, N., Lee, J. J., Kelly, A. M., Kozlowski, E., … Simon, H. U. (2008). Catapult-like release of mitochondrial DNA by eosinophils contributes to antibacterial defense. Nature Medicine, 14, 949-953.
DOI: 10.1038/nm.1855.

Zhe, C., Xi, W., Lingling, D., Liuqun, J., Xiaogang, J., Ying, L., … Meng, L. (2017). Suppression of microRNA-384 enhances autophagy of airway smoth muscle cells in asthmatic mouse. Oncotarget, 8, 67933-67941.
DOI: 10.18632/oncotarget.18913

LEGEND TO THE FIGURE

FIGURE 1: Total and differential cells count in BALF (A-E). Representative illustration of BALF cells (400× magnification, arrows indicate eosinophils) (G). Analysis of the activity of the EPO enzyme (F). Histopathological analysis in lung. Representative photomicrographs of stained sections with H&E (200x and 1000x magnification, arrow indicate inflammatory infiltrate) (H). Morphometric analysis perivascular and peribronchial with H&E staining (I,J). Representative photomicrographs of stained sections with alcian blue (200× and 1000x magnification, arrows indicate globet cells) (K). Data represent the mean ± SD, n = 20 animals per group. * $p < 0.05$, ** $p < 0.01$ and *** $p < 0.001$ (One-way ANOVA followed by Tukey test). DPBS: dulbecco phosphate buffered saline; EPO: eosinophil peroxidase; 3-MA: 3-methyladenine; OVA: ovalbumin; TCC: total cells count.

FIGURE 2: Assessment of respiratory system mechanics: resistance (Rn), tissue damping (G) and tissue elastance (H) (A-C). Cytokine levels in lung (IL-5, IL-13, IFN-γ, IL1-β, TNF-α and IL-10) (D-I). Analysis of the NFκB p65 protein by immunofluorescence in lung sections (J). Data represent the mean ± SD, n = 10 animals per group. * $p < 0.05$, ** $p < 0.01$ and *** $p < 0.001$ (One-way ANOVA followed by Tukey test). DPBS: dulbecco phosphate buffered saline; IFN: interferon; IL: interleukin, 3-MA: 3-methyladenine; OVA: ovalbumin; TNF: tumor necrosis factor.

FIGURE 3: ROS production in lung (A). Activity of antioxidant enzymes (SOD, CAT and GPx) in lung (B-E). Mitochondrial energy metabolism (Complex II, SDH, complex IV) in lung (F-H). NA^+, K^+-ATPase activity analyses in lung (I). Data represent the mean ± SD, n = 10 animals per group. * $p < 0.05$, ** $p < 0.01$ and *** $p < 0.001$ (One-way ANOVA followed by Tukey test). CAT: catalase; DCF: dichlorofluorescein; DPBS: dulbecco phosphate buffered saline; GPx: glutathione peroxidase; 3-MA: 3-methyladenine; OVA: ovalbumin; ROS: reactive oxygen species; SDH: succinate dehydrogenase; SOD: superoxide dismutase.

FIGURE 4: Immunofluorescence microscopy of EETs in BALF eosinophils (630x magnification, arrows indicate EETs formation) (A). Quantification of extracellular DNA traps in BALF (B). Analysis of cell death in BALF cells by Annexin V/PI (C). Data represent the mean ± SD, n = 20 animals per group. *** $p<0.001$ (One-way ANOVA followed by Tukey test). BALF: bronchoalveolar lavage fluid; DPBS:

dulbecco phosphate buffered saline; EETs: eosinophil extracellular traps; EPO: eosinophil peroxidase; 3-MA: 3-methyladenine; OVA: ovalbumin; PI: propidium iodide.

FIGURE 5: Detection and quantification of AVOs in BALF eosinophils (A-C). Analysis of LC3B in BALF eosinophils and lung tissue by immunofluorescence (D,E). Analysis of LC3B and protein kinase B (AKT) in lung by Western blot (F,G). Data represent the mean ± SD, n = 20 animals per group. * $p < 0.01$ (One-way ANOVA followed by Tukey test). AKT: protein kinase B, AVOs: acidic vesicle organelles; BALF: bronchoalveolar lavage fluid; DPBS: dulbecco phosphate buffered saline; EPO: eosinophil peroxidase; 3-MA: 3-methyladenine; LC3B: light chain 3B; OVA: ovalbumin.

FIGURE 1

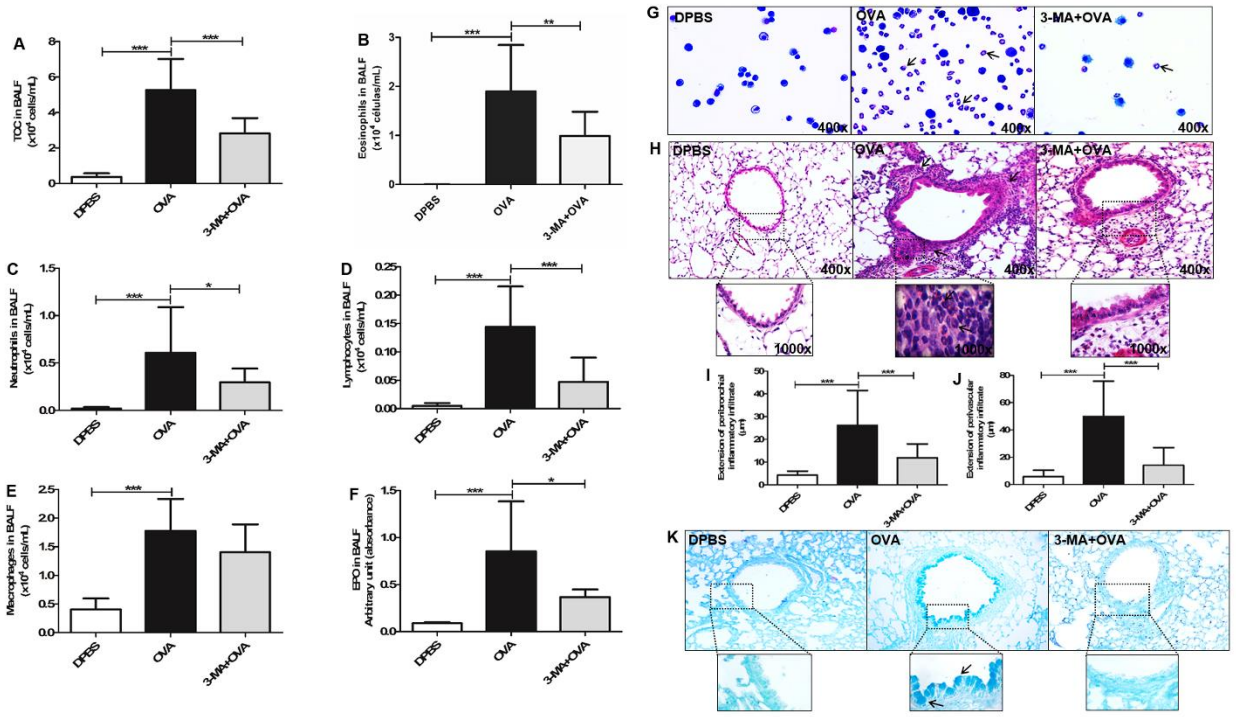

FIGURE 2

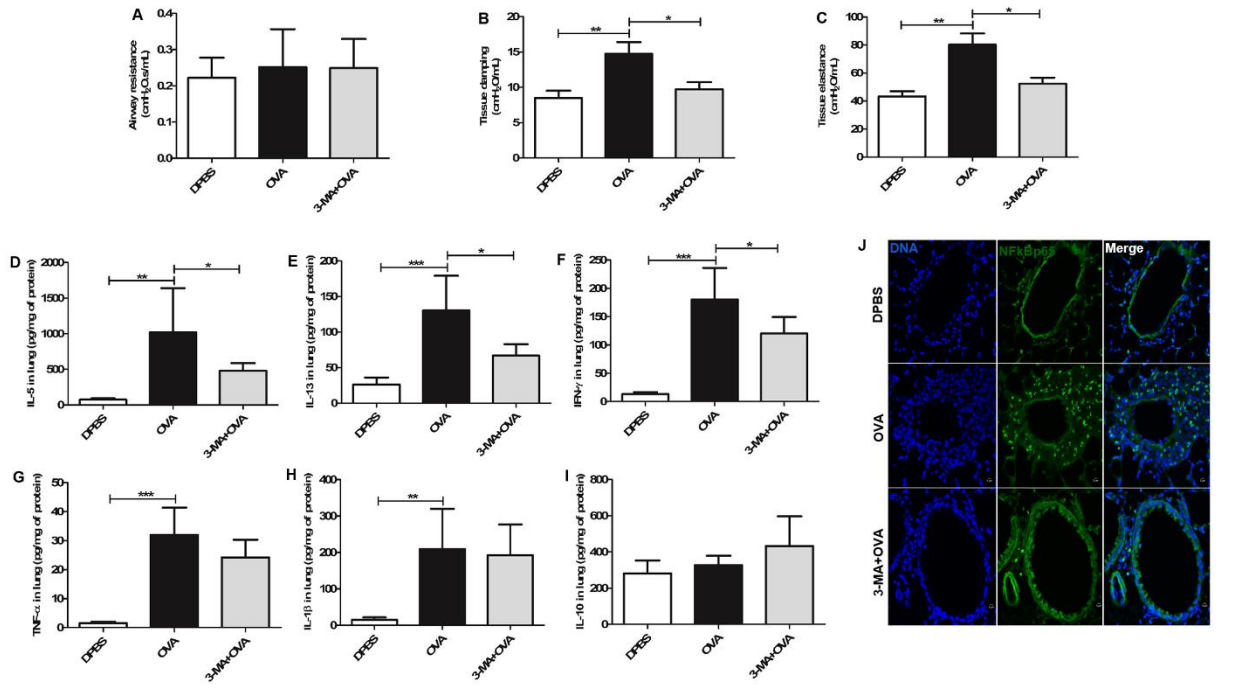

FIGURE 3

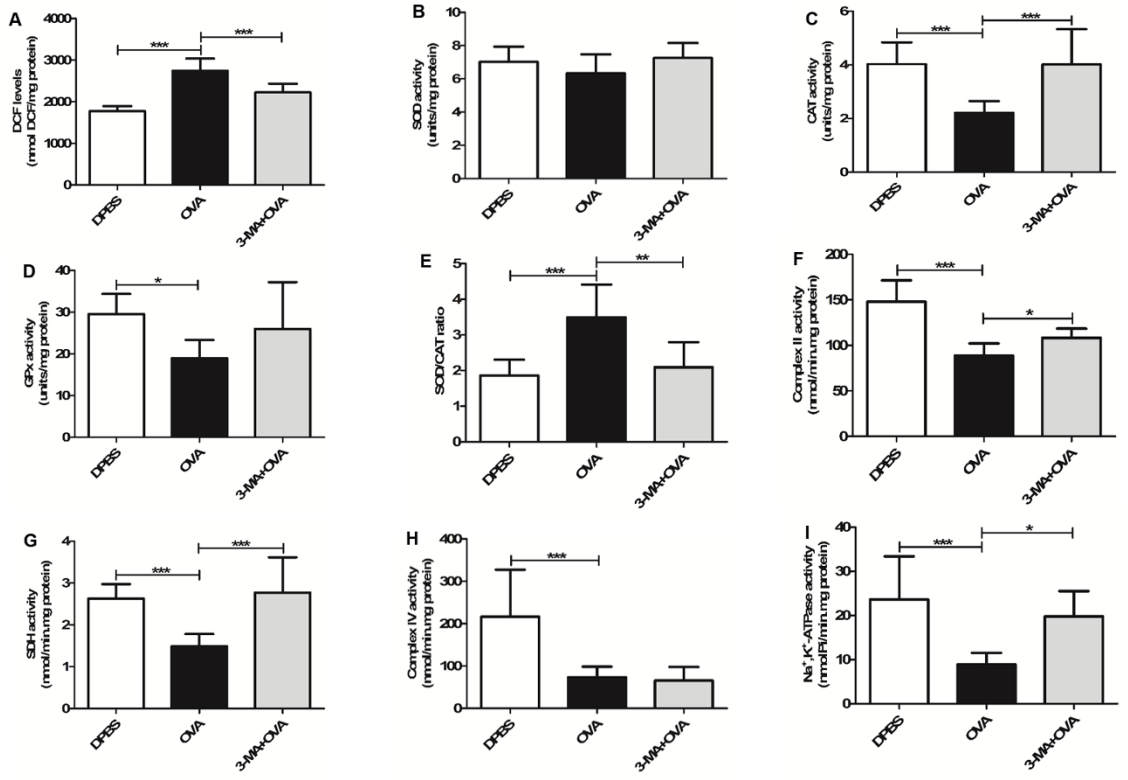

FIGURE 4

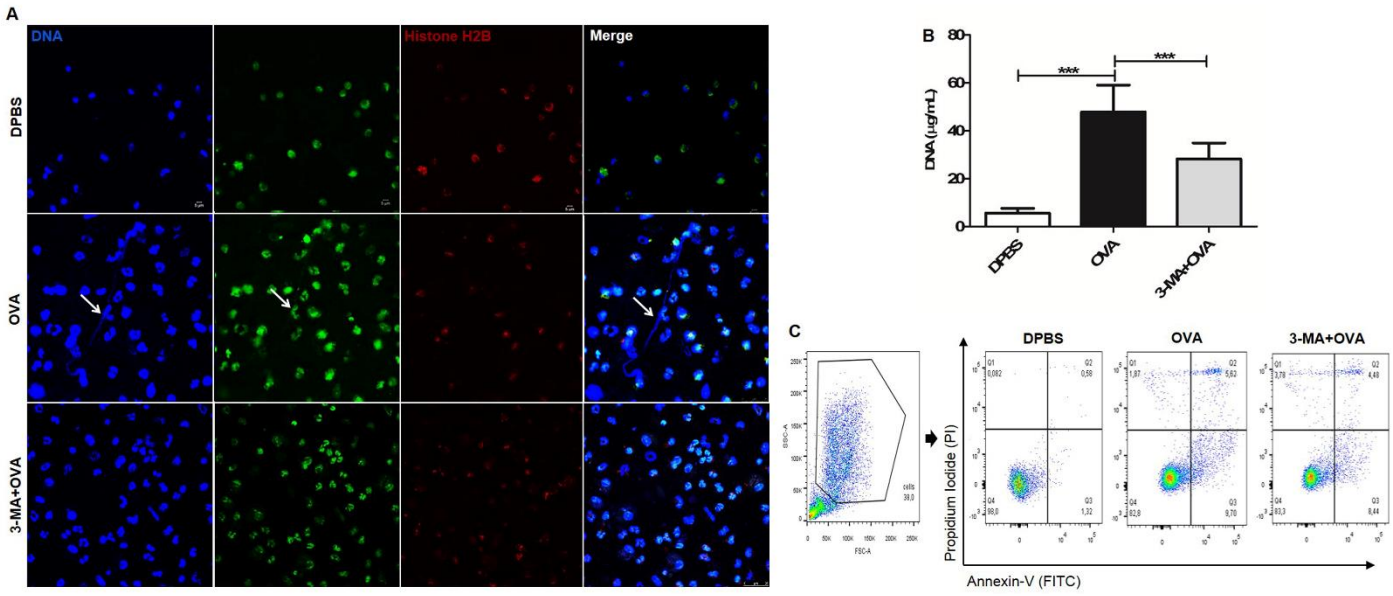

FIGURE 6

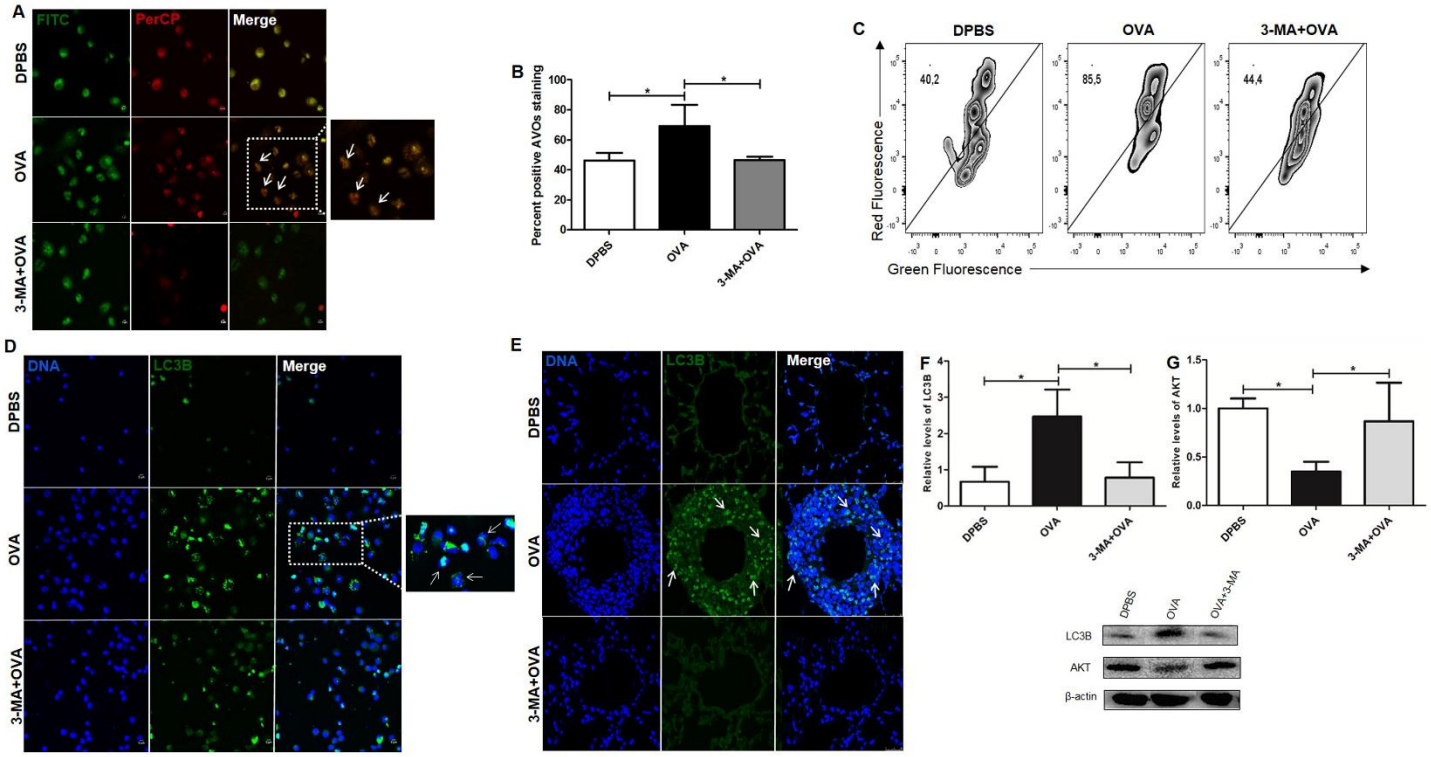
A
FITC
PerCP
Merge
DPBS
OVA
3-MA+OVA
B
Percent positive AVOs staining
100
80
60
40
20
0
*
*
DPBS
OVA
3-MA+OVA
C
DPBS
OVA
3-MA+OVA
40,2
85,5
44,4
Red Fluorescence
Green Fluorescence
D
DNA
LC3B
Merge
DPBS
OVA
3-MA+OVA
E
DNA
LC3B
Merge
DPBS
OVA
3-MA+OVA
F
Relative levels of LC3B
4
3
2
1
0
*
*
DPBS
OVA
3-MA+OVA
G
Relative levels of AKT
1.5
1.0
0.5
0.0
*
*
DPBS
OVA
3-MA+OVA
DPBS
OVA
OVA+3-MA
LC3B
AKT
β-actin

Pontifícia Universidade Católica do Rio Grande do Sul
Pró-Reitoria de Graduação
Av. Ipiranga, 6681 - Prédio 1 - 3º. andar
Porto Alegre - RS - Brasil
Fone: (51) 3320-3500 - Fax: (51) 3339-1564
E-mail: prograd@pucrs.br
Site: www.pucrs.br